



Miniaturized Platforms for High Throughput Biocatalysis

Ana Rita Cardoso Martins

Thesis to obtain the Master of Science Degree in

Biotechnology

Supervisor: Dr. Pedro Carlos de Barros Fernandes

Examination Committee

Chairperson: Prof. Luís Joaquim Pina da Fonseca

Supervisor: Dr. Pedro Carlos de Barros Fernandes

Member of the Committee: Prof. Maria Henriques Lourenço Ribeiro

October 2016

ACKNOWLEDGEMENTS

First of all I would like to express my sincere gratitude to Dr. Pedro Fernandes, my supervisor. I would like to thank you for accepting me to develop this work and for all the trust and freedom that was given to me to on the lab and for the encouragement to test every new idea. For all the knowledge, guidance, advices and for all of the hours spent discussing data and exchanging impressions, thank you. Words might not be enough to express how grateful I am.

To all of my lab friends and colleagues, especially to Inês, Rosarinho, Sónia and Sofia, for all the coffee-breaks, lunches, successes and failures we shared and for all of the support and friendship, thank you.

To my MSc friends and to all of my other closest friends that usually do not understand half of what I am saying when they ask me about my work, thank you for all the patience and for saying that everything would turn out great. I think it did! You are the ones you kept me from going insane by taking my mind out of work and by turning these last few years into something amazing.

Finally, to the most important people in my life, mom, dad, brother – thank you for everything, for all the sacrifices, all the belief, trust, patience and love. I am forever grateful to you.

ABSTRACT

The ability to perform very specific reactions has attracted great interest to enzymes, especially to take advantage of such characteristics to apply in (industrial) bioprocessing. New trends have been raising up in the last years, namely regarding the use of miniaturized devices.

Two immobilization methods were used in parallel throughout the work: covalent binding in Amberlite IRC-86 and entrapment in PVA, being the latter the one who showed better immobilization efficiency (94%) and overall performance.

The optimal temperature and pH found for the enzyme immobilized in Amberlite IRC-86 was 55°C and pH 4 whereas for PVA it was 65°C and pH 4.5. No temperature shifts compared to the free form were observed, only higher tolerances to heat upon immobilization in both supports. With Amberlite IRC-86 a shift from pH 5 to 4 was observed upon immobilization. In the entrapped enzyme system, the reaction showed signs of needing convective flow at the reactional volume of 1 mL, whereas for the covalently-linked enzyme the threshold occurred with 3 mL.

The kinetics of agitated and non-agitated systems were compared to investigate the impact of the reactional volume and agitation presence/absence in the reaction performance and the results were found to be dependent of the immobilization method.

A scaled down approach with MTP was used to evaluate the influence of geometric and dynamic parameters on the reaction with the goal of optimizing the operational conditions and establish microtiter plates as a reliable and efficient high-throughput platform for fructose production.

Key words:

Inulin; Enzyme Immobilization; Amberlite IRC-86; PVA; Miniaturized Systems; Microtiter Plates

RESUMO

A capacidade de realizar reações específicas tem atraído um grande interesse para os enzimas, especialmente para tirar partido de tais características e aplicá-las em bioprocessos (industriais). Novas tendências têm surgido nos últimos anos, nomeadamente em relação ao uso de dispositivos miniaturizados.

Dois métodos de imobilização foram usados em paralelo ao longo deste trabalho: ligação covalente em Amberlite IRC-86 e aprisionamento em PVA, sendo o último o que mostrou melhores eficiências de imobilização (94%) e desempenho geral.

A temperatura e pH ótimos para o enzima imobilizado em Amberlite IRC-86 foi de 55°C e pH 4 enquanto para o PVA foi de 65°C e pH 4,5. Não se observaram quaisquer desvios de temperatura relativamente à forma livre, apenas aumentos na tolerância ao calor aquando a imobilização em ambos os suportes. Com Amberlite IRC-86 observou-se um desvio no pH de 5 para 4 aquando a imobilização. A reação com o enzima aprisionado mostrou sinais de precisar de agitação ao volume reacional de 1 mL, enquanto para o enzima ligado covalentemente tal ocorreu aos 3 mL.

A cinética dos sistemas agitados e não agitados foi comparada para investigar o impacto do volume reacional e da presença/ausência de agitação no desempenho da reação, sendo os resultados dependentes do método de imobilização.

Uma abordagem à escala reduzida com microplacas foi usada para avaliar a influência de parâmetros geométricos e dinâmicos na reação com o objetivo de otimizar as condições operacionais e estabelecer as microplacas como plataformas de alta produção, fiáveis e eficientes para a produção de frutose.

Palavras-chave:

Inulina; Imobilização de enzimas; Amberlite IRC-86; PVA; Sistemas miniaturizados; Microplacas

TABLE OF CONTENTS

Acknowledgements	iii
Abstract.....	v
Resumo	vii
Table Index.....	xiii
Figure Index.....	xv
Abbreviations List	xvii
1. Introduction.....	1
1.1. General overview on enzyme relevance	1
1.1.1. Enzyme relevance in the market	1
1.1.2. Enzyme engineering	1
1.1.3. Enzymes as green catalysts	2
1.2. Enzyme immobilization	3
1.2.1. Entrapment	7
1.2.2. Encapsulation	9
1.2.3. Support based immobilization	10
1.2.4. Cross linking	15
1.3. Inulin hydrolysis for fructose production	17
1.3.1. Fructose production	17
1.3.2. Inulin and inulinase	18
1.3.3. Optimal reaction conditions	20
1.4. Process scaling	23
1.4.1. Mechanical agitation and size scaling	24
1.5. Miniaturized systems	25
1.5.1. Microtiter plates	26
1.5.2. Microfluidic devices	30
2. Objectives.....	33
3. Materials and Methods	35

3.1.	Materials	35
3.2.	Immobilization procedures.....	35
3.2.1.	Amberlite immobilization.....	35
3.2.2.	PVA immobilization.....	36
3.3.	Characterization of immobilized and free inulinase (pH and temperature)	37
3.4.	Biotransformation with the free and immobilized enzyme	37
3.5.	Hydrodynamic environment within scale up	38
3.6.	Microtiter plate assays	39
3.7.	Enzyme activity.....	40
3.8.	Analytical methods	40
4.	Results	41
4.1.	Hydrolysis of <i>Dahlia</i> tubers inulin with inulinase immobilized in Amberlite IRC-86.....	41
4.1.1.	Characterization of immobilized and free inulinase (pH and temperature)	41
4.1.2.	Time courses of product formation of the free and immobilized enzyme	41
4.2.	Hydrolysis of <i>Dahlia</i> tubers inulin with inulinase immobilized in PVA	43
4.2.1.	Time courses of product formation of the free and immobilized enzyme	43
4.3.	Hydrolysis of chicory root inulin with inulinase immobilized in PVA	46
4.3.1.	Characterization of immobilized and free inulinase (pH and temperature)	46
4.4.	Hydrodynamic environment within scale up	46
4.5.	Microtiter plates assays	48
4.6.	Enzyme Activity	51
4.6.1.	Inulinase immobilized in Amberlite IRC-86: activity over <i>Dahlia</i> tubers inulin.....	51
4.6.2.	Inulinase immobilized in PVA beads: activity over Chicory root inulin	51
5.	Discussion	55
5.1.	Optimal pH and temperature	55
5.2.	Biotransformation with the free and immobilized enzyme	57
5.3.	Hydrodynamic environment within scale up	62
5.4.	Microtiter plates assays	62
5.5.	Enzyme activity.....	67

6. Conclusions and Future Work..... 71

7. References 73

TABLE INDEX

Table 1 – Main advantages and disadvantages of enzyme immobilization [5], [8], [11].	4
Table 2 – Critical shaking speed (N_{crit}) for the different plates and filling volumes used in both agitators (orbital diameters of 1.5 mm and 25 mm). Calculations were performed considering the $\rho_{water, 50^{\circ}C}$ as 988.10 kg.m ⁻³ , $\rho_{water, 55^{\circ}C}$ as 985.65 kg.m ⁻³ , $\sigma_{water, 50^{\circ}C}$ as 0.0679 N.m ⁻¹ and $\sigma_{water, 55^{\circ}C}$ as 0.0671 N.m ⁻¹ .	49
Table 3 – Overview of the dimensionless numbers (Fr_a , Re_f and Ph) calculated for the different agitators and MTP used.	49
Table 4 – Theoretical angle of the liquid inside the wells formed against the walls of the MTP.	50
Table 5 – Summary of the kinetic parameters (V_{max} and K_M) for the free and Amberlite IRC-86 immobilized inulinase, with and without agitation in reactional volumes of 1, 3 and 10 mL.	51
Table 6 – Summary of the kinetic parameters (V_{max} and K_M) for the free and PVA immobilized inulinase, with and without agitation in reactional volumes of 1 and 10 mL. Values obtained through a non-linear regression from Hyper32® software.	53
Table 7 – Immobilization efficiency for the two types of supports and methods used.	55
Table 8 – Summary of the optimal pH and temperatures observed for the different substrates and supports tested.	56
Table 9 – Inulin hydrolysis rates (g.L ⁻¹ .min ⁻¹) at 1, 3 and 10 mL, with and without agitation (440 rpm) for the different immobilization methods tested and the free enzyme. In all cases the R^2 was higher than 0.94, except for Amberlite IRC-86 without agitation at 3 and 10 mL where no linear correlation was observed.	58
Table 10 – Liquid height to vessel diameter ratio for the different reactional volumes under study.	61
Table 11 – Qualitative comparison between Amberlite IRC-86 and PVA-based immobilization systems.	61

FIGURE INDEX

Figure 1 – Main characteristics involved in process development and optimization (adapted from [5]).....	2
Figure 2 – Overview on the application of protein engineering methods towards enzymes.	2
Figure 3 – Schematic representation of immobilization by entrapment. During the formation of the polymeric network (represented by the blue lines), the enzyme (E) is retained. The catalytic reaction occurs due to the ability of substrates and products to pass through it.	7
Figure 4 – Formation of calcium alginate gel beads by dripping of the solution into CaCl ₂ (source: [5]).....	8
Figure 5 – Schematic representation of enzyme (E) encapsulation.	9
Figure 6 – Schematic representation of support-based immobilization through adsorption.	10
Figure 7 – Schematic representation of covalent binding in support-based immobilization.	12
Figure 8 – Examples of carrier coupling using an amino group of the enzyme. In the first case the matrix is pre-activated with epoxy groups. In the bottom, the matrix is activated with cyanogen bromide. (source: [5])	13
Figure 9 – Schematic representation of enzyme immobilization by cross linking.	15
Figure 10 – Inulin structure.	18
Figure 11 – Scale up approach based on the most conventional methods of gradually increasing the reactor's scale. Typical approaches are based on rules of thumb, practices and correlations such as the 1:10 scale up ratio [92].	23
Figure 12 – Different configurations available for microtiter plates. A wide range of characteristics are available to be combined accordingly to the researcher's purposes.	27
Figure 13 – Amberlite IRC-86 beads with a harmonic mean size of 0.58 to 0.78 mm. The functional group of this weak acid cation exchanger is carboxylic acid.	36
Figure 14 – Final form of the PVA beads in acetate buffer 0.1 M pH 4.5.	37
Figure 15 – General experimental setup for the biotransformation and enzyme activity measurements. In the picture Amberlite IRC-86 is being incubated inside jacketed vessel at 55°C in a reactional volume of 10 mL.....	38
Figure 16 – Reaction vessels for the 1 mL (A) and 10 mL (B) reactions.	39
Figure 17 – Magnetic stirrers used in the 1 mL (A) and 10 mL (B) reaction vessels.	39
Figure 18 – Microtiter plates used for the study of the hydrodynamic studies. (A) 96-square-shaped well, round-bottomed plate (well length: 0.8 cm); (B) 24-square-shaped well, pyramidal-bottomed plate (well length: 1.7 cm); (C) 24-round-shaped well, flat-bottomed plate (well diameter: 1.6 cm). The filling content of the shown plates is Amberlite IRC-86 (in brown) and PVA beads (in white).	40
Figure 19 – Effect of the temperature and pH on <i>Dahlia</i> tubers inulin hydrolysis with Amberlite IRC-86 immobilized enzyme (—●—) and free enzyme (—●—).....	41

Figure 20 – Time course of product formation for the 1 mL reaction system with the free and Amberlite IRC-86 immobilized enzyme with and without magnetic agitation (440 rpm). Free enzyme on the main axis and immobilized enzyme on the secondary axis. 42

Figure 21 – Time course of product formation for the 3 mL reaction system with the free and Amberlite IRC-86 immobilized enzyme with and without magnetic agitation (440 rpm). Free enzyme on the main axis and immobilized enzyme on the secondary axis. 42

Figure 22 – Time course of product formation for the 10 mL reaction system with the free and Amberlite IRC-86 immobilized enzyme with and without magnetic agitation (440 rpm). Free enzyme on the main axis and immobilized enzyme on the secondary axis. 43

Figure 23 – Time course of product formation for the 1 mL reaction system with the free and PVA immobilized enzyme with and without magnetic agitation (440 rpm). Free enzyme on the main axis and immobilized enzyme on the secondary axis. 44

Figure 24 – Time course of product formation for the 3 mL reaction system with the free and PVA immobilized enzyme with and without magnetic agitation (440 rpm). Free enzyme on the main axis and immobilized enzyme on the secondary axis. 45

Figure 25 – Time course of product formation for the 10 mL reaction system with the free and PVA immobilized enzyme with and without magnetic agitation (440 rpm). Free enzyme on the main axis and immobilized enzyme on the secondary axis. 45

Figure 26 – Effect of the temperature and pH on Chicory root inulin hydrolysis with PVA immobilized enzyme (—○—) and free enzyme (—●—). 46

Figure 27 – Reaction rates for the 1 mL ($0.184 \text{ g.L}^{-1}.\text{min}^{-1}$ at 423 rpm) and 10 mL ($0.1408 \text{ g.L}^{-1}.\text{min}^{-1}$ at 737 rpm and $0.1556 \text{ g.L}^{-1}.\text{min}^{-1}$ at 881 rpm) reactional systems with Amberlite IRC-86 immobilized enzyme. The 1 mL reaction at 423 rpm was used as the scale up basis. 47

Figure 28 – Effect of magnetic stirring in the initial velocity of the reaction of hydrolysis of inulin with Amberlite IRC-86 immobilized enzyme in a 10 mL reactional system. 48

Figure 29 – Comparative studies of the reaction rate of inulin hydrolysis with both immobilized enzymes under various agitation speeds (110, 170, 450 and 700 rpm) and shaking diameters (1.5 and 25 mm). Different configuration MTP were used: Plate A – 96-square-shaped well, round-bottom; Plate B – 24-square-shaped well, pyramidal-bottom; Plate C – 24-round-shaped well, flat-bottom. 50

Figure 30 – Michaelis-Menten plots for the free enzyme. Activity measurements were performed with chicory root inulin concentrations ranging from 10 to 120 g.L^{-1} at pH 4.5 and 50°C . (A) 1 mL reactional system with agitation; (B) 1 mL reactional system without agitation; (C) 10 mL reactional system with agitation; (D) 10 mL reactional system without agitation. Plots obtained through Hyper32® software. 52

Figure 31 – Michaelis-Menten plots for the PVA immobilized inulinase. Activity measurements were performed with chicory root inulin concentrations ranging from 10 to 120 g.L^{-1} at pH 4.5 and 50°C . (A) 1 mL reactional system with agitation; (B) 1 mL reactional system without agitation; (C) 10 mL reactional system with agitation; (D) 10 mL reactional system without agitation. Plots obtained through Hyper32® software. 52

ABBREVIATIONS LIST

BSA	Bovine Serum Albumin
d	Maximum internal diameter of the shaking vessel or the stirrer diameter (m)
D	Agitator diameter
D_w	Well diameter (m)
D_o	Orbital shaking diameter (m)
DP	Degree of polymerization
DNS	2,4-dinitrosilylic acid
Fr_a	Axial Froude number
g	Gravitational acceleration ($m.s^{-2}$)
K_M	Michaelis constant
MTP	Microtiter plate
MW	Molecular weight
N_i	Rotational speed (rpm)
n	Scale up factor
N	Mixing frequency (1/s)
N_{crit}	Critical shaking frequency (1/s)
Ph	Phase number
PVA	Polyvinyl alcohol
Re	Reynolds number
Re_f	Reynolds number adapted for liquid film
rpm	Rotations per minute
SEM	Scanning electron microscopy

T	Vessel diameter
t_m	Mixing time
V_L	Filling volume (m^3)
V_{max}	Maximum reaction rate
Z	Liquid column height in the vessel

SYMBOL LIST

ρ	Fluid density ($kg.m^{-3}$)
σ	Surface tension ($kg.s^{-2}$)
μ	Fluid viscosity (Pa.s)
u	Fluid velocity ($m.s^{-1}$)

1. INTRODUCTION

1.1. General overview on enzyme relevance

1.1.1. Enzyme relevance in the market

The ability to perform very specific reactions has attracted great interest to enzymes, especially to take advantage of such characteristics to apply in industrial processes. However, with the increasing worldwide demands regarding process development, new breakthroughs are needed in the enzyme field to satisfy such demands and to amplify their use in the more diverse areas [1].

Enzymes are used in areas from research and development, to cosmetics, medication or food manufacturing [1]. Currently hydrolytic enzymes account for almost 75% of all industrial enzymes [1]. Hydrolases are enzymes such as proteases, amylases, lipases and celluloses used for degradation of natural substances [2], [3]. For example, α -amylases can be applied to convert starch to sugar syrups [1].

Enzymes can be divided accordingly to the sector in which they are used. Technical enzymes are perhaps the most used by the ordinary consumer in goods like detergents, textiles and fuel alcoholic industries [2]. This kind of enzymes was valued at \$4.2 billion in 2014 by research associations and are expected to reach \$6.2 billion in 2020 [4].

The use of enzymes to improve flavors, textures or nutritional values is of extreme importance in the food sector where enzymes are under some strict regulations in order to be used [1]. Nonetheless this enzyme sector is expected to reach about \$2 billion by 2020 [4].

1.1.2. Enzyme engineering

A prerequisite for any industrial process is its rational design and development [5]. For that, information about the biocatalyst, the reaction itself and the environment in which the reaction occurs is necessary (Figure 1). The goal is to maximize the reaction outcome (higher selectivity, yields and purity) while minimizing the overall consumption of biocatalyst, raw materials and other utilities [5].

The optimization of a reaction can include parameters such as pH, temperature, cofactors, substrate and product concentrations and buffers composition among others [5]. The reactor material and the physical properties can also influence greatly the system. However, the best optimization conditions often come through trial and error procedures.

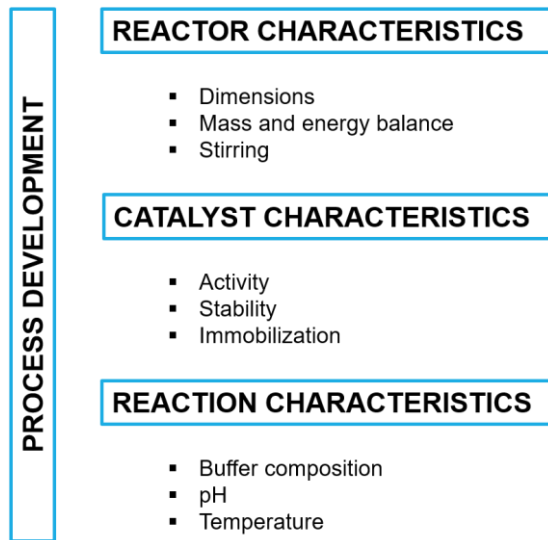


Figure 1 – Main characteristics involved in process development and optimization (adapted from [5]).

The rapid and recent developments in the biotechnology field have led to the development of novel improved and customized catalysts by means of recombinant DNA techniques and others such as site-directed mutagenesis and in vitro evolution via gene shuffling. Such advances, when applied to protein engineering, have shown great developments in changing the catalytic features of native enzymes and enough evidence to be a promising strategy to optimize processes [2] [6].

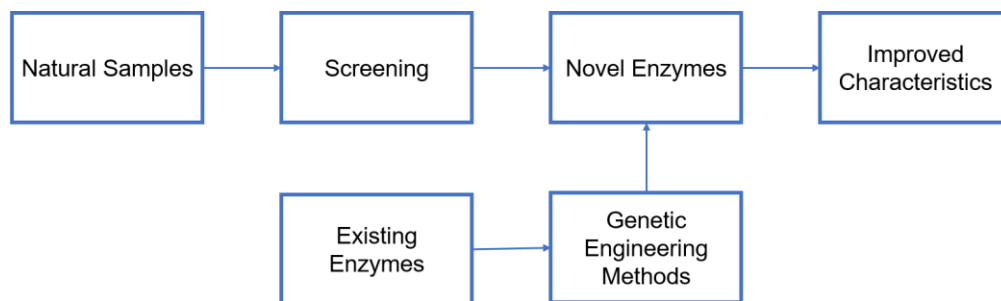


Figure 2 – Overview on the application of protein engineering methods towards enzymes.

1.1.3. Enzymes as green catalysts

Regarding sustainable process development, biocatalysts are an essential key factor. Biocatalysts can operate under mild reaction conditions in diverse environments and their use has also obviated the need of often toxic reagents that protect and/or activate certain functional groups [6]. This reduces the number of

intermediate reactive steps, decreases the need for extra utilities, as well as the use of reagents, many often toxic and expensive [2], [7].

Reactions with biodegradable biocatalysts are thus preferred since the reaction can be more direct with less waste production and less requirements for purification, which results in both more economic and environment friendly processes [6]. The conscientiousness for green process development is a very important aspect to implement in a world with a non-stop increasing population where many of Earth's natural resources are close to exhaustion [5].

1.2. Enzyme immobilization

An enzyme is a biological catalyst that promotes the transformation of chemical species in living organisms even under very mild conditions [8]. Enzymes have the ability to catalyze reactions with a very high degree of substrate specificity, which decreases the formation of by-products [8], [9]. Enzymes are a remarkable discovery in the field of bioprocess technology and are involved in very complex biochemical transformations that may not be accessible to regular organic chemistry methods [8], [9]. Biotechnology industries are currently concerned with enhancing enzyme productivity and develop new techniques to increase their shelf life, which are fundamental requisites for large-scale and economic formulation [9].

Enzymatic reactions can be performed with enzymes dissolved in aqueous liquid phase (homogeneous biocatalysis) or attached to surfaces (heterogeneous biocatalysis), which involves enzymes in a water-insoluble (solid) form [8], [10]. The latter methodology, also known as enzyme immobilization, refers to the confinement of an enzyme to a phase (matrix/support), different from the one for substrates and products, that can be used repeatedly and continuously with retention of its catalytic activity [8], [9].

By allowing the recovery of and reuse of costly enzymes, heterogeneously catalyzed reactions have shown to be successful in improving both the technical and economic performance of several industrial processes being preferred over their free form due to their extended availability that eases downstream processing [8]–[11]. Nevertheless, a large number of processes rely on non-immobilized biocatalysts by using a second liquid phase, such as an organic solvent or an ionic liquid, where the biocatalyst can be immobilized homogeneously [5].

Properties such as catalytic activity and operational stability tend to change when the free enzyme is immobilized, most probably due to changes in the native three-dimensional conformation of the enzyme that can occur upon binding, or differences in the microenvironment in which the enzyme interacts with its substrate and the support itself [8]. The integrity of the structural stability during the biochemical reaction is thus highly encouraged. Improved enzyme performance, via increased stability and reuse, leads to higher catalyst productivities which, in turn, control the enzyme costs per kg product and part of the economic viability of the process [6], [9], [11]. Paradoxically one of the main problems with immobilization is precisely

the loss of catalytic activity [8]. Macromolecular substrates can be a problem as their access to the enzyme's active site may be limited by steric hindrance, which in turn may reduce the activity [8]. These problems can be obviated by choosing the right residues to be involved in the immobilization and the right support.

Clearly, immobilization has great advantages, especially in process development. However it also should be taken into account the respective downsides of it. The main advantages and disadvantages of this approach are summarized in Table 1.

Table 1 – Main advantages and disadvantages of enzyme immobilization [5], [8], [11].

Advantages	Disadvantages
Catalyst reuse and recycling	Carrier or matrix cannot be recycled
Enhanced enzyme activity	Activity loss or reduction
Easier product-biocatalyst separation	Diffusional limitations, lowering reaction rates
Better stability, especially towards organic solvents and heat	Additional costs for carrier or immobilization matrix and immobilization procedure
Reduced costs of downstream processing	
Modification of substrate selectivity and enantioselectivity and multi-enzyme reactions	
Wider choice of reactor (fixed bed reactors and continuous operation)	
Easier reactor operation	

Although seeming like an indispensable strategy for (industrial) process development, truth is that only a few processes based on enzyme immobilization are actually successfully [12]. Nonetheless, products such as high-fructose syrups, semi-synthetic penicillins or amino acids rely heavily on immobilized enzymes such as glucose isomerase, penicillin acylase or amino acid acylase, respectively [8], [12].

Attachment to appropriate surfaces allows to concentrate the activity of the enzyme towards a specific location and might even protect it from degradation [8]. The main components involved in any immobilization procedure are the enzyme, the type of support and the mode of attachment between the enzyme and the matrix. The most common methods of attachment range from reversible physical adsorption and ionic linkages to stable covalent bonds which will be discussed further on.

Choice of Support

The characteristics of the support are of crucial importance to get full advantage of the immobilized system. When considering a support, properties such as an available high internal surface area, physical strength, resistance to compression, hydrophilicity, inertness towards the enzyme, biocompatibility, resistance to microbial attack, regenerability and availability at low cost must be considered [9], [10]. Characteristics

related with pore size, mean particle diameter and swelling behavior are equally important as they can restrict the type of reactor used (e.g. stirred tank vs. fluidized bed) [8]. In particular, the size of the pores or the particles determine the total surface area available for immobilization. Regarding this subject, porous and non-porous supports are available, being the former the most widely used. When compared with non-porous, porous supports have higher surface areas and loading capacities, and as the enzyme is inside the pores, it offers more protection from the environment [8]. Still, non-porous supports show fewer diffusional limitations [8].

Supports can be classified into inorganic and organic, and the latter into natural and synthetic polymers. Inorganic supports offer great stability against degradation however the majority of the supports used in industry are of organic nature [9].

The most widely used matrix is agarose. This polymer has all of the desired characteristics referred above: high porosity, high capacity, hydrophilic character and commercial availability. Besides, the absence of charged groups prevents nonspecific adsorption of substrate and products [8]. However this support is rather expensive, which makes it of crucial importance the need to regenerate and reuse the matrix. Another example of a polymer is chitosan which has been reported to be non-toxic, biocompatible, amenable to chemical modification and highly affinitive to protein due to its hydrophilic nature. However its application to the food and pharmaceutical industry is limited due to the tedious and time consuming immobilization process [13].

Regarding synthetic polymers, Amberlite ion-exchange resins are available in different varieties, accordingly to the differences in the functional groups present at the surface of the beads and, in the case of mixture resins, their cation to anion ratio, among others. These resins are insoluble, compatible with most organic solvents and diluted acids and bases, resistant to biodegradation and, in general, capable of being regenerated.

Amberlite MB-150, a strongly acidic cationic and strongly basic anionic mixture resin, has been reported in the immobilization of α -amylase [14] and β -galactosidase [15]. Other types have been reported in the immobilization of urease (Amberlite MB-1) [16], inulinase (Amberlite IRC-50) [17] or lipase (Amberlite IRC-50 and IR-4B) [18].

A new trend that has been gaining relevance is the use of immobilization carriers made of responsive materials. The use of such materials is of great interest in measuring pH, temperature, electrical fields, shear stress, or dissolved oxygen levels within the reaction medium [19]. However, these methods are still limited to the small range of analytes available [10].

An example of such was the rational development of silica materials that are phosphorescently labeled inside the pores [20]. The development of this underivatized support aimed to immobilize enzymes whilst it could be used to determine the support's internal oxygen concentration in heterogeneous oxygen-dependent biocatalysis [20]. One of the main outcomes of measuring the internal oxygen levels could be of

great help in order to optimize the immobilized enzyme and overcome eventual diffusional limitations. By using the oxidative deamination of D-methionine as a model system, the authors concluded that the biocatalyst was almost as effective as the free enzyme and that the immobilized enzyme was perfectly distributed throughout the mesostructured silica support [20].

Biocatalytic reactions can also change the protonic gradient of the bulk, which ultimately changes the pH at which the reaction occurs. Studies to determine the pH in immobilized enzymes based on dual-lifetime referencing (DLR) have been carried [21]. Cephalosporin C amidase was immobilized into Sepabeads EC-EP, pre-labeled with lipophilic variants of two luminophores in the matrix, in a stirred reactor at pH 8.0 [21]. Changes of about 1 pH unit were recorded whilst substrate addition, evidencing the importance of measuring the intraparticle pH levels as an important tool to assess, for example, substrate depletion or formation of acidic products [21]. The great promise regarding this system is its ability to be applied to other agitated systems with particles in suspension.

A non-support related but similar approach for monitoring reactions based on flavin-dependent oxidoreductases has been tested for high-throughput microtiter-plate-based activity assays [22]. Several enzymes were put in the presence of selected redox dyes, capable of acting as electron acceptors, and the decolorization of the dye was followed and visible within a few minutes [22]. This showed that the dyes used could be applied to activity assays of other flavin-dependent oxidoreductases. The method showed to be economical as only low concentrations of dye were necessary to assure substrate saturation and thus maximal reaction velocities [22]. It also benefits from the fact that the assay is based on the direct enzymatic reduction of the dye and not on the coupled detection of a product.

Microscopic techniques have also been applied to deepen the knowledge on the structure-activity relationship of immobilized enzymes. Haloalkane dehalogenase was used in the free form, as a cross-linked enzyme aggregate (CLEA) and as a CLEA entrapped in PVA lenses (Lentikats®) [23]. Electron microscopy showed higher catalytic activities for CLEAs subjected to strong morphological changes induced by sonication, when compared to unsonicated CLEAs whereas the particle size of CLEAs did not show evidence of being determinant for the catalytic activity. Confocal microscopy to Lentikats® revealed that the catalytic activity was affected by other factors besides the biocatalyst loading, namely the pore size as narrower pores resulted in higher activities for CLEAs than for the free enzyme [23]. These observations illustrate the usefulness of microscopic techniques to gather information regarding the events that occur during immobilization, as well as their potential to be applied in optimization procedures.

Mode of attachment

The modes of attachment between the enzyme and the support can be classified in reversible and irreversible. Reversibly immobilized enzymes can be detached from the support by changing the conditions that influence the strength of the interaction (e.g. pH, ionic strength, temperature, or polarity), whereas irreversibly immobilized enzymes cannot be detached without destroying either the support or the activity

of the enzyme [24]. Reversible methods are very attractive especially due to economic reasons, this because if the enzymatic activity becomes corrupted, the support can be regenerated and re-immobilized with new enzyme. This kind of immobilization is thus of particular interest for labile enzymes.

The strength of the binding is usually inversely related to the ease with which it can be reversed, thus enzymes can be attached to the support via interactions ranging from reversible physical adsorption and ionic linkages to stable covalent bonds [8]. The most common procedures of irreversible enzyme immobilization are entrapment in organic or inorganic polymer matrices, covalent binding to prefabricated supports and cross linking of enzyme molecules [6].

An equilibrium between the reversibility of the binding and its stability is often difficult to fulfil, and generally the stability, through strong bonds, is preferred over reversibility [8].

1.2.1. Entrapment

Enzyme entrapment (Figure 3) is based on the occlusion of an enzyme within a polymeric network, such as an organic polymer or sol-gel matrix, that allows the substrate and products to pass through while it retains the enzyme [6], [8]. This method of immobilization occurs *in situ* as the enzyme is present during the synthesis of the polymeric network but it should be noted that the enzyme is not bound to the matrix or membrane [6]. By being retained, entrapment protects the enzyme from the direct contact with the environment, which in turn minimizes shear stress, gas bubbles and hydrophobic solvents effects. The major drawback is though the low enzyme loading and the intrinsic mass transfer limitations through membranes or gels [25]. Considering the way in which the enzyme is immobilized, entrapment does not have the best performance when it comes to prevent enzyme leakage, which makes covalent attachment often required (see Chapter 1.2.4.2) [6].

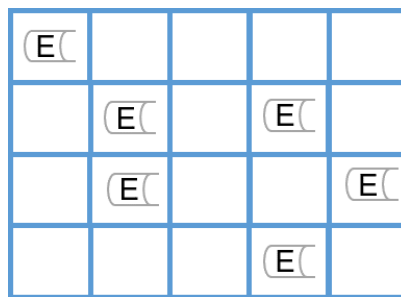


Figure 3 – Schematic representation of immobilization by entrapment. During the formation of the polymeric network (represented by the blue lines), the enzyme (E) is retained. The catalytic reaction occurs due to the ability of substrates and products to pass through it.

Among the different entrapping approaches are gels, fibers and micro-encapsulation [25].

The natural polysaccharide sodium alginate is a very simple and widely-known method of entrapment. Generally, the alginate is mixed with the biocatalyst solution and dropped into a calcium chloride solution in which water-insoluble alginate gel beads are formed (Figure 4) [26]. Carrageenan is also a natural polysaccharide used in a similar way: a saline mixture of carrageenan, together with the biocatalyst is dropped into a gelling reagent (potassium chloride, ammonium, calcium or aluminum cations) [5]. The gel can be hardened by glutaraldehyde or other cross-linking agent, often enhancing biocatalyst stability [5].

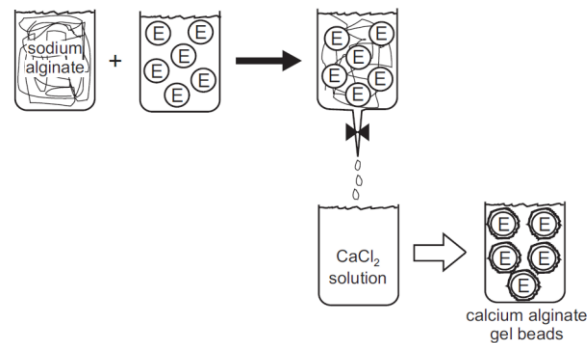


Figure 4 – Formation of calcium alginate gel beads by dripping of the solution into CaCl₂ (source: [5]).

Regarding synthetic immobilization methods, polyacrylamide gels are also very used. In this approach the biocatalyst, acrylamide and a cross linker agent are mixed together with an initiator and a stimulator to promote the polymerization reaction [5].

Mesoporous silica has great advantages such as its high surface area, uniform pore distribution, tunable pore size [27] and high adsorption capacity [28], [29]. In fact, a recent breakthrough regarding the stable entrapment and release of enzymes on demand was based on the use of this support together with β -glucosidase as a model enzyme. In the work developed by Zlateski *et al.* the immobilized enzyme was further entrapped within the pores of the support to increase its stability and prevent enzyme leaching. To do so, additional silica was grown amorphously inside the pores, leading to a decay of > 80% on the enzyme activity [30]. Afterwards, the release scheme was promoted by the use of fluoride-containing buffers to dissolve both the silica from the inside of the pores as well as from the support structure. Ultimately the entrapped enzyme showed to be unreactive but highly stable towards heat and its activity boosted from unreactive to values comparable to those of the free form upon release [30]. The method showed not only improved operational, storage and heat stability but mainly the potential of using the triggered release of the enzymes for storage purposes.

Recently great developments have been observed with hydrogels, due to its applicability to enzyme immobilization. PVA is a hydrophilic synthetic polymer frequently used as a biomaterial given its natural polymer-like biocompatibility. PVA-based gels are permeable, non-degradable and have high mechanical stability. Ultimately, their properties can be further improved by cross-linking with boric acid or sodium sulfate [31]. The immobilization method consists in mixing the biocatalyst with the PVA solution and then promoting

its gelification by freezing and thawing [32] or UV light [33]. Other approaches rely in its extrusion to solutions such as polyethers (polyethylene glycol (PEG) or polypropylene glycol), where the gelification occurs instantly, forming small flexible beads of tunable diameter (e.g. 3–4 mm) and hemispherical-like shape [34] with low diffusion limitations (thickness of 200–400 µm) [35]. Therefore, this approach is advantageous for industrial process application due to its relative inexpensiveness, easiness of preparation, adaptableness to stirred tank reactors and easiness of downstream processing for biocatalyst recover.

Additives such as PEG or PVA can have stabilizing effects on these sol-gel entrapped enzymes. A study concerning the effect of PVA in entrapment showed that physical properties, such as the hardness and surface area, of the sol-gel can be greatly influenced by the PVA content [36]. As for PEG, *Candida rugose* immobilized-lipase activity in the hydrolysis of olive oil was studied in the presence and absence of PEG 1450, and the results showed that the most active biocatalyst was in the presence of PEG [37].

PVA gels are also used as cell immobilization matrices, proving their mechanical resistance to abrasion, stabilizing effects over wide pH ranges and conferring low mass transfer resistances to the system, when compared to natural polysaccharide alginate, for example [38].

In order to bypass the problems associated with the large scale production of (R)-cyanohydrins by (R)-oxynitrilases, mainly catalyst leaching and long-term stability, Vorlop *et al.* developed a 2-step method based on the cross-link of the enzyme prior to its entrapment in PVA. This method showed to have negligible catalyst leaching and diffusion, long-term stability, high activities and great recycling abilities, as it was reused 20 times without loss of the enzymatic activity [39].

1.2.2. Encapsulation

Encapsulation (Figure 5) is a very similar method to entrapment, being even difficult to distinguish sometimes. Encapsulation also protects the enzyme from the external environment and its application in large scale process is often limited by their mass transfer limitations [25]. Nonetheless, efficient encapsulation has been achieved with alginate–gelatin–calcium hybrid carriers that provided great mechanical stability and significantly prevented enzyme leakage [40].

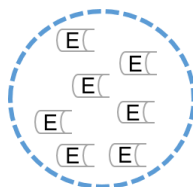


Figure 5 – Schematic representation of enzyme (E) encapsulation.

1.2.3. Support based immobilization

The performance of supported enzyme preparations is dependent both on the properties of the enzyme and the carrier material. It is the interaction between them that governs the system's (bio)chemical, mechanical and kinetic properties [6]. Immobilization to a prefabricated support, such as a synthetic organic polymer, a biopolymer or an inorganic solid, can provide rigidity [11]. However the use of a carrier is associated with dilution of the volumetric activity, caused by the introduction of a large portion of non-catalytic bulk which can account for 90–99% of the mass or volume of the catalyst [6], [11], [25]. This results in lower yields and productivities.

As previously stated, the design of the system is one of the most, if not the most, important factor to consider as it can compromise the entire process. Regardless of the laborious and time-consuming process, this is especially important in carrier-bound design as it often leads to activity losses in the order of 50% or more [6]. This is one of the main driving forces towards the development of carrier-free systems, as it will be opportunistically discussed.

Support binding can be of physical (hydrophobic and van der Waals interactions), ionic or covalent nature. A variety of supports have been used ranging from biopolymers (water-insoluble polysaccharides such as cellulose, starch, agarose and chitosan and proteins such as gelatin and albumin) to inorganic solids (alumina, silica, zeolites and mesoporous silicas) [6].

1.2.3.1. Adsorption

Enzyme immobilization on solid carriers can be achieved using a broad variety of chemical and physical methods. Among them is the fastest and most universal method: immobilization by adsorption (Figure 6). In physical adsorption the attachment of the enzymes to the matrix is mainly through hydrogen bonding, ionic interactions and van der Waals forces [8], [41]. This simple and inexpensive method usually preserves the catalytic activity of the enzyme as little or no conformational changes occur in the active center [11]. However enzyme leakage is a problem, especially in aqueous solvents, as the physical bonding is generally too weak to keep the enzyme fixed under conditions of high reactant and product concentrations and high ionic strength [6], [11]. This can be a problem upon process and downstream processing design.

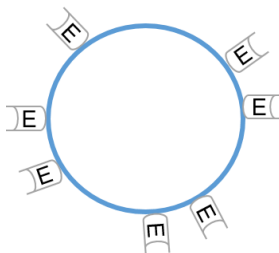


Figure 6 – Schematic representation of support-based immobilization through adsorption.

The adsorption of the enzyme towards the carrier is dependent on the affinity between them, thus to achieve a successful immobilization the existence of specific functional groups on the surface of both the enzyme and the carrier has to be assured [41]. Interesting methods based on the use of mono- and polyclonal antibodies for the specific and coupled immobilization and purification of proteins have been discussed [42]. However high affinity antibodies are often not desired because of the need to use drastic conditions to promote desorption of the enzyme [42].

The carrier criteria of choice regards to cost, availability, stability and the type of reactor in sight. In general the non-soluble carriers used can be divided into organic and inorganic origin. Chitin, chitosan, cellulose and alginate, all already mentioned, are of organic origin and provide the great advantage of being readily modified to match the conditions for a given enzyme [41].

Taking the *Yarrowia lipolytica* lipase as an example, its immobilization on octyl-agarose and octadecyl-Sepabeads® supports by physical adsorption resulted in higher yields and in a 10-fold increase in stability over that of free lipase. Such observation was accounted to the hydrophobicity of the octadecyl-Sepabeads® that enhanced the affinity between the enzyme and the support [43].

In a recent work, this immobilization method was tested for the immobilization of various lipases and phospholipases in octyl-glutamic [44] and octyl-amino [45] agarose beads. These heterofunctional supports were designed specifically to prevent enzyme desorption whilst keeping the immobilization reversible, contrary to previous attempts with octyl-glyoxyl agarose beads [46]. The introduction of glutamic acid and amino groups (ethylenediamine and hexylenediamine) in octyl-agarose permitted the establishment of ionic bonds responsible for assuring the enzyme adsorption to the support in case of suppression of the hydrophobic adsorption (e.g. addition of non-ionic or organic detergents). In both cases it was first guaranteed that the enzyme was immobilized via interfacial activation and only then the establishment of ionic bridges was allowed. Heterofunctional supports for the later multipoint or multisubunit immobilization of enzymes have also been applied to lipases [42]. Overall these mixed adsorption methods showed complex effects on the stability of the enzymes, as they showed to be very enzyme-dependent (for instance, only one lipase and one phospholipase showed clear advantages in terms of stability upon immobilization in octyl-amino supports [45]). At the end, the supports were prone to be regenerated and reused after enzyme inactivation through a washing step with ionic detergents or guanidine [44]. Adsorption is thus an (economically) attractive method in large scale processes where the enzymes in use are inexpensive [25].

1.2.3.2. *Ionic binding*

Within the reversible non-covalent immobilization techniques there is yet ionic binding. In ionic bonding the enzymes are bound through salt linkages, being this kind of interaction generally stronger than the ones previously mentioned [6], [8].

This simple and reversible method struggles with the optimal conditions under which the enzyme remains fully active and strongly bound [8]. Besides, more challenges may arise from the use of a highly charged

support as well as charged substrates or products. As the optimum pH and stability may change, so can the reaction kinetics due to diffusion or partition phenomena.

Regarding the types of supports used, polysaccharide biopolymers such as dextran, agarose and chitosan are among the most used [11]. These supports can be functionalized with a variety of chemical groups (e.g. quaternary ammonium, diethylaminoethyl and carboxymethyl derivatives) to achieve proper ionic interaction [11].

Indeed, an aminoacylase from *Aspergillus oryzae* was used in the Tanabe process for the production of L-amino acids by resolution of racemic acyl amino acids. Aminoacylase was immobilized on DEAE-Sephadex, which consists of cellulose modified with diethylaminoethyl functionalities [6]. On the other hand, there are other functionalized resins for ionic binding such as the macroporous acrylic polymer Amberlite FPC3500 (cationic) or FPA54 (anionic) [11].

1.2.3.3. Covalent binding

Among the most popular methods of immobilization are the ones based on the formation of covalent bonds, which are of special interest when there is a requirement to obtain an enzyme-free product [8]. Due to the nature of the interaction, covalent immobilization shows the strongest bonding between the enzyme and the support, moreover it benefits from the fact that the enzyme is not leached from the surface upon use [6], [8]. Meanwhile, this feature can also be a disadvantage because if the enzyme becomes irreversibly deactivated, both the enzyme and the support become unviable [6], [8]. Generally, the amino acid residues that are not involved in the active site or in the substrate-binding site of the enzyme, are the ones used to form the covalent bond with carriers [5] (Figure 7).

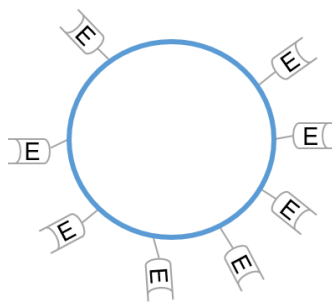


Figure 7 – Schematic representation of covalent binding in support-based immobilization.

Properties such as catalytic activity or thermal stability can become altered upon immobilization [25]. In order to have high activities it is thus extremely important that the amino acids with a role in the enzyme's catalytic activity do not bind the support, which can be difficult to fulfill in some cases [8]. There are some methods available to obviate this problem.

Coupling methods can be divided into the ones that focus on the activation of the matrix by addition of an agent such as cyanogen bromide, and the ones that modify the polymer backbone to produce an activated group (e.g. spacers with epoxy groups) [8] (Figure 8).

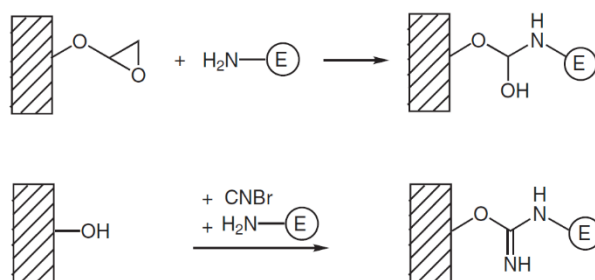


Figure 8 – Examples of carrier coupling using an amino group of the enzyme. In the first case the matrix is pre-activated with epoxy groups. In the bottom, the matrix is activated with cyanogen bromide. (source: [5])

The biocatalyst is thus attached to a support through the hydroxyl or amino groups in the side chains of amino acids like arginine, aspartic acid (carboxylic group) and cysteine (thiol group) [5], [9]. Lysine is also very used through its above-average-reactivity ϵ -amino group, which acts as the point of covalent attachment, providing good bond stability [47]. The degree of reactivity with which this reaction occurs is thus based on different functional groups, giving rise to binding through amide, ether, thio-ether, or carbamate bonds [8], [9]. In order to improve the immobilization and decrease steric hindrance effects, spacer arms can be used. Epoxide groups are of special interest due to their stability and capacity to react with amino acids even under mild conditions, plus they can readily bind lysine [11]. It is often good practice to quench the residual groups, after immobilization, with a primary amine to avoid non-specific interactions [47].

Covalent coupling can rely on the use of synthetic resins, biopolymers or inorganic polymers for support [6]. In polymers such as mesoporous silica and chitosan there is evidence of increased half-life and thermal stability [28].

Several improvements have been being done to enhance enzyme binding. For that, supports with multiple reactive functional groups were developed to, for example, specifically include amine groups [11]. The reason for this is that amine groups can ionically bind with protein carboxylic acids and thus, as the proximity is bigger, improve the covalent bond between the lysine residues and the epoxide groups [11]. Besides amine groups, resin epoxide groups can also be combined with thiol groups to bind cysteine residues [11].

Penicillin G acylase (PGA) has a very important role in the pharmaceutical industry, namely in the synthesis of precursors for β -lactamic antibiotics. Epoxy acrylic carriers (e.g. Sepabeads®) have shown great performances in industry due to their simple immobilization procedure, where the nucleophilic groups mainly of lysine residues covalently bind the epoxy groups of the carrier, however PGA immobilization struggles with these supports as the reaction performance is negatively affected [48]. To improve this reaction

aldehyde-based spacers were introduced in the carrier, through glutaraldehyde activation, and the results showed a 3-fold increase in the reaction rate against the reaction in the unmodified support [48]. These spacers have thus highlighted the importance that increasing the distance between the enzyme and the carrier has in obviating diffusion limitations.

A similar approach was followed by Basso and coworkers, which found a series of lysine residues on the surface of an endoinulinase from *Bacillus stearothermophilus* and an exoinulinase from *A. niger* that were not involved with the active site. The inulinases were covalently immobilized to amino – where a pre-activation with glutaraldehyde was necessary – and epoxy – where the immobilization relied in the excellent reactivity between these groups and the ϵ -amino group of the lysine residues – Sepabeads® [49]. In both cases the immobilization efficiency and the activity registered were very high, suggesting that the procedure optimized the enzyme orientation and conformation, which facilitated the access of inulin to the active site as well as the product release, observations that are not that recurrent in immobilization procedures [49].

1.2.3.4. *Site-directed covalent immobilization*

Through the last chapters some problems (e.g. leaching, enzyme stability, recoverability and reusability, etc.) regarding the immobilization techniques discussed herein have been highlighted. Indeed, part of these have been solved by recent breakthroughs in enzyme immobilization which even made some processes more affordable. Nonetheless many were not solved as they concerned one very specific issue: the enzyme orientation.

Studies focused on controlling the orientation of immobilized enzymes, by exploring specific interactions, revealed greater stabilities (by 50% or even 73%) when compared to their nonspecific counterpart [7]. This is especially important for long-term reuse and economic viability of processes. More, the position of certain amino acid residues can also affect the enzyme orientation, as it was described for nitroreductase cysteine residues [50].

Regarding the orientation and selectivity of the immobilization procedure, engineered approaches based on fusion proteins and derivatized supports have also been tested. The enzyme D-amino acid oxidase was fused with a cationic binding module and further immobilized onto a negatively charged acid-derivatized mesoporous glass [51]. This approach assured a selective immobilization due to its positive charge at pH 7, while all of the other proteins had mainly a negative charge. As for the orientation, the charge asymmetry in the cationic module influenced the immobilization in a way that only the positively charged module interacted with the support, leaving the enzyme available to react [51]. The main advantage with this approach is the fact that the binding of the fusion protein to the support is reversible under high salt conditions, and thus the support can be used repeatedly [51]. The potential to eliminate intermediate purification processes also constitutes a very attractive advantage.

1.2.4. Cross linking

One simple and popular way of immobilization is through covalent immobilization with bi- or multifunctional reagents (Figure 9) [5]. Nevertheless, these cross linking reagents must not modify the structural nor the functional properties of the enzymes during immobilization [9].

Glutaraldehyde is the mostly widely used bifunctional cross-linker reagent, though others can be used, due to its ability to form stable inter and intra covalent bonds between subunits [5], [9]. Its inexpensiveness and availability are also an important factor for its widespread use [6].

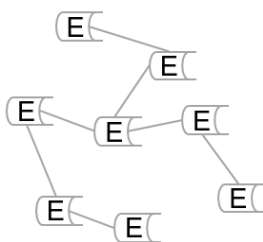
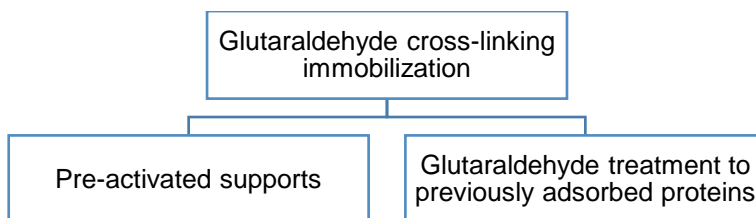


Figure 9 – Schematic representation of enzyme immobilization by cross linking.

1.2.4.1. Glutaraldehyde

Similar to the covalent immobilization discussed in Chapter 1.2.3.3, cross-linking immobilization via glutaraldehyde can also follow different approaches.



Relatively to the immobilization, both the use of pre-activated supports and the glutaraldehyde treatment to previously adsorbed proteins on supports with primary amino groups follows an analogous mechanism. However, with pre-activated supports the chemical modifications only occur to the groups involved in the immobilization, while a glutaraldehyde treatment *a posteriori* may change the whole enzyme surface [52].

Glutaraldehyde is a very reactive agent of a small size which can access even the more internal regions of proteins, thus it is not uncommon for glutaraldehyde to cause the enzymes to lose their activity [6]. This can happen if important amino acids involved in the catalysis become cross-linked. Similarly to covalent attachment, the immobilization of proteins with few lysine residues may be more difficult and the introduction of reagents to provide amino groups (e.g. poly-lysine or polyethyleneimine) can be employed to partially solve the problem [6].

Enzymes like glutaryl acylase (GAC), D-aminoacid oxidase (DAAO) and glucose oxidase (GOX) were immobilized on glutaraldehyde pre-activated supports (MANAE-glut) and non-activated supports (MANAE-agarose) where the enzyme was then treated with glutaraldehyde to allow for the covalent attachment to the support [52]. The activity was measured for the various enzymes and while GAC kept 100% of the activity in both supports, GOX and DAAO decreased their activities from 100% in MANAE-agarose to 80% and 40% in MANAE-glut, respectively [52]. Regarding stability, it was also observed that glutaraldehyde treatment to adsorbed proteins had better results than with pre-activated supports [52]. Nevertheless, both immobilization methods showed better performances than with just adsorbed enzymes.

1.2.4.2. *Self-immobilization*

It has already been mentioned (Chapter 1.2.3) that solid supports for enzyme immobilization may reduce the catalyst's volumetric and specific activity. This factor has been leading to an increasing interest in carrier-free immobilized enzymes, such as cross-linked enzyme crystals (CLECs) and cross-linked enzyme aggregates (CLEAs), where activities of 10 to 1000 times relatively to the biocatalyst immobilized in a support have been reported [53]. Similarly to cross linking, carrier-free immobilization can also rely on the use of bifunctional agents, such as glutaraldehyde, to bind enzymes to each other [11], [53]. CLEAs and CLECs have been found to be especially powerful for catalysis in organic media [54], [55].

Cross-linked enzyme aggregates (CLEA)

Immobilization through CLEA relies on the fact that when aqueous protein solutions are added together with salts, organic solvents or non-ionic polymers, the proteins tend to aggregate and precipitate [6], [9], [56]. The further cross-link of these aggregates makes them permanently insoluble. The non-covalent nature of the bonds in these aggregates allows the retention of the tertiary structure without denaturation and the catalytic activity is preserved [6]. Just as protein precipitation (e.g. ammonium sulfate or polyethylene glycol) is often used for purification purposes, CLEA have the double advantage of being applied both to immobilization and purification of enzymes [6].

The main advantages related with CLEA focus on their easy preparation from crude enzyme extracts, more concentrated enzymatic activity, tunable particle size, negligible diffusional limitations, higher operational and storage stability and lower associated costs due to the absence of a carrier [11], [56]. The application of CLEA to industrial scale bioprocessing seems like an attractive option due to their high activities, yields and stabilities, even at high temperatures, but the method still struggles with aspects of mechanical strength and recoverability from the medium in which they are [6].

One way to bypass this limitation is through the encapsulation (see Chapter 1.2.1 and 1.2.2) of the CLEA. This approach was tested for the encapsulation of PGA CLEA into PVA beads (Lentikats®) and, even though the CLEA activity decreased by 40% upon encapsulation, the mechanical properties of the CLEA as well as the stability in the presence of organic solvents were improved [57].

Cross-linked enzyme crystals (CLEC)

In protein crystals, enzymes are close to each other. When these crystals are cross-linked they result in CLEC, biocatalysts of increased physical strength [11]. As part of the crystallization to which enzymes are subjected, they exhibit controllable particle size (from 1 up to 100 μm) [53], [56].

Contrary to CLEA, CLEC are suitable for industrial bioprocessing due to their high operational stability in harsh conditions, ease of recycling and high volumetric productivities [11], [53]. However the major drawback relies precisely in the laborious and costly crystallization process, as highly purified enzymes are required, which ultimately contributes highly to the economic viability of the process [11], [58].

1.3. Inulin hydrolysis for fructose production

An increasing interest is being given to fructose production through inulin enzymatic hydrolysis in terms of the best operating conditions, substrate and enzyme origin as well as immobilization techniques [59]. The influence of reaction kinetics and deactivation rates is also crucial to further improve the reaction.

1.3.1. Fructose production

Fructose ($\text{C}_6\text{H}_{12}\text{O}_6$) is known to be the sweetest natural sugar. It has two enantiomers, D-fructose and L-fructose, being the latter not found in nature [60], [61]. Due to its sweetness, reported to be 1.3 to 2.0 times that of sucrose [62], fructose is emerging in the world of low caloric sweeteners facing the competition with sucrose, which causes problems related to corpulence, cariogenicity, arteriosclerosis and diabetes [61], [63].

The demand for fructose syrups has been increasing over the years, however its high cost has revealed to be limitative to its commercial diffusion [60]. As fructose does not cause any disturbances in the metabolic balance of diabetics and is free of other side effects linked with sucrose metabolism in humans [61], [62], it would be of high relevance to develop a low cost process for its production. This would also be important from an economic point of view, since a process that uses sucrose can be ran similarly through the use of a smaller quantity of fructose.

Nowadays, fructose is being obtained by sucrose inversion thanks to the enzyme invertase or from hydrolyzed corn starch, in which the hydrolysate, previously treated with α -amylase and glucoamylase, is then isomerized by glucose isomerase [24], [60], [61], [64], [65]. The latter is the main process used in industry today, but is characterized by a strong thermodynamic limitation as the values of the equilibrium concentrations of fructose and glucose are around 50% [65]. In fact, the final sugar syrup obtained from this reaction yields a mixture of about 42% fructose, 50% glucose and 8% oligosaccharides [60], [61], [64]. The

subsequent concentration of fructose syrups is carried out by column chromatography techniques, which can be costly to operate [60], [64], [66].

An attractive way of reducing the costs associated with the production of fructose is by changing the raw material. Thus, materials naturally rich in fructans, or inulin, are a promising bet. Inulin solutions are not naturally sweet, but if the polymer is converted to D-fructose monomers, it can be used as a sweetener [61].

Fructose can be obtained by acid hydrolysis of inulin (sulfuric, hydrochloric, phosphoric, citric, oxalic, and tartaric acids have been used to catalyze this reaction, at pH values of 1–2, and 80–100°C for 1–2 h) [60], [62], [66]. However this process did not achieve great developments as low pH promotes fructose degradation and product contamination with difructose dianhydrides, which will have additional costs regarding its recover in ion exchange resins from the final solution [61], [63]–[66].

A different approach for fructose production relies in the enzymatic hydrolysis of inulin. This reaction is catalyzed by the enzyme inulinase and it has been shown to be a promising process as one enzymatic step yields up to 95% pure fructose [64], [67]. This process is preferable due to higher specificity and lower by-product formation [65].

1.3.2. Inulin and inulinase

Inulin is a linear fructan-type polysaccharide consisting of β -2,1 linked D-fructofuranose molecules, attached to a terminal glucose molecule through a sucrose-type linkage at the reducing end (Figure 10) [17], [64], [65], [68].

Inulin occurs as an energy reserve in various plants and can be found in Jerusalem artichoke, dahlia, chicory, garlic, asparagus root and salsify [17], [65], [69]. The degrees of polymerization (DP) and branching depend on the polymer's origin. In vegetable origin inulin, the number of fructose units linked to a terminal glucose can vary from few units to about 70, meaning that inulin is a mixture of oligomers and polymers [60]. Commercially available inulin, derived from these sources, has an average DP of about 27–29. On the other hand, bacterial inulin has DPs ranging from 10 000 to 100 000 [60].

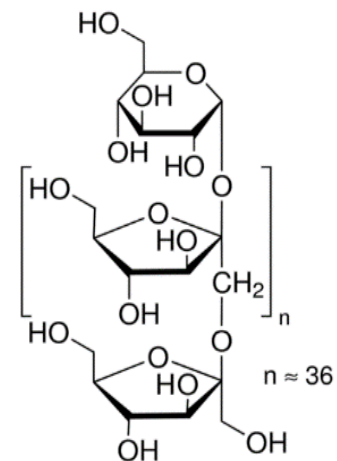


Figure 10 – Inulin structure.

Pure inulin is almost insoluble in cold water, but it can be easily dissolved in hot water. In plants, part of the inulin is present as fructose polymers with lower chain length, which are more soluble. These polymers have higher glucose contents (5-15%) when compared with pure inulin (3%) [65].

Most of inulin applications are directly related with its DP. Oligofructose and other short chain inulins are widely used in the food industry as low-calorie sweeteners, fat replacers or texture modifiers while longer chain inulins are more useful in the pharmaceutical industry [70], [71]. Due to its glycosidic bond this

carbohydrate cannot be digested by human digestive enzymes, yet it can be used as an effective prebiotic to stimulate the growth and activity of beneficial bacteria in the digestive tract [72]. Inulin may enhance the growth of probiotics (*Bifidobacterium*, *L. casei*, *L. plantarum*), inhibit the growth of harmful bacteria such as *E. coli* and *Clostridia* [68], [73] and be used as a means for strategic drug release [74].

Inulinases can have two distinct actions on inulin molecules. The enzyme that hydrolyses β -1,2-fructan links in inulin is commonly referred to as endo-inulinase or β -1,2-fructan fructanohydrolase (E.C. 3.2.1.7) [60]. An endo-inulinase has an internal action on those linkages, yielding a series of oligosaccharides (mainly inulotriose, inulotetraose and inulopentaose) of special interest for the food and pharmaceutical industry [75], [76]. In the case of an exo-inulinase, or β -D-fructan fructanohydrolase (E.C. 3.2.1.80), there is an endwise action that separates the first D-fructose molecule and proceeds until the last linkage within inulin is broken and D-glucose is released as a minor product [75].

Despite the fact that these two inulinases showed similar properties, it has been shown that a mixture of both can achieve better inulin conversions to fructose than the pure endo or exo enzyme [65]. Such observation may be due to the amplified action when combined, i.e. as endo-inulinases break inulin into many oligosaccharides, the attack points for exo-inulinase are increased, which ultimately increases the reaction rate of inulin hydrolysis. The activities of pure endo or exo-inulinase were studied and compared to a mixture of both. Higher activities were observed in the mixture than by summing the other two, regardless of inulin concentration [77].

When syrups with high fructose content are aimed, a synergetic action of exo- and endo-inulinase is explored to achieve total inulin hydrolysis [78]. On the other hand, partial hydrolysis by exo-inulinase is used to produce short chain fructans, such as oligofructose, used as a functional sweetener [69].

Several inulinases have been described as originating either from plant material such as inulin-containing roots and tubers or from microorganisms, comprehending bacteria, fungi and yeast [17], [65]. Previous works indicate that the most commonly employed microorganisms are fungal strains belonging to *Aspergillus* sp., *Penicillium* and *Fusarium* [65], [79] and yeast strains belonging to *Kluyveromyces* sp. [63], [80].

Plant sources are not as productive as the microbial ones, which seem to be the most capable of satisfying industrial requirements [66], though bacteria do not show an inulinase yield comparable to that of filamentous fungi and yeasts [60]. Nonetheless, bacteria's thermophilic nature could turn out to be a great advantage in this context where higher temperatures are used in the fermentation and also allow for a higher substrate solubility [80]. Several improvements have been made to develop the best microbial source with the best properties and highest yields. A list of microorganisms used for the production of inulinases can be found elsewhere [60].

Inulinases often show a certain activity towards β -2,6-fructan links, meaning that they can also hydrolyze sucrose into fructose and glucose [60]. Sucrose hydrolytic enzymes are called invertases (E.C. 3.2.1.26; β -

D-fructo-furanoside-fructo-hydrolase) [60]. Both inulinase and invertase belong to β -fructosidases, still they can be distinguished based on the ratio (α) of their activities (Equation 1).

$$\alpha = \frac{\text{Inulinase Activity}}{\text{Invertase Activity}} \quad \text{[Equation 1]}$$

Where $\alpha > 10^{-2}$ classifies the enzyme as an inulinase whereas $\alpha < 10^{-4}$ classifies it as an invertase [81]. A true inulinase or invertase behavior seldom exists, instead enzymes usually show a type of activity over the other. After inulinase action over inulin, it is desirable to hydrolyze the ultimate link between glucose and fructose through an inulinase with invertase activity [60]. In such case, the presence of sucrose can even be beneficial to improve the enzyme's yield. In cases where the enzyme has no invertase activity, sucrose presence can have inhibitory effects [63], [80].

Genetic engineering methods are already being applied to modify the inulinase genes in recombinant microorganisms to enhance the reaction's products [82]. Computational methods also have shown evidence of being powerful tools in the rational design of efficient biocatalysts and in the understanding of the enzyme-substrate interactions [49].

An extensive review on inulinase applications and inulin advantages in bioprocesses can be found elsewhere [76]. More thorough reviews on inulin's physicochemical properties, isolation and purification methods and biotechnological applications may also be consulted elsewhere [70], [71], [83].

1.3.3. Optimal reaction conditions

Many works have been being done regarding enzyme activity and stability. For that the effects of temperature and pH were studied, despite the fact that enzyme's response to these factors depends mainly on the source strain used for its production.

1.3.3.1. *pH, temperature and substrate concentration*

Inulin chemical stability at $\text{pH} \leq 4$ decreases with increased heating times and temperature, while in neutral and basic environment it is chemically stable regardless of pH, heating time and temperature [68]. Thus, its application in food systems may be limited in acidic products, especially when the process occurs at temperatures above 60°C.

Batch reactor performance with *Aspergillus* inulinase to evaluate temperature and pH influence showed that the hydrolysis degree (the sum of glucose and fructose relative to the total carbohydrate content) of 20% (w/w) inulin was maximum at 60°C and pH 4.5. Nonetheless at 65°C 95% of the enzyme maintained its activity [65].

Inulin concentration influence on the hydrolysis rate was also studied in said conditions for 24 hours. Results proved that the ideal substrate concentration should be >13% with an inulinase concentration of 2 units per gram of inulin. Hydrolysis of 98-99% were achieved in 48 hours [65]. Despite the fact that, from a kinetic point of view, high substrate concentrations determine high reaction rates, inulin concentrations higher than 13% no longer showed to affect the reaction rate, yet it is an important factor for enzyme stabilization [65]. Indeed, stored inulinase from *K. fragilis* in the presence of inulin (55°C, 4h) showed no activity loss whereas in the absence of inulin deactivation it was observed and only 20% of its maximum activity was retained in the same conditions [84].

Inulin batch hydrolysis of 1 mL of inulinase solution from *A. niger* in 49 mL of a 5% inulin solution, at 55°C and pH 4 for refined inulin (DP = 24) and chicory extract (DP = 8) showed lower hydrolysis degrees for the first, being the maximum (54%) achieved after 16 hours with the less refined chicory inulin [85]. This evidence seems to correlate with the properties of exo-inulinases, as the higher the DP the less available ends are within the mixture.

Similarly, in a study regarding inulin acid hydrolysis with different oligofructose samples, it was observed that for identical pH and temperature conditions, the fructose production rate was higher for the shorter oligomers than for the longer ones. This is due to the relatively high content of fructosyl ends available for bond cleavage in the smaller oligomers. [86]

The microbial enzymes reported so far have pH optima in the range of 3.5–5.5 and temperature optima between 45–55°C [65]. Optimal temperature values were generally higher for bacteria and yeasts than for fungi. Regarding pH, fungal inulinases tend to exhibit an optimum pH between 4.5 and 7.0, yeast inulinases between 4.4 and 6.5 and bacterial inulinases between 4.8 and 7.0 [80].

Besides the information on optimal temperatures and pH, information regarding a relative broad interval can be useful for a greater flexibility in operational conditions, especially when considering industrial processes where optimal temperature and pH are often not used. While the pH optima range seems to be very suitable, the enzymes may generally be considered as too temperature labile for industrial use [65], since industrial inulin hydrolysis is carried out at 60°C in order to prevent microbial contamination and also because it allows the use of higher inulin concentrations due to increased solubility [64].

1.3.3.2. *Kinetic parameters*

Kinetic properties of inulinases are highly dependent on enzyme and substrate origin, inulin DP, as its variation during the reaction does not allow a precise estimation of the kinetic parameters [85], as well as temperature. Studies with *A. ficuum* inulinase at 30, 40 and 50°C showed increasing K_M values of 3.52, 5.35 and 7.89 mM, respectively, and also confirmed the Michaelis-Menten behavior of the reaction [87]. Additional data regarding a thorough review on kinetic parameters and assay conditions can be found elsewhere [60].

1.3.3.3. Immobilized inulinase for fructose production

Immobilized enzymes are an attractive way to carry reactions of industrial relevance. These enzymes have different kinetic parameters, activities and stabilities when compared with the corresponding free form. The majority of the available data report immobilized inulinases in batch reactors [66], [67], [84] and continuous packed bed reactors (PBR) [24], [67], [78], [84].

Several supports have been used and evaluated for continuous use of immobilized enzyme for fructose production in packed bed column reactors. Tests in supports such as casein, chitin [66] and sodium alginate for free and immobilized inulinase, from *A. fuminatus*, led to optimum pH values of 5.5 and temperatures of 60°C [64]. Overall improved heat stability was observed and the immobilized enzyme retained 70% of its activity after 48 hours at 60°C [64]. As for the K_M , values for the various immobilized inulinases varied from 0.2 to 0.5 mM [64].

Immobilized inulinase from *A. ficuum* on chitin supports revealed that the optimal glutaraldehyde concentration was of 3%. The optimal pH of 4.5 and the optimum temperature of 60°C were similar to those obtained for the free enzyme. Non-surprisingly, the immobilized enzyme was more stable than the free form [67]. Using the same immobilization method at 40°C and inulinase on Jerusalem artichoke tuber juice in batch reactors for 4 hours led to a hydrolysis of 80% whereas 10 hours increased the hydrolysis to 90%. In the PBR process, under the same conditions, a hydrolysis of almost 90% was achieved after a residence time of 4.5 hours [67].

Similar experiments were made on chitin, casein and cellulose with *A. candidus* inulinase. Maximum immobilization yields (45.8%) and thermal stability (76% of inulinase activity was retained after 1h at 55°C) were obtained with cellulose supports. In all cases the best temperature to the immobilized form was 55°C against the 45°C of the free enzyme [66].

A. niger inulinase immobilization in PVA hydrogels for continuous and batch production has also been reported. Under continuous operation, a product yield of 75% was observed after 20 days, while in the batch reactor remained at 80% after 10 consecutive batch runs. Increased biocatalyst stability was observed when the immobilization was performed with 1% (v/v) of glutaraldehyde solution [88].

The optimal pH and temperature for a preparation of *A. niger* inulinases immobilized on Amberlite IRC-50 was 5.5 and 50°C, respectively. These optimal parameters were then estimated by a model which gave similar results (pH 5.2 and 54°C) [89]. In another approach, the same enzyme was immobilized in polyurethane foam also at pH 5.5 and 50°C to evaluate the stability of the enzyme. It was observed that the enzyme had a half-life of 48 days and maintained 49.4% of its initial activity for 42 days and 24 cycles [90].

A different approach was followed when the goal was to find the optimal conditions for inulin total hydrolysis at pH 5.0 in a PBR. Inulin solutions from 2.5 to 10% (w/v), temperatures between 30 and 60°C and flow

rates from 0.5 to 8.0 mL.min⁻¹ were studied. From a kinetic point of view it was expected to use higher temperatures since these allow for better solubility of inulin solutions. Complete hydrolysis was carried for 45 days at 40°C and only for 2 days at 60°C [78], in which the enzyme showed a half-life of 16 days.

A more hydrodynamic approach, also conducted in a PBR, aimed to assess the reactor's influence in the reaction. Thus, while all of the other conditions remained unchanged, several H/D ratios (3.9, 10.3 and 21.3) were tested and the best performance was observed for H/D of 10.3. Aminoethylcellulose-immobilized inulinase from *K. fragilis* acting on a 7% inulin solution led to almost full conversion in 6 hours at 40°C. Enzyme half-life was about 14 days [84].

1.4. Process scaling

In bioprocessing engineering it is of the uppermost importance to scale the laboratory-bench or pilot scale process to achieve large-scale production levels. A reaction scale up involves considerations both from a scientific point of view, on the reaction performance, as well as from an engineering perspective, regarding the reactor design and its physical properties. For this, it is essential to assure that the product properties and the reaction itself are the same regardless of the scale in which it occurs. To keep in mind that the scale up of a system depends heavily on the type of reaction under study and that the physical factors of the system such as the mixing, power consumption, mass transfer, heat transfer and/or the rheology cannot be considered as one but rather as a commitment between all [91].

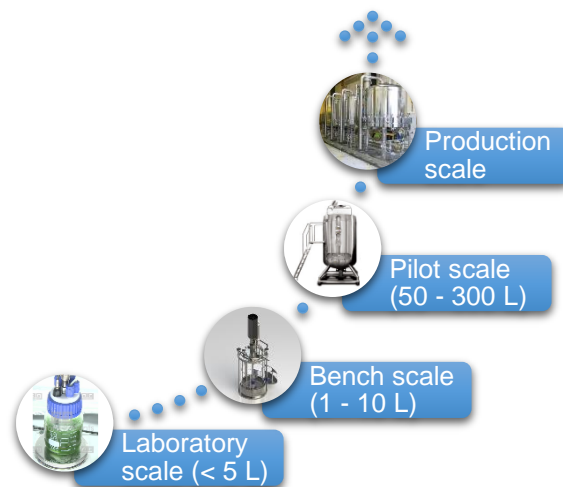


Figure 11 – Scale up approach based on the most conventional methods of gradually increasing the reactor's scale. Typical approaches are based on rules of thumb, practices and correlations such as the 1:10 scale up ratio [92].

1.4.1. Mechanical agitation and size scaling

Regarding the mechanical agitation, the scale up cannot simply be based on an increase of the impeller size and/or speed. Instead, a commitment between the stirring speed necessary for an efficient mixing has to be balanced together with the amount of shear stress that does not compromise the system. The implementation of one or more impellers, their configuration and distance between each other should also be analyzed. In aerated systems additional considerations must be taken since the scale up is mainly based on oxygen transfer rates (OTR), as mass transfer resistance from the gas to the liquid phase is often found to limit the productivity [92], [93]. The following subchapters focus only on the scaling of non-aerated systems, therefore the main aspects and considerations regarding the scale up of aerated bioreactors should be consulted elsewhere [92], [94].

Geometric similarity

When considering geometric similarity to upscale, it is considered that the ratio between the large scale and the small scale is applied in every length dimension and that all of the lengths in the large scale can be obtained by multiplying the small scale by such ratio or factor (Equation 2) [95]. When increasing the reaction scale by means of increasing the reactor size, it has to be noted that the geometric shapes of the remaining components of the system (e.g. bottom, impeller number and type, baffles) must be proportionally kept the same.

$$R = \frac{D_2}{D_1} = \frac{T_2}{T_1} = \frac{Z_2}{Z_1} \quad \text{[Equation 2]}$$

Where D is the agitator diameter, T is the vessel diameter and Z is the liquid column height in the vessel.

Rotational speed

In mechanically stirred vessels, under turbulent regime, the rotational speed necessary in the large scale system is related to the small scale system through Equation 3.

$$N_{i,1} = N_{i,2} \left(\frac{1}{R}\right)^n \quad \text{[Equation 3]}$$

Where N_i refers to the rotational speed (rpm), R to the previously calculated dimensionless ratio and n to the scale up factor.

If the criteria is to keep the Froude number constant, then n equals 1, which also ensures a constant tip speed of the agitator. If, on the other hand, it is chosen to keep constant the Reynolds number, then n will be 2. This criteria is often used when hydrodynamic similarity between both scales is desired [95]. When considering equal solid suspensions, n assumes the value of 0.75.

The Reynolds number (Re) is a dimensionless number that characterizes the turbulence of a fluid, representing the ratio of inertial to viscous forces. In the case of microfluidic devices its value is usually low

($Re < 100$), meaning that the viscous forces are dominating and thus, laminar flows are obtained [96]. In the case of turbulent regimes, as usually desired in large cylindrical-shaped reactors, the convective forces are dominant over the viscous forces and $Re > 2000$ [97]. The Reynolds number for stirred tank reactors can be calculated through Equation 4.

$$Re = \frac{\rho N d^2}{\mu} \quad \text{[Equation 4]}$$

Where ρ is the fluid density ($\text{kg}\cdot\text{m}^{-3}$), N is the mixing frequency (1/s), d is the maximum internal diameter of the shaking vessel or the stirrer diameter (m) and μ is the fluid viscosity (Pa.s).

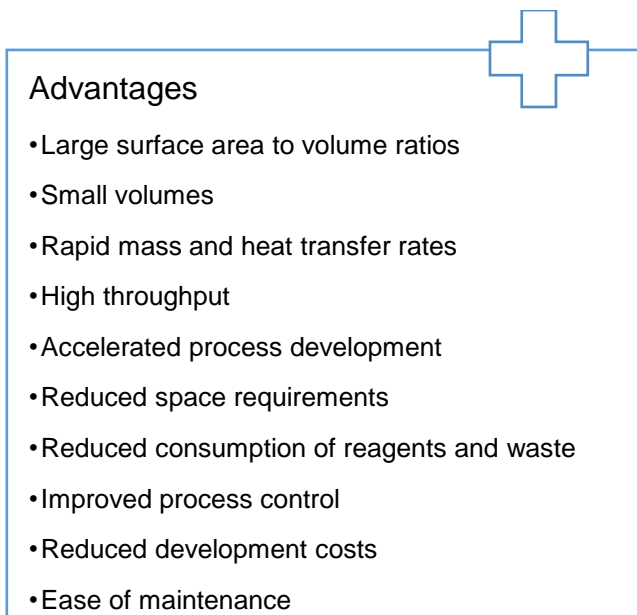
Heat transfer

During the course of a reaction, there is an inevitable amount of heat produced by the reaction and the stirring system that needs to be removed. However, when the reactor volume increases, the surface area available for such heat transfer decreases [5]. Consequently, to dissipate the same amount of heat that has been introduced into the system, the heat transfer rate must be increased in proportion to the vessel size. For that, strategies concerning the material of the cooling system and the design of the cooling system itself (e.g. cooling jacket, internal coils) have to be analyzed in order to define the best method.

1.5. Miniaturized systems

In the past few years, the use of miniaturized devices in bioprocess development has shown numerous advantages when compared to the traditional batch technology. One of the main goals associated with miniaturization is the need to develop cheaper, faster and more efficient reaction systems (i.e. with smaller requirements of raw materials and other utilities) [98]. Yet, the goal is not only to achieve better biotransformation results but also to increase its throughput and reproducibility.

Miniaturization is contributing to the reduction of the waste production and raw materials used as well, leading to the development of more environmental-friendly projects [99]. The main advantages of this emerging technology are presented below [6], [96], [99]–[101].



Miniaturization englobes mainly two types of systems: multi-well plates and microfluidic devices [99].

1.5.1. Microtiter plates

Microtiter plates (MTP) are miniaturized systems that consist in a flat platform with multiple wells that can be used as “small parallelized reactors”, which can be interpreted as miniaturized shake flasks of small volumes (nL – mL) [102]. These MTP are available in a wide range of well number, geometries and volumes, depending on the manufacturer and the purposes of the researcher (Figure 12).

Among the advantages of using MTP are the easiness in the handling procedures, the multiplex capacity to test different conditions in a single run and the economic gains from using small volumes of reagents. The main disadvantages of MTP however rely on plate-to-plate variability, bowl and edge effects resulting from the intrinsic variations between the inner and outer wells [103] and physical effects, such as the increased surface tension forces acting on the fluids. Indeed there are reports describing differences of up to 1.6°C between outer and inner wells, the effect of thermal gradients in absorption values [104] as well as the influence of evaporation [103]. These examples are one of the main reasons why not using the outer wells of the MTP is a good laboratory practice to bypass experimental noise [103].

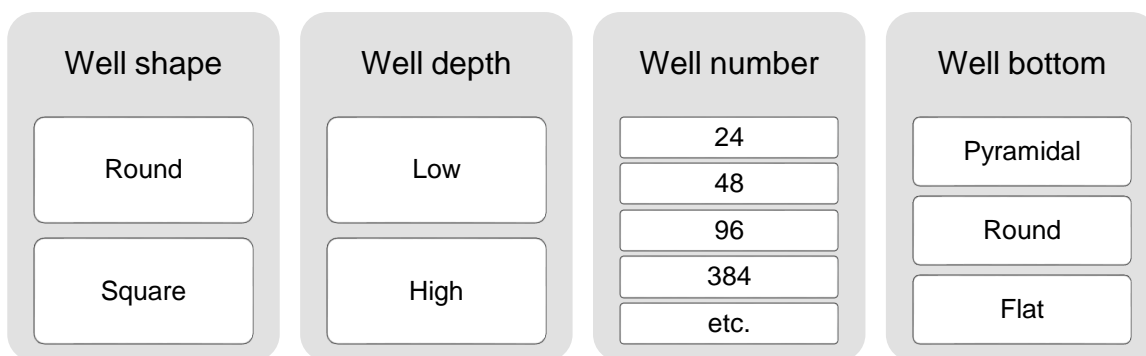


Figure 12 – Different configurations available for microtiter plates. A wide range of characteristics are available to be combined accordingly to the researcher’s purposes.

MTP are a key element in biotechnology and the development of ultraminiaturized plates (1536-well plates) is now being applied for advanced high throughput screening experiments in which more than 100 000 compounds can be handled per day [105]. Thanks to the non-stoppable developments in technology, the handling and automation of MTP is fairly easy to do. It is now possible to combine side equipment such as pipettes, microplate readers, thermostated agitators, auto-samplers, and online software to control, manipulate and analyze all data, increasing the relevance of these systems in R&D and even their application for industrial purposes. Indeed, plate readers can be attached and perform a whole analysis to the data in less than 90 seconds, evidencing the high throughput potential of these miniaturized systems. The main problems associated with these concern more to the response detection in terms of sensitivity and rapidness than to the MTP itself.

Among the fields to which MTP can be applied to, one of the most relevant is the evaluation of reaction kinetics in biocatalytic systems. Indeed, the development of an automated platform capable initiating, following the reaction over time and generating the corresponding kinetic parameters was achieved while reducing the reaction volume from the micro- to the nanoliter scale [106].

The development of a fully automated process sequence in 96-deep square wells, from the fermentation stage of *E.coli* TOP10 until the analytical assays of the bioconversion reaction of cyclohexane monooxygenase has also been reported [107]. The system also allowed for the rapid determination of the kinetic parameters of the reaction and for the continuous control of the process. The data from the microscale process was used to scale it up to a 75 L scale, based on the oxygen transfer coefficients involved, showing that microscale automation is a promising strategy for rapid process development [107].

On the other hand, MTP are widely applied in the high throughput screening of cultivation systems with the main goal of perform and screen reactions in a short period of time with minimal volume consumption.

One research group used 96-square deep-well MTP to study the changes in metabolic fluxes of glucose metabolism in several knockout mutants of *B. subtilis* with a ¹³C-labelled compound. This approach seemed

to be the most favourable since the low volumes needed compensated for the high costs of the tracer. The experiment showed comparable results to those obtained in 30 mL shake flasks [108].

A scale-down approach through the use of a 48-well MTP was recently used for vinegar production, showing comparable results to those of a 9 L bioreactor [109], which was used for the prediction of the proper cultivation conditions in the MTP. This approach included the design of a custom made lid to reduce evaporation losses while providing a suitable oxygen supply to the cultivation [110].

Examples regarding the effect of the hydrodynamic environment in biofilm formation are also documented in 96-well MTP and compared to macroscale methodologies [111]. When comparing shaking to static conditions, the SEM studies at the microscale level revealed differences in the length of the biofilm's cells, which were not evident at the macroscale [111]. Such results highlight the role that hydrodynamic effects might have upon miniaturized systems and the importance of using microscale methods and techniques of increased detail to avoid the loss of relevant information.

Mammalian cells have also benefited from cultivation in MTP. Several groups have focused on finding the best cultivation conditions by studying their performance in a wide array of geometries and conditions. Recently, a group used 96-deep well MTP for the high throughput production of a protein from transient transfection of mammalian cells [112]. The study focused on finding the optimal operating conditions, namely by comparing MTP with different well geometries, working volumes and agitation at different speeds and orbital diameters as these factors influence the mixing conditions and the mass transfer of oxygen to the culture medium. Ultimately it was concluded that the best conditions were with a 96-round-deep well and round bottom MTP with a working volume of 1 mL, agitated at 1000 rpm and a 3 mm orbital diameter [112].

1.5.1.1. Mixing of shaken bioreactors

Mixing efficiency and hydrodynamic conditions should be addressed in order to assure a good performance and productivity by the reactional system under study. The agitation mechanism in MTP is often performed by shaking as this is the simplest and most efficient way to promote mixing, still magnetic stirring can also be used although in a lesser extent.

When considering enzyme kinetics, it is of the uppermost importance to ensure a rapid and efficient mixing upon solution addition to guarantee a higher reproducibility of the assays. However, when working at the microscale, the small volume additions are often not subjected to proper mixing, resulting in mixing times as long as minutes [113].

There are several methods to quantify mixing efficiency, however the most used to follow fluid motion are visual methods helped by microscopic, photo or video techniques [114], [115]. Fluorescence experiments through the addition of alkali tracers were used to assess mixing times in shaken 96-round well MTP, revealing the existence of "dead-zones" at low shaking speeds, where t_m were in the order of minutes, which were reduced to only a few seconds at higher shaking speeds [116].

The shaking speed at which the centrifugal forces of the shaker instrument overcome the surface tension of the liquid inside the well is known as critical shaking speed. The critical shaking frequency (N_{crit}) for 48-well, 96-well and 24-round well MTP can be calculated accordingly to Equation 5 [113], [117], [118].

$$N_{crit} = \sqrt{\frac{\sigma D_w}{4 \pi V_L \rho D_o}} \quad \text{[Equation 5]}$$

Where σ is the surface tension ($\text{kg}\cdot\text{s}^{-2}$), D_w is the well diameter (m), V_L is the filling volume (m^3), ρ is the fluid density ($\text{kg}\cdot\text{m}^{-3}$) and D_o is the shaking diameter (m).

It has been reported that below the critical frequency, increases in the shaking frequency of 96-well MTP did not change the liquid distribution, therefore in order to induce liquid motion inside the wells, increase the interfacial mass transfer area and decrease the mixing times, this value should be exceeded [113], [117].

The gas-liquid mass transfer phenomena is rather well understood in MTP due to the emphasis given to fermentation studies. It is known that sufficient oxygen supply is fundamental for the cultivation of aerobic microorganisms, mammalian and plant cells. However, in order to do so the minimum shaking speed predicted must guarantee the rapid mixing and oxygen transfer, factor which is often overlooked during screening experiments [119]. To avoid oxygen supply deficits, adjustments in the shaking conditions can be made by changing the frequency, the well size or the filling volume, for example.

Reports have showed that decreases in the filling volume have led to increases in the OTR and, consequently, in increases of the rate of substrate oxidation and conversion to product [107]. A strong influence of the shaking diameter in the maximum OTR was reported [120] and alterations in the well geometry from round to square have proved to be beneficial to the mixing efficiency and oxygen supply [113]. The same was observed for 48-well MTP, in which the positive effects over the OTR were compared to those of baffles in shake flasks [121].

The mixing process in shaken and stirred reactors can be characterized through dimensionless numbers, such as the Reynolds number (Re) (Equation 4). However, in shaken systems, the Re is usually calculated using the diameter of the well (D_w) instead of the impeller diameter (D_i) plus considering a few other factors of importance in MTP operation (Equation 6) [122].

$$Re_f = \frac{\rho \pi N D_w^2}{2 \mu} \left(1 - \sqrt{1 - \frac{4}{\pi} \left(\frac{V_L^{\frac{1}{3}}}{D_w} \right)^2} \right)^2 \quad \text{[Equation 6]}$$

The Phase number (Equation 7) was adapted as an analogy of a partially filled rotating horizontal drum from liquid films to water-like solutions [123] and acts as an indicator of the operational conditions of the fluid flow regarding the inputted rotational movement in shaken reactors [124]. This number is widely used as an additional tool for a more thorough analysis of the operation in shaken reactors.

$$Ph = \frac{D_o}{D_w} \times (1 + 3 \log_{10} Re_f) \quad \text{[Equation 7]}$$

Where D_o is the shaking diameter, D_w is the diameter of the wells of the MTP and Re_f is the Reynolds number. When $Ph > 1.26$, together with the axial Froude number > 0.4 , it is considered that we have in-phase conditions, meaning that the operating conditions are favorable and that the fluid follows the rotational movement. For $Ph < 1.26$ the operating conditions are out-of-phase, meaning that the fluid cannot follow the shaking movements, remaining at the bottom of the shake flask, which can occur when large flasks, low filling volumes, small shaking diameters or very viscous fluids are used [117], [124]. The assessment of this number constitutes a way to assure that the fluid flow is appropriate, as otherwise the mixing and the reproducibility of the operating conditions would be rather poor.

Sometimes it might be necessary to change the shaking diameter instead in order to have in-phase conditions since high agitation frequencies could lead the liquid to fall off of the MTP's wells [124]. Indeed an experiment in which the shaking diameter was the variable under study showed that the liquid flow in square wells was out-of-phase when $D_o = 25$ mm but changed to in-phase conditions when $D_o = 50$ mm. This observations highlight the importance of a proper selection of the shaking parameters for the successful use of 96-square well MTP [113].

The axial Froude number (Equation 8), in this context ($Fr_a > 0.4$), means that the centrifugal acceleration is strong enough to project the fluid bulk against the surrounding walls of the wells.

$$Fr_a = \frac{u^2}{g D_o} = \frac{2 (\pi N)^2 D_o}{g} \quad \text{[Equation 8]}$$

Where u is the fluid velocity ($\text{m}\cdot\text{s}^{-1}$), N is the mixing frequency (s^{-1}), D_o is the shaking diameter (m) and g is the gravitational acceleration ($\text{m}\cdot\text{s}^{-2}$).

The theoretical angle of the liquid inside the wells can be calculated by applying the arc tangent to the Froude number of Equation 8 [120], [123].

1.5.2. Microfluidic devices

Microfluidic devices focus on the transport of little amounts of fluids (e.g. nanoliter scale) through small microchannel compartments with no mixing input to the system. These microreactors are suitable for continuous operation and the reaction space is within the microchannel itself [99]. Their use as a means to develop higher throughput methods in process development also relies with their potential of being applied to test and optimize a wide range of biocatalysts, unit operations and reaction conditions, altogether or not, to assess if and how they influence each other. An interesting way to do so is by implementing each operation and/or condition into modules prone to, later on, being combined by the researcher, increasing the extent of conditions and reactions tested [96], [101], [125].

The physical effects that dominate fluid flow (e.g. surface tension) are also rather different when compared to the conventional large scale systems [100]. In this kind of system the fluid flow in the microchannel follows a direct, precise and pre-established path mostly under a laminar regime with dominating surface tension forces where the mass transport rate is dominated by molecular diffusion (micro-mixing). As the mixing of the fluids is promoted by the contact between them at the molecular scale, the mixing times are decreased and diffusional limitations minimized [99]. These effects can be described by dimensionless numbers such as the Reynolds number, the Bond number and the Péclet number, respectively [96], [100]. Further insights into the hydrodynamics of microfluidic environments may be found elsewhere [126].

Microfluidic systems have greater surface-to-volume ratios that allow heat and mass transfer to occur in just a few instants [96]. These properties make these systems suitable for very exothermic reactions, as this factor is often overlooked when designing small scale bioreactors, and allows for higher selectivities and more accurate kinetic parameters [101].

Many reactions, in order to happen, are dependent on the products formed in previous reactions. The implementation of cascade reactions into miniaturized microfluidic systems is of great interest, however these reactions are limited by their compatibility as in some catalytic cascades the catalysts are not compatible with each other [100]. An approach to minimize such problem relies in the implementation of several in-line isolated operations that could facilitate the reactions without the interference of intermediate products, which would not be present for the next reaction [100]. The fact that these reactions occur isolated from each other would add another great advantage, which is the elimination of the need to remove the interfering intermediate byproducts prone to cause product contamination or enzyme deactivation, if present in the reaction zone.

Stimulus-responsive polymers with swelling/shrinking properties can be implemented as part of the microfluidic device's hardware which can be used to create valves, when the stimulus threshold is reached, ultimately controlling fluid flow [127]. An interesting review, focusing on stimuli such as light, temperature, redox state or pH can be found elsewhere [19].

Interestingly enough, microfluidic devices can also be manufactured for the purpose of delivering chemical and mechanical signals, which is of the uppermost importance in cell culture [128]. From the quantification of cellular responses, to the control of cellular microenvironments or the *in vitro* generation of tissues for biomedical and pharmaceutical research, microfluidic platforms have proved to be an outstanding tool for the development of systems biology [128].

Despite the whole potential of microreactors on homogeneous reactions and separation procedures, such as liquid-liquid extraction [129] and two phase systems [130], [131], their capacity to handle solids in heterogeneous biocatalysis is still quite limited due to the dimensions of the channels that, in turn, limit the size of the solids to be used [132]. Strategies of enzyme immobilization in the internal surface of the micro

reactor's channels have been implemented successfully [133], [134] and it has been reported that enzyme leaching from porous beads in a packed-bed microreactor was lower than that of a batch reactor [135].

High throughput methods can rise simply by numbering up (parallelization) the optimized small scale reactor, instead of the more conventional scale up approach, as the former is a faster and simpler process [96], [98]. From an economical point of view, it is advantageous since the costs associated with the redesign, pilot-scale experiments and validation are reduced, which in turn allows the speed up of the process development [101]. This approach may not be the most straightforward in the handling and operational aspects, when considering the high number of systems working in parallel [96].

Generally better results are reported to relatively fast reactions performed under mass or heat transfer controlled conditions [100], [132]. Enzyme catalyzed reactions are usually slow ($k_{rate} = 0.1 - 100 \text{ s}^{-1}$) and not limited by mass transference effects unless transport across phase boundaries is involved, as in multiphase biocatalytic processing [100]. Still, there are reports showing how some reactions benefited from microsystems, making them good systems for process intensification through miniaturization.

In practical terms, microwell plates seem to be currently the better candidates in terms of experimental throughput, such as the screening capacity of the biocatalysts used or reaction conditions tested per time, as the automation level of in-line analysis is more developed in these than in microfluidic reactors [100].

It should be noted that miniaturization might not be suitable for every reaction and, even if it is suitable, the system performance and/or the economic gains coming from it might not be greatly improved with such approach. This method must be analyzed case-by-case in contrast with the more conventional ones.

2. OBJECTIVES

The main goal of this project is to study the behavior and applicability of miniaturized systems, such as small vessels and microtiter plates, in biochemical engineering and to establish them as robust platforms for high throughput biocatalysis and rapid process development.

In order to do so, the enzymatic hydrolysis of inulin by inulinase was chosen as the model reaction and the enzyme will be subjected to two different immobilization protocols – entrapment in PVA and covalent binding in Amberlite IRC-86 – which will be oftentimes compared.

The biocatalyst will be characterized in terms of optimal pH and temperature for the subsequent assays which will be divided in four segments:

- (i) Importance of agitation in small-scale reactors
Studies at several volumes (1, 3 and 10 mL) will be made with and without magnetic stirring to assess the importance of having agitation to overcome diffusional limitations in relatively small volumes
- (ii) Evaluation of common scale up criteria
The hydrodynamic environment changes upon reaction scale up will be evaluated and compared to the original system
- (iii) Influence of geometric and dynamic parameters in the reaction rate
Microtiter plates will be thoroughly tested on their high throughput capacity to study how effects such as the agitation rate, the shaking diameter, the well shape and dimensions or the filling volume might affect the overall reaction rate
- (iv) Evaluation of the kinetic parameters of free and immobilized inulinase
The kinetic parameters of the enzyme will be determined and compared at several reactional volumes, for different substrate sources (*Dahlia* tubers and chicory root), in the presence and absence of agitation to see how these factors affect the enzyme kinetics

The analytical methods to be performed will rely on spectrophotometric techniques, more specifically in the DNS method for the quantification of reducing sugars.

3. MATERIALS AND METHODS

3.1. Materials

Reagents

The purified liquid Fructanase mixture (exo-inulinase + endo-inulinase in 50% glycerol and 0.02% Na azide) was acquired from Megazyme (Wicklow, Ireland). The substrate inulin, from *Dahlia tubers* and chicory root, were acquired from Acros Organics (Geel, Belgium). The immobilization support, Amberlite IRC-86 in hydrogen form, was acquired from Fluka Analytical and the reagents used in the immobilization protocol, polyethylenimine 50% aqueous solution and glutaraldehyde 24% (w/w) were obtained from Sigma-Aldrich and Acros Organics (Geel, Belgium), respectively. Polyvinyl alcohol (Lentikat liquid 250) was obtained from GeniaLab (Braunschweig, Germany). Polyethylene glycol, with an average MW of 600 (PEG 600) was acquired from Acros Organics (Geel, Belgium). Bradford reagent (for 1-1,400 µg/ml protein) was obtained from Sigma-Aldrich (St Louis, U.S.A.).

Equipment

For the analytical measurements, a SPECTROstar Nano spectrophotometer, from BMG LabTech, was used.

A heating bath LAUDA E100 (Ecoline, Staredition) was used to carry the reactions at the proper temperature in the magnetic stirred vessels. For microtiter plate tests, a Heidolph Titramax 1000 shaker adapted with a Heidolph Heizmodul Inkubator 1000 temperature control and an Agitorb 160E orbital agitator from ARALAB were used.

3.2. Immobilization procedures

3.2.1. Amberlite immobilization

Inulinase was immobilized onto Amberlite IRC-86 (Figure 13) based on the method described by Obón and co-workers [136] and adapted by Rocha and co-workers for immobilization in Amberlite IRC-50 [89]. First, 10 g of Amberlite IRC-86 were washed in 100 mL of distilled water for an hour and vacuum filtered. The same procedure was then applied but with acetate buffer 0.1 M pH 4.5 instead. The support modification procedure started with a 2-hour long incubation of 25 mL of polyethylenimine 10% with Amberlite IRC-86. The beads were recovered by vacuum filtration and activated by incubation with 50 mL of glutaraldehyde 10%, also during 2 hours. The support was recovered by vacuum filtration and incubated with 10 mL of diluted inulinase (10-fold in acetate buffer 0.1 M pH 4.5) at 4°C during 2 hours. Lastly, the support with the immobilized enzyme was vacuum filtered, washed with acetate buffer 0.1 M pH 4.5, vacuum filtered and

stored at 4°C until further use. All of the steps were performed under gentle magnetic stirring at room temperature, unless stated otherwise.



Figure 13 – Amberlite IRC-86 beads with a harmonic mean size of 0.58 to 0.78 mm. The functional group of this weak acid cation exchanger is carboxylic acid.

3.2.2. PVA immobilization

Inulinase entrapment in PVA was based on the methodology developed by Fernandes and co-workers [137]. Lentikat® liquid was heated up to 95°C, until it was completely dissolved, and then allowed to cool down to 50°C. 1 mL of a 5-fold diluted enzyme solution (in acetate buffer 0.1 M pH 4.5) was added to 5 mL of Lentikat® liquid and mixed through magnetic stirring in a 25 mL jacketed vessel. After allowing the mixing of the solution, the preparation was extruded through a peristaltic pump into 50 mL of PEG 600, also under magnetic stirring, and left for a 2-hour long incubation. Afterwards the beads were collected, drained and washed with acetate buffer 0.1 M pH 4.5 for 30 minutes. Both supernatants were collected and assayed for protein quantification. PVA beads were then soaked in acetate buffer 0.1 M pH 4.5 and stored at 4°C until further use (Figure 14).

The efficiency of the immobilization procedure was determined by the following equation (Equation 9).

$$IE (\%) = \frac{E_0 - E_w}{E_0} \times 100 \quad \text{[Equation 9]}$$

Where E_0 refers to the amount of enzyme present in the enzyme solution prepared, and E_w refers to the amount of enzyme present in the washing solutions (PEG 600 and acetate buffer 0.1 M pH 4.5).



Figure 14 – Final form of the PVA beads in acetate buffer 0.1 M pH 4.5.

3.3. Characterization of immobilized and free inulinase (pH and temperature)

The effects of pH and temperature on enzyme activity were evaluated in 30 minutes batch runs by incubating 15 mg of Amberlite IRC-86 or 3 beads (appx 70 mg) of PVA immobilized enzyme in 1 mL of inulin solution 50 g.L⁻¹ in acetate buffer 0.1 M in a pH range of 4–5.5 and in a temperature range of 45–70°C. For the free enzyme, 16.67 µL of inulinase diluted 100-fold in acetate buffer 0.1 M pH 4.5 were used similarly. Blanks with enzyme free solutions were performed likewise. Determination of enzyme activity was determined through the rate of reducing sugars formation in the reaction medium and converted in relative activity. All trials were performed in duplicate.

3.4. Biotransformation with the free and immobilized enzyme

Experiments with the free and immobilized enzyme were carried out in magnetically stirred (440 rpm) 1, 3 and 10 mL vessels. 50 µL of 10-fold diluted enzyme or 200 mg of Amberlite IRC-86 immobilized enzyme were added to 3 mL of *Dahlia* tuber's inulin 50 g.L⁻¹ prepared in acetate buffer 0.1 M pH 4 at 55°C. For the PVA immobilized enzyme, 50 µL of a 100-fold diluted enzyme solution or 210 mg of bead weight were added to 3 mL of chicory root inulin 50 g.L⁻¹ prepared in acetate buffer 0.1 M pH 4.5 at 50°C. Proportions were kept for the remaining volume trials. Samples were collected periodically, quenched in dinitrosalicylic acid (DNS) reagent and assayed for quantification of reducing sugars. The reaction rate was defined as the amount of reducing sugars formed over the course of the reaction and the calculations were based on the linear evolution of the measurements made, in general, in the first 30 minutes. All trials were performed in duplicate. Equivalent trials without magnetic stirring were also performed.



Figure 15 – General experimental setup for the biotransformation and enzyme activity measurements. In the picture Amberlite IRC-86 is being incubated inside jacketed vessel at 55°C in a reactional volume of 10 mL.

3.5. Hydrodynamic environment within scale up

To study the hydrodynamic effects of scaling the reaction from 1 to 10 mL, the tests were performed by adding either 67 or 670 mg of Amberlite IRC-86 immobilized enzyme to 1 or 10 mL of 50 g.L⁻¹ *Dahlia* tubers inulin solution prepared in acetate buffer 0.1 M pH 4 at 55°C, respectively. Samples were collected every 10 minutes, quenched in DNS reagent and assayed for quantification of reducing sugars. Reaction rates were determined as described in Chapter 3.4. All trials were performed in duplicate.

The 1 mL reaction was performed in a 1.2 cm diameter vessel under magnetic stirring at 423 rpm (Figure 16A). The system was scaled to 10 mL in a vessel with a diameter of 2.5 cm (Figure 16B) using Equation 2 [95].

The rpm of the scaled 10 mL vessel will thus be related to the small 1 mL vessel, through Equation 3 [95].

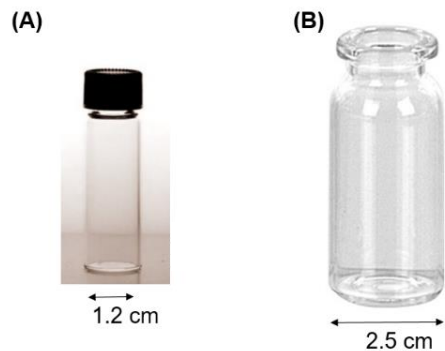


Figure 16 – Reaction vessels for the 1 mL (A) and 10 mL (B) reactions.

The dimensions of the small scale magnetic agitator are 0.8 cm in length and 0.3 cm in diameter (Figure 17A) and for the 10 mL reaction vessel are 1.5 cm in length and 0.5 cm in diameter (Figure 17B).

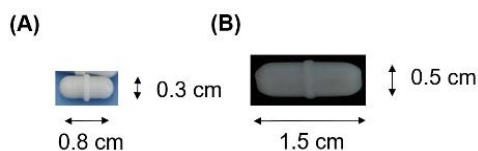


Figure 17 – Magnetic stirrers used in the 1 mL (A) and 10 mL (B) reaction vessels.

3.6. Microtiter plate assays

To study the reaction in a shaken environments, microtiter tests were performed by adding either 70 mg of PVA beads or 67 mg of Amberlite immobilized enzyme to 1 mL of 50 g.L⁻¹ *Dahlia* tubers inulin solution prepared in acetate buffer 0.1 M pH 4 at 50°C or 55°C, respectively. Three different MTP were used (Figure 18):

- A. Square-shaped, round-bottomed 96-well plate (well length: 0.8 cm)
- B. Square-shaped, pyramidal-bottomed 24-well plate (well length: 1.7 cm)
- C. Round-shaped, flat-bottomed 24-well plate (well diameter: 1.6 cm)

In order to keep the Froude number constant, trials in the MTP shaker (orbital diameter of 1.5 mm) occurred at 450 and 700 rpm while trials in the orbital shaker (orbital diameter of 2.5 cm) occurred at 110 and 170 rpm. Similar assays with a reaction volume of 3 mL were performed for plate B and proportions were kept the same. Samples were collected at 0 and 60 minutes, quenched in DNS reagent and assayed for quantification of reducing sugars.

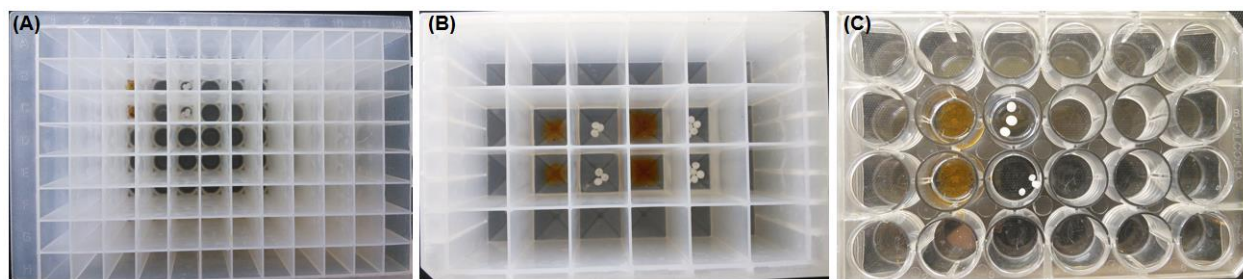


Figure 18 – Microtiter plates used for the study of the hydrodynamic studies. (A) 96-square-shaped well, round-bottomed plate (well length: 0.8 cm); (B) 24-square-shaped well, pyramidal-bottomed plate (well length: 1.7 cm); (C) 24-round-shaped well, flat-bottomed plate (well diameter: 1.6 cm). The filling content of the shown plates is Amberlite IRC-86 (in brown) and PVA beads (in white).

3.7. Enzyme activity

The experimental set up for the determination of the kinetic parameters proceeded accordingly to the conditions described in Chapter 3.4. For *Dahlia* tubers inulin, the tested concentrations for the free and Amberlite immobilized enzyme were of 10, 20, 30, 50, 75 and 100 g.L⁻¹. Samples were collected at 0 and 20 minutes, according to the “sacrificial well” methodology [138]. On the other hand, the chicory root inulin concentrations for the activity for the free and PVA immobilized enzyme were of 10, 20, 30, 50, 75, 100 and 120 g.L⁻¹. Samples were collected at 5, 10, 15 and 20 minutes. Enzyme activity was determined through the rate of reducing sugars formation in the reaction medium and all trials were performed in duplicate. The initial reaction rates were plotted as a function of the substrate concentrations for the three reactional volumes.

3.8. Analytical methods

Quantification of reducing sugars was performed by the 2,4-dinitrosilylic acid (DNS) method [139]. Fructose was used for the establishment of a standard curve. The method was adapted to be performed in 96-well plates. For that, 10 µL of sample were added to 90 µL of distilled water and 100 µL of DNS reagent. The solutions were then incubated in a closed system plate for 5 minutes at 100°C and, afterwards, allowed to cool down to room temperature. 500 µL of distilled water were added to the wells and, after mixing, 200 µL were transferred to a 96-well microplate. Absorbance was read at 540 nm. Blanks were either performed with distilled water or the substrate solution. Standard deviations did not exceed 10%.

Protein quantification was performed accordingly to the Bradford method, also adapted to be performed in 96-well microplates, as described in [140].

4. RESULTS

4.1. Hydrolysis of *Dahlia* tubers inulin with inulinase immobilized in Amberlite IRC-86

4.1.1. Characterization of immobilized and free inulinase (pH and temperature)

The influence of temperature and pH on the enzyme activity of the immobilized enzyme was assessed. The optimal parameters determined were a pH of 4 and a temperature of 55°C for the immobilized enzyme (Figure 19). For the free enzyme the optimal pH observed was 5 and the optimal temperature was also of 55°C.

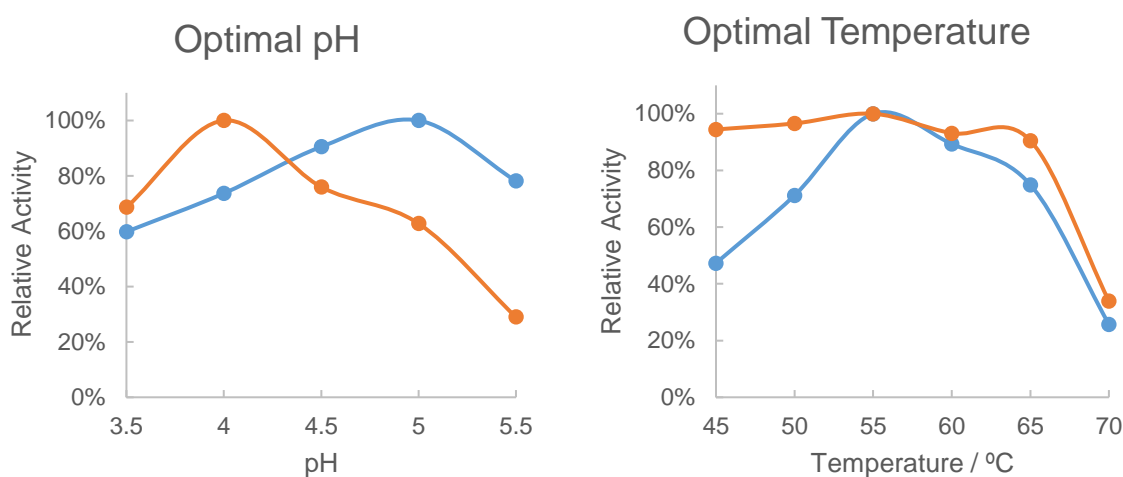


Figure 19 – Effect of the temperature and pH on *Dahlia* tubers inulin hydrolysis with Amberlite IRC-86 immobilized enzyme (—○—) and free enzyme (—●—).

4.1.2. Time courses of product formation of the free and immobilized enzyme

Following some preliminary studies on the overall reaction performance (data not shown), a more extensive study towards the effect of magnetic agitation on the reaction was carried. For this, the reducing sugars formation for all 1, 3 and 10 mL volumes was monitored in the first hour of reaction with and without magnetic agitation (Figure 20, Figure 21 and Figure 22).

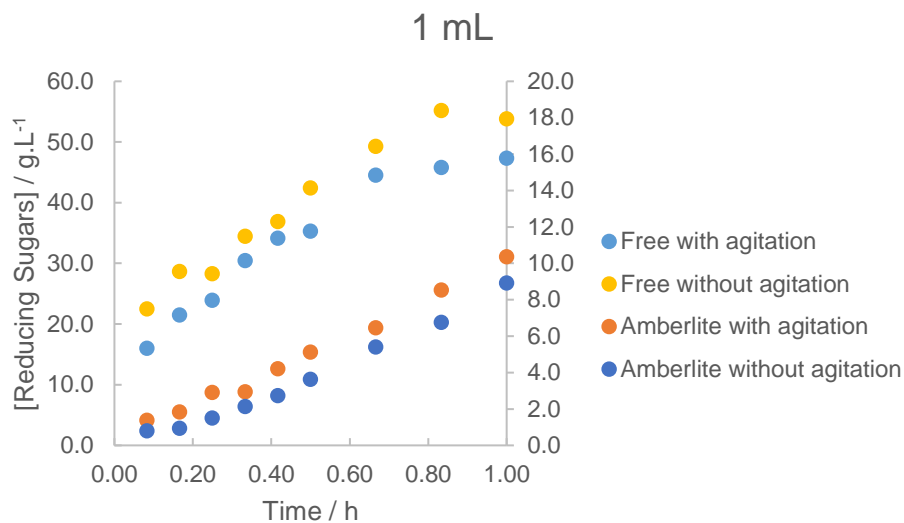


Figure 20 – Time course of product formation for the 1 mL reaction system with the free and Amberlite IRC-86 immobilized enzyme with and without magnetic agitation (440 rpm). Free enzyme on the main axis and immobilized enzyme on the secondary axis.

In the case of the 1 mL reaction system, it is possible to observe that the free enzyme has higher hydrolysis than the immobilized form. Regarding the immobilized enzyme, Figure 20 shows that the agitated system has better performances, however such behavior is not observed for the free enzyme. In both cases the time course of product formation has a linear behavior throughout the, at least, first half hour.

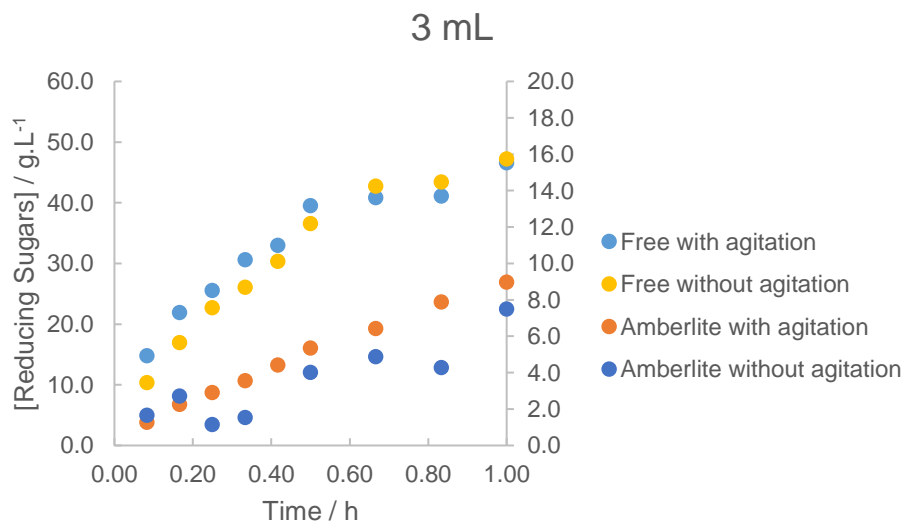


Figure 21 – Time course of product formation for the 3 mL reaction system with the free and Amberlite IRC-86 immobilized enzyme with and without magnetic agitation (440 rpm). Free enzyme on the main axis and immobilized enzyme on the secondary axis.

Relatively to the 3 mL reactional system, it is possible to observe a similar behavior in the sense that the free enzyme has higher hydrolysis than the immobilized enzyme and that in the first 30 minutes the reaction seems to follow a linear behavior. However, this trend is not observed for the non-agitated immobilized enzyme.

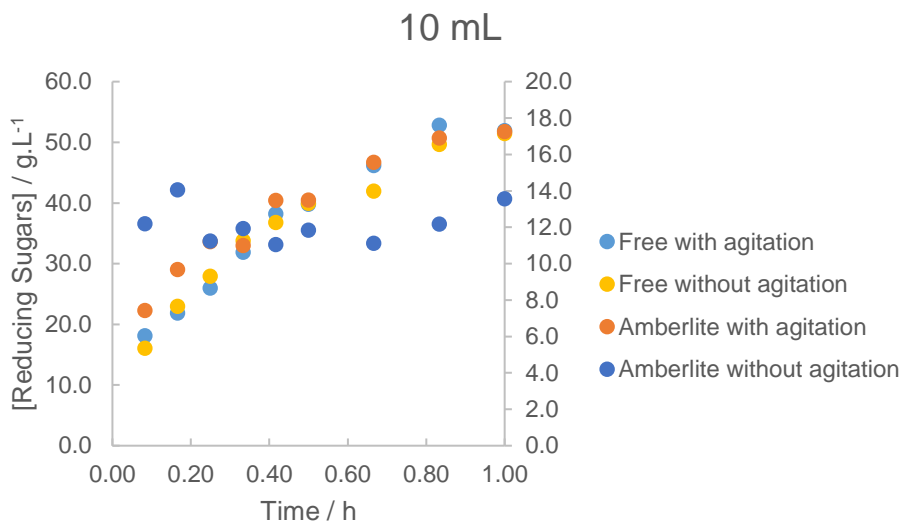


Figure 22 – Time course of product formation for the 10 mL reaction system with the free and Amberlite IRC-86 immobilized enzyme with and without magnetic agitation (440 rpm). Free enzyme on the main axis and immobilized enzyme on the secondary axis.

Regarding the 10 mL reaction system, the results regarding the free enzyme are very similar to the previous ones, whereas there is agitation or not, which suggests that agitation is not crucial in this case. However, the opposite occurs in the immobilized enzyme system, as the reaction without agitation shows a rather random behavior instead of a linear one, as in the agitated immobilized enzyme system.

4.2. Hydrolysis of *Dahlia* tubers inulin with inulinase immobilized in PVA

4.2.1. Time courses of product formation of the free and immobilized enzyme

Similarly to the described in Chapter 4.1.2, the effect of magnetic agitation in the different reaction volumes was studied and the time courses of the PVA immobilized enzyme were compared to those of the free enzyme (Figure 23, Figure 24 and Figure 25).

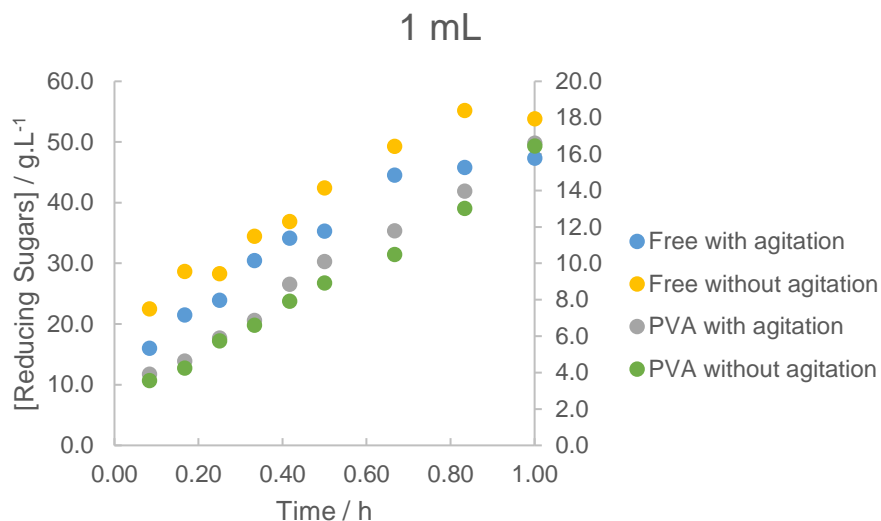


Figure 23 – Time course of product formation for the 1 mL reaction system with the free and PVA immobilized enzyme with and without magnetic agitation (440 rpm). Free enzyme on the main axis and immobilized enzyme on the secondary axis.

For the PVA immobilized enzyme it can be seen that the presence or absence of agitation does not seem to have a great impact in the time course of product formation at the beginning of the reaction, as both reactions show a linear behavior in the first 30 minutes (Figure 23). However, after 30 minutes the reducing sugars concentration in the agitated system is slightly higher than in the non-agitated. As for the free enzyme, higher reducing sugars concentrations are seen for the non-agitated system throughout the whole hour in which the reaction was followed, still the agitated system shows more linear trends at the beginning than the non-agitated.

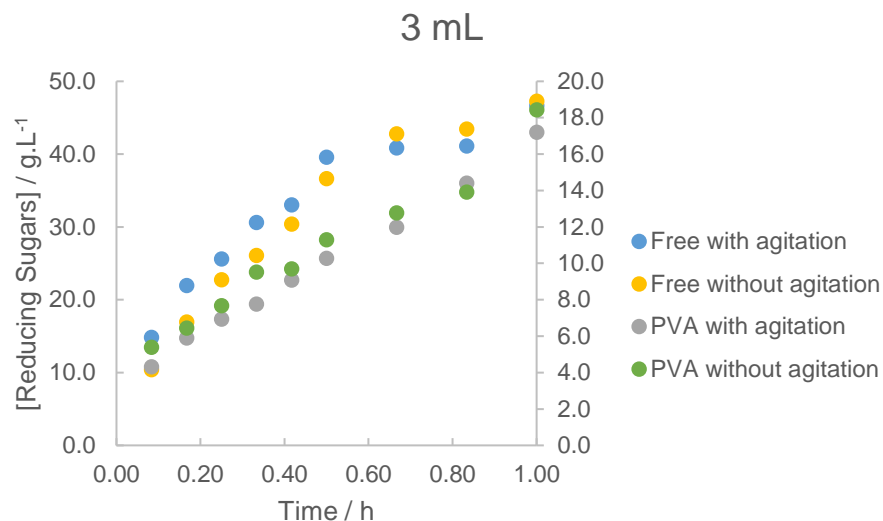


Figure 24 – Time course of product formation for the 3 mL reaction system with the free and PVA immobilized enzyme with and without magnetic agitation (440 rpm). Free enzyme on the main axis and immobilized enzyme on the secondary axis.

In the 3 mL reactional system the higher concentrations of reducing sugars are observed for the free enzyme in the agitated system, in the first half hour. The PVA immobilized enzyme without agitation allows for slightly higher concentrations than the agitated system, however in the agitated system the reaction shows a more linear behavior over its course than in the non-agitated system (Figure 24).

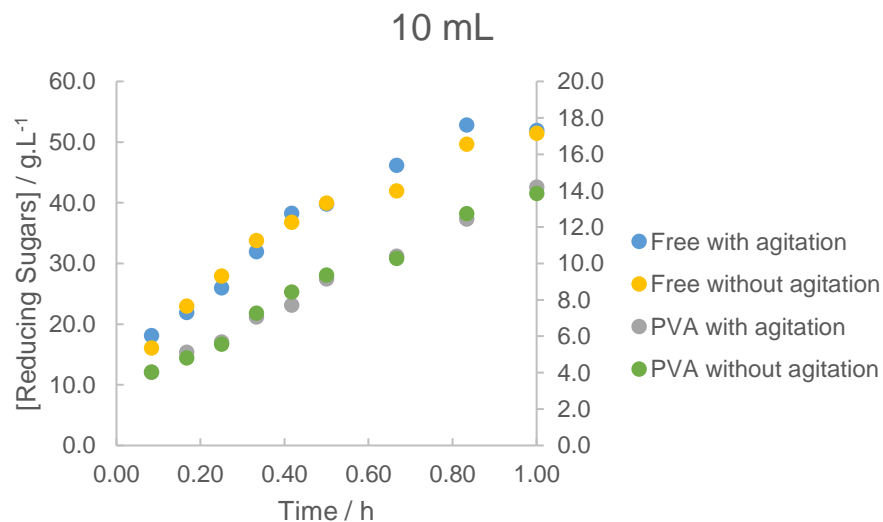


Figure 25 – Time course of product formation for the 10 mL reaction system with the free and PVA immobilized enzyme with and without magnetic agitation (440 rpm). Free enzyme on the main axis and immobilized enzyme on the secondary axis.

In general, in the 10 mL reaction system (Figure 25) there are not differences whereas agitation plays a crucial role in the reaction or not, as the product formation of the agitated and non-agitated systems is basically equal within both the free and PVA immobilized enzyme.

4.3. Hydrolysis of chicory root inulin with inulinase immobilized in PVA

4.3.1. Characterization of immobilized and free inulinase (pH and temperature)

The influence of temperature and pH on the enzyme activity for the PVA immobilized enzyme was also assessed. The optimal parameters determined for both the free and immobilized enzyme were a pH of 3.5–4 and a temperature of 65°C (Figure 26).

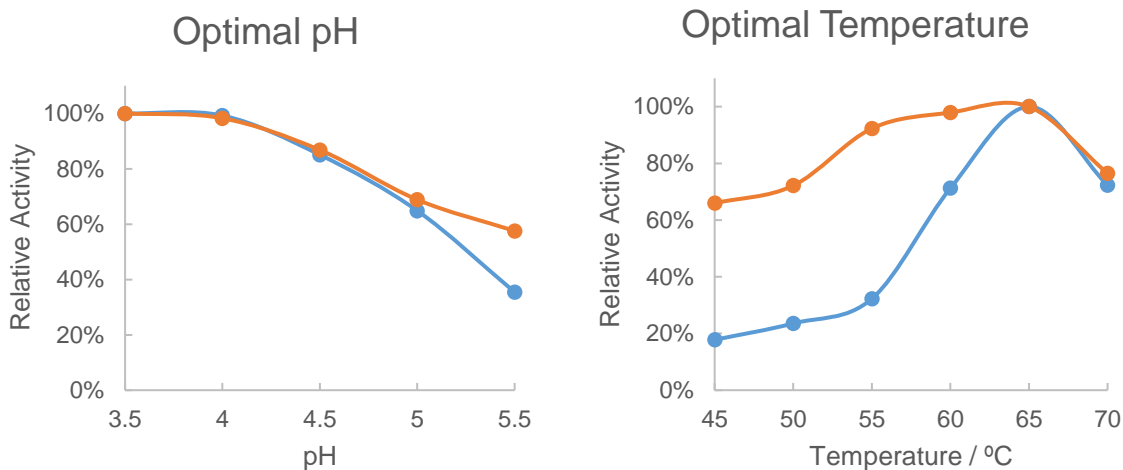


Figure 26 – Effect of the temperature and pH on Chicory root inulin hydrolysis with PVA immobilized enzyme (—●—) and free enzyme (—●—).

4.4. Hydrodynamic environment within scale up

One important factor when scaling a reaction is to assure that the reaction performance remains the same as before the scaling. One approach to scale a reaction is based simply on keeping all of the proportions of the vessels, in which the reaction occurs, the same.

In the scaling of the reaction from the 1 mL to the 10 mL system, two proportional vessels were used. Nonetheless, the agitation speed was also adapted for the 10 mL system by using Equation 3. It was considered that the scale up could occur in two scenarios, one in which n assumed the value of 1 and other in which the value would be of 0.75. The results obtained are in Figure 27.

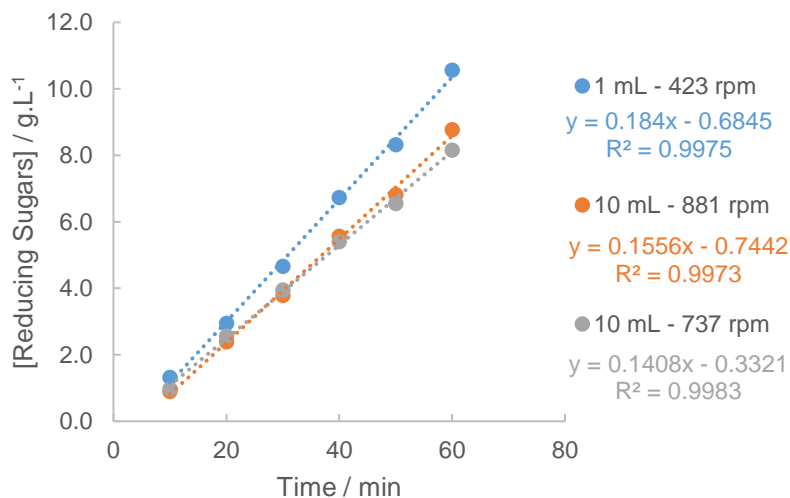


Figure 27 – Reaction rates for the 1 mL (0.184 g.L⁻¹.min⁻¹ at 423 rpm) and 10 mL (0.1408 g.L⁻¹.min⁻¹ at 737 rpm and 0.1556 g.L⁻¹.min⁻¹ at 881 rpm) reactional systems with Amberlite IRC-86 immobilized enzyme. The 1 mL reaction at 423 rpm was used as the scale up basis.

From the results obtained in Figure 27 it is possible to observe that when the reaction occurs at a 10 mL scale, the hydrolysis rate is not as high as when it happens in a 1 mL, regardless of considering equal liquid motions ($n = 1$) or equal solid suspensions ($n = 0.75$).

A further study to assess the overall performance of the reaction in the 10 mL vessel was carried simply by changing the magnetic agitator speed. The results obtained for the initial reaction rates as a function of the rpm can be found in Figure 28, where it is possible to observe that the initial velocity tends to increase as the speed of the magnetic agitator also increases. However in the last tests, at 900 and 1200 rpm, it can be seen that the velocity decreases abruptly.

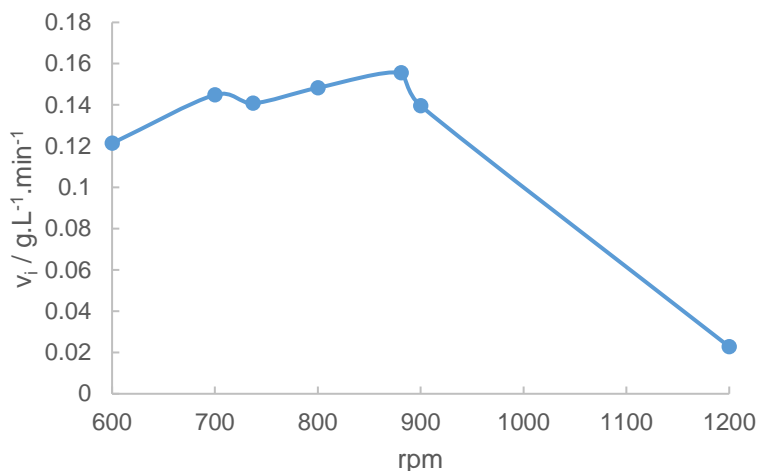


Figure 28 – Effect of magnetic stirring in the initial velocity of the reaction of hydrolysis of inulin with Amberlite IRC-86 immobilized enzyme in a 10 mL reactional system.

4.5. Microtiter plates assays

In a variation of the former studies, the reaction was also tested in different environments, namely regarding the filling volume, the wells geometry and dimensions, the agitation frequency and the orbital diameter of the agitator.

In a first step the critical shaking speed (N_{crit}) necessary to input to the MTP was calculated through Equation 5 (Table 2). From the results obtained it is possible to see that the temperature has little, if none, influence over the N_{crit} in the range of the tested conditions. Therefore, for the subsequent calculations the physical properties of water were assumed to be at 50°C.

It should be noted, however, that the reports that show that Equation 5 is valid for 24-round well and 96-well MTP relate to filling volumes of 200 μL [113] and not deep-well plates, as the used herein. Still, it will be assumed that such difference does not compromise its applicability to the used systems.

Table 2 – Critical shaking speed (N_{crit}) for the different plates and filling volumes used in both agitators (orbital diameters of 1.5 mm and 25 mm). Calculations were performed considering the $\rho_{water, 50^\circ C}$ as 988.10 kg.m^{-3} , $\rho_{water, 55^\circ C}$ as 985.65 kg.m^{-3} , $\sigma_{water, 50^\circ C}$ as 0.0679 N.m^{-1} and $\sigma_{water, 55^\circ C}$ as 0.0671 N.m^{-1} .

Plate	D_w / mm	V_L / mL	Temperature / °C	Agitator 1	Agitator 2
				$D_o = 1.5 \text{ mm}$	$D_o = 25 \text{ mm}$
				N_{crit} / rpm	N_{crit} / rpm
A	8	1	50	324.0	79.4
			55	322.4	79.0
B	17	1	50	472.3	115.7
			55	470.0	115.1
		3	50	272.7	66.8
			55	271.3	66.5
C	16	1	50	458.2	112.2
			55	455.9	111.7

In order to keep the Froude number constant within the two agitation diameters, the agitation rates of the two agitators were equalized through Equation 8. Therefore, the established 450 and 700 rpm for Agitator 1 correspond to 110 and 170 rpm in Agitator 2, respectively (Table 3 and Table 4).

Table 3 – Overview of the dimensionless numbers (Fr_a , Re_f and Ph) calculated for the different agitators and MTP used.

Plate	V_L / mL	Agitation rate / rpm	Agitator 1 $D_o = 1.5 \text{ mm}$			Agitation rate / rpm	Agitator 2 $D_o = 25 \text{ mm}$		
			Fr_a	Re_f	Ph		Fr_a	Re_f	Ph
A	1	450	0.17	1.33E+03	1.95	110	0.17	3.26E+02	26.69
		700	0.41	2.07E+03	2.05	170	0.41	5.04E+02	28.46
B	1	450	0.17	1.92E+03	0.96	110	0.17	4.71E+02	13.26
		700	0.41	2.99E+03	1.01	170	0.41	7.27E+02	14.10
	3	450	0.17	4.30E+01	0.52	110	0.17	1.05E+01	5.98
		700	0.41	6.68E+01	0.57	170	0.41	1.62E+01	6.81
C	1	450	0.17	1.38E+03	0.98	110	0.17	3.36E+02	13.41
		700	0.41	2.14E+03	1.03	170	0.41	5.20E+02	14.29

From the data present in Table 3 and Chapter 1.5.1.1, half of the working conditions were designed to be in-phase ($Fr_a > 0.4$ and $Ph > 1.26$) while the other half to be out-of-phase. Therefore, the lower agitation rates in Agitator 1 and 2, at 450 and 110 rpm, respectively, will always be expected to be out-of-phase. Similarly, the higher agitation rates will be associated with in-phase conditions. Exceptionally, plates B and C in Agitator 1 were out-of-phase even at the higher agitation rate, this was due to the fact that for these

plates to be under in-phase conditions, while keeping the same experimental conditions as the others, the stirring speed would have to be higher than 3000 rpm, which turned to be impossible.

Both immobilized enzymes were used to study the influence that parameters such as the agitation rate, shaking diameter, filling volume or well configuration have upon the reaction's initial velocity. The results obtained are shown in Figure 29.

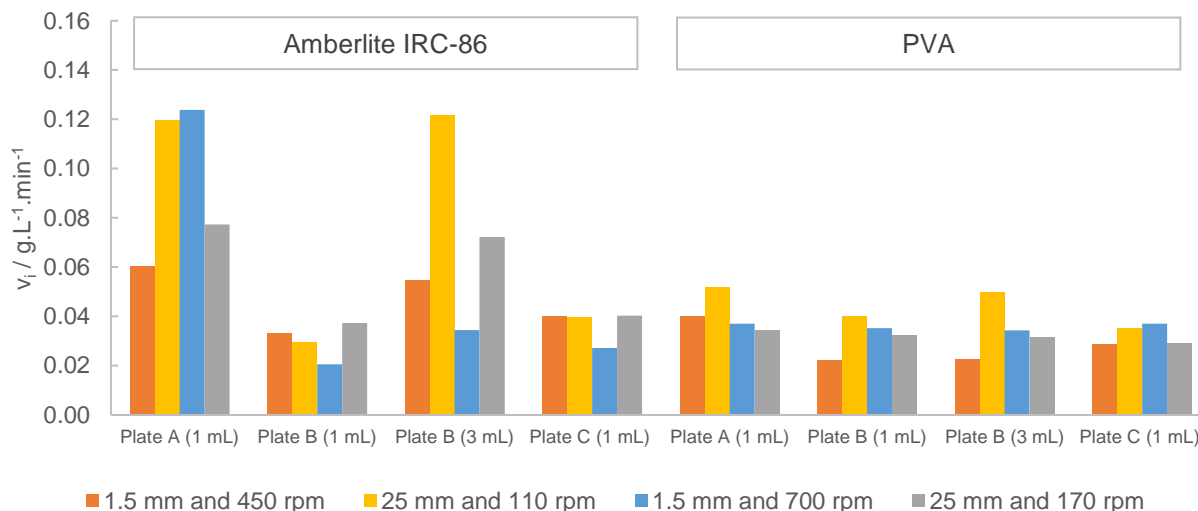


Figure 29 – Comparative studies of the reaction rate of inulin hydrolysis with both immobilized enzymes under various agitation speeds (110, 170, 450 and 700 rpm) and shaking diameters (1.5 and 25 mm). Different configuration MTP were used: Plate A – 96-square-shaped well, round-bottom; Plate B – 24-square-shaped well, pyramidal-bottom; Plate C – 24-round-shaped well, flat-bottom.

The application of the arc tangent to the axial Froude number (Equation 8) gives the theoretical angle that the liquid inside the wells makes against the walls. Values are in Table 4.

Table 4 – Theoretical angle of the liquid inside the wells formed against the walls of the MTP.

Orbital diameter / mm	1.5		25	
Agitation rate / rpm	450	700	110	170
Froude number	0.17	0.41	0.17	0.41
Theoretical Angle / Degrees	9.65	22.35	9.65	22.35

4.6. Enzyme Activity

4.6.1. Inulinase immobilized in Amberlite IRC-86: activity over *Dahlia* tubers inulin

In order to determine the kinetic parameters of the hydrolysis reactions, activity measurements at different substrate concentrations for the different reaction volumes of 1, 3 and 10 mL were performed. Note, however, that due to the previous results (Figure 21 and Figure 22), the 3 and 10 mL immobilized system without agitation will not be considered for the kinetic parameters estimation, as the methodology adopted assumes a linear evolution of the product formation and such behavior was not observed. Further assays relying on the most conventional methods, of collecting samples in shorter periods of time, could be considered.

To determine the kinetic parameters, K_M , K_M^{app} , V_{max} and V_{max}^{app} , it was assumed that the enzyme followed a typical Michaelis-Menten kinetics. Thus, the data regarding the initial velocities ($\text{g.L}^{-1}.\text{min}^{-1}$) were plotted against the different substrate concentrations (g.L^{-1}) for a non-linear regression. The results obtained are in Table 5.

Table 5 – Summary of the kinetic parameters (V_{max} and K_M) for the free and Amberlite IRC-86 immobilized inulinase, with and without agitation in reactional volumes of 1, 3 and 10 mL.

	FREE					
	1 mL		3 mL		10 mL	
	Agitated	Non-agitated	Agitated	Non-agitated	Agitated	Non-agitated
$V_{max} / \text{g.L}^{-1}.\text{min}^{-1}$	2.98	2.94	2.50	2.70	2.50	2.60
$K_M / \text{g.L}^{-1}$	80.62	70.89	63.31	74.53	60.00	70.00
	AMBERLITE IRC-86					
	1 mL		3 mL		10 mL	
	Agitated	Non-agitated	Agitated	Non-agitated	Agitated	Non-agitated
$V_{max}^{app} / \text{g.L}^{-1}.\text{min}^{-1}$	0.39	-	0.40	-	0.29	-
$K_M^{app} / \text{g.L}^{-1}$	127.80	-	135.90	-	125.60	-

4.6.2. Inulinase immobilized in PVA beads: activity over Chicory root inulin

Similarly to the described in Chapter 4.6.1, the kinetic parameters were also determined for the enzyme immobilized in PVA with Chicory root inulin as substrate. In order to do so, activity measurements at different substrate concentrations for the reaction volumes of 1 and 10 mL were performed (see Chapter 3.7). It was also assumed that the enzyme followed a typical Michaelis-Menten kinetics [141]. The data regarding the initial velocities ($\text{g.L}^{-1}.\text{min}^{-1}$) was plotted against the different substrate concentrations (g.L^{-1}) through Hyper32[®] software. The results obtained are in Figure 30, Figure 31 and Table 6.

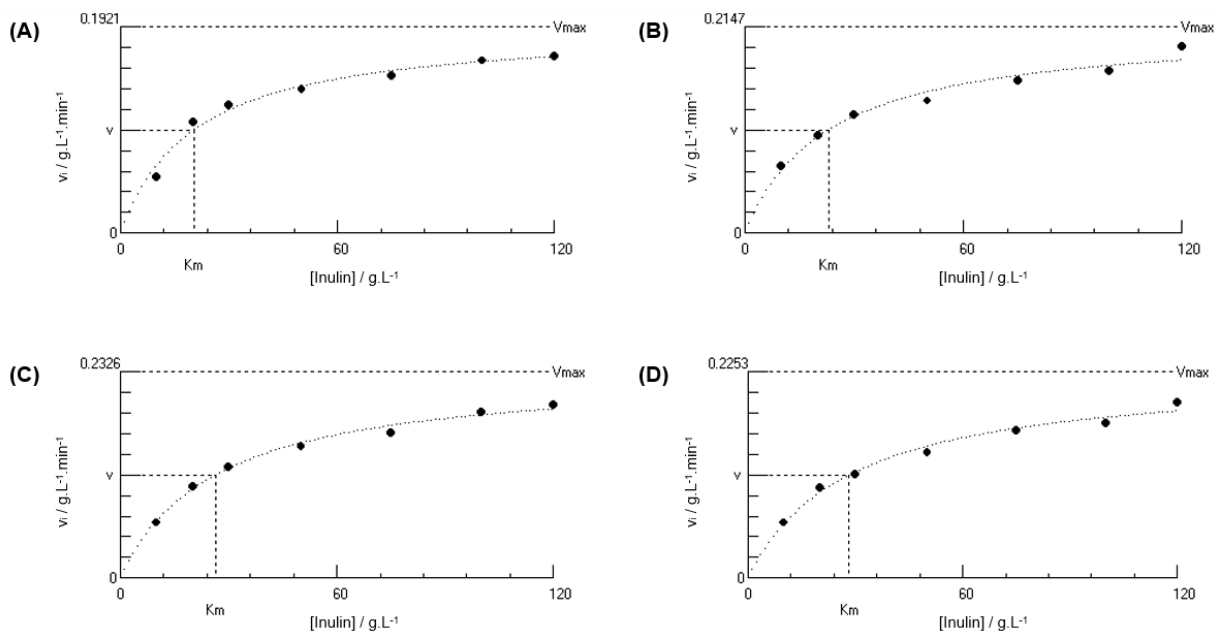


Figure 30 – Michaelis-Menten plots for the free enzyme. Activity measurements were performed with chicory root inulin concentrations ranging from 10 to 120 g.L⁻¹ at pH 4.5 and 50°C. (A) 1 mL reactional system with agitation; (B) 1 mL reactional system without agitation; (C) 10 mL reactional system with agitation; (D) 10 mL reactional system without agitation. Plots obtained through Hyper32[®] software.

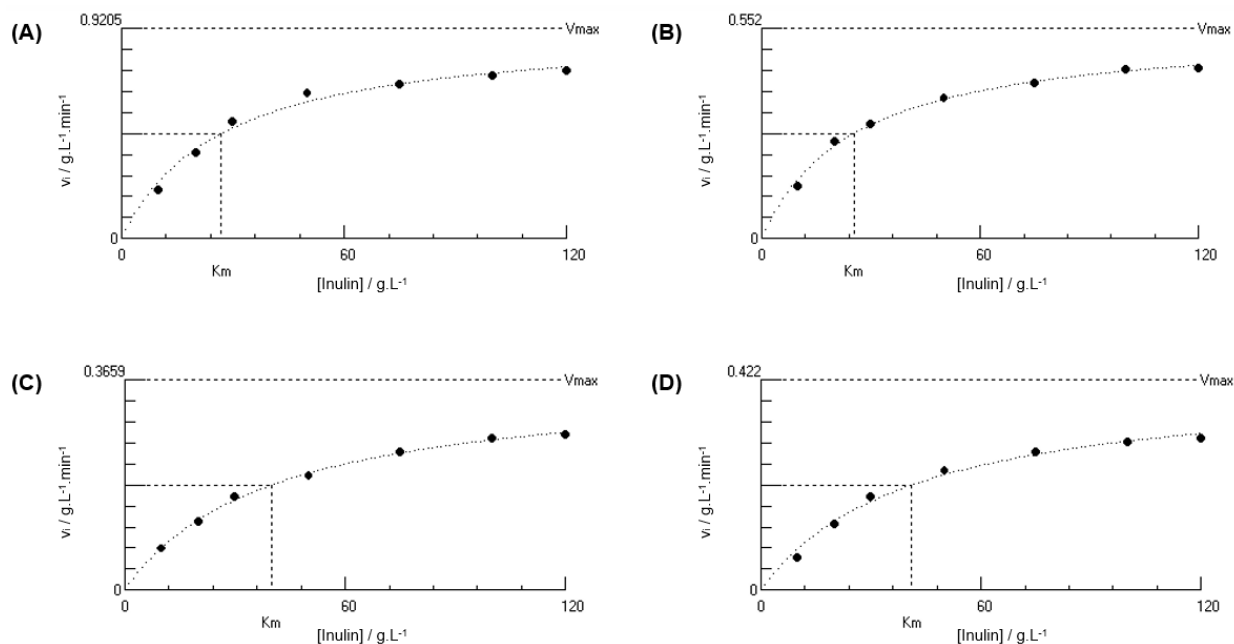


Figure 31 – Michaelis-Menten plots for the PVA immobilized inulinase. Activity measurements were performed with chicory root inulin concentrations ranging from 10 to 120 g.L⁻¹ at pH 4.5 and 50°C. (A) 1 mL reactional system with agitation; (B) 1 mL reactional system without agitation; (C) 10 mL reactional system with agitation; (D) 10 mL reactional system without agitation. Plots obtained through Hyper32[®] software.

Table 6 – Summary of the kinetic parameters (V_{max} and K_M) for the free and PVA immobilized inulinase, with and without agitation in reactional volumes of 1 and 10 mL. Values obtained through a non-linear regression from Hyper32® software.

	FREE			
	1 mL		10 mL	
	Agitated	Non-agitated	Agitated	Non-agitated
$V_{max} / \text{g.L}^{-1}.\text{min}^{-1}$	0.19 ± 0.02	0.22 ± 0.03	0.23 ± 0.02	0.23 ± 0.02
$K_M / \text{g.L}^{-1}$	20.23 ± 7.80	22.98 ± 9.99	26.33 ± 6.34	28.23 ± 9.21
	PVA			
	1 mL		10 mL	
	Agitated	Non-agitated	Agitated	Non-agitated
$V_{max}^{app} / \text{g.L}^{-1}.\text{min}^{-1}$	0.92 ± 0.11	0.55 ± 0.04	0.37 ± 0.02	0.42 ± 0.06
$K_M^{app} / \text{g.L}^{-1}$	26.95 ± 9.88	25.42 ± 5.63	39.95 ± 5.90	41.17 ± 14.17

5. DISCUSSION

Oftentimes the immobilization efficiency with Amberlite IRC-86 showed to perform poorly (~30%) as the amount of enzyme immobilized in the support was rather low (data not shown). In order to solve this problem, a small change in the immobilization protocol was made and the glutaraldehyde solution was left for incubation overnight, leading to some improvement of the results (~60%). However, as the optimization of the immobilization conditions was not the main priority of this work, this aspect was not further studied. In that sense, additional studies on this subject could be performed, namely by assessing the optimal pH, glutaraldehyde concentration or incubation times for immobilization onto this specific support as well as an analytical analysis (e.g. FTIR [142]) to confirm the success of the chemical functionalization. This could be of crucial importance since the optimal conditions for glutaraldehyde activation could be underestimated. Nonetheless, the chosen approach, of increasing the glutaraldehyde incubation time, showed satisfactory results.

Table 7 – Immobilization efficiency for the two types of supports and methods used.

Support	Immobilization Method	Immobilization Efficiency
Amberlite IRC-86	Covalent binding	60%
PVA	Entrapment	94%

The immobilization protocol for Amberlite IRC-86 does not allow for precise efficiency calculations as the washing steps executed are often not meticulously quantified in terms of the washing buffer added as well as the reagents added for the support functionalization, which is why the shown value (Table 7) should only be taken of as a rough approximation. Nonetheless, it was seen that the approach with the covalent binding resulted in poorer results when compared with the ones obtained with the enzyme entrapment in PVA. Similar observations regarding the poor efficiency of the method for Amberlite IRC-86 have already been reported [64] as well as the far better results obtained with PVA entrapment [88].

5.1. Optimal pH and temperature

In order to develop the upcoming studies it was necessary to first determine the optimal pH and temperature of the reactions involving both inulin from *Dahlia* tubers (Figure 19) and chicory root (Figure 26). A summary of the results can be found in Table 8.

Table 8 – Summary of the optimal pH and temperatures observed for the different substrates and supports tested.

Inulin source	<i>Dahlia</i> tubers		Chicory root	
Enzyme support	Free	Amberlite IRC-86	Free	PVA
pH	5	4	3.5-4	3.5-4
Temperature	55	55	65	65

Regarding the reaction in which the substrate is inulin from *Dahlia* tubers, it is possible to see a shift in the optimal pH from 5 to 4 upon immobilization, suggesting that the immobilization favors the reaction to occur in more acidic environments than those of the free enzyme, an interesting point when considering the industrial purposes in which this reaction can be applied to. However this result is not as common as the many reported increases in the optimal pH for an immobilized enzyme when considering that the support used had an overall negative charge, even after functionalization [24], [64], [66], [78], [89]. Such event might be due to the previously mentioned lack of studies for the glutaraldehyde optimization, as there could still be a high amount of positive charges on Amberlite IRC-86 beads' surface resulting from the support modification with polyethylenimine, leaving it to act like an anionic exchanger instead. An uneven positive charge distribution across the support might have led to the creation of microenvironments close to the immobilized enzyme. If so, a higher density of negative charges might have built up, creating more basic environments around the enzyme (higher pH) than that of the solution (lower pH), where the measurement takes place [143]. Methods and notes regarding the monitoring of these particular pH microenvironments were previously discussed, being many focused on the use of opto-chemical sensors [21], [144].

As for the temperature, it is possible to see that 55°C is the optimal temperature for both the free and immobilized enzyme. Nevertheless, the major difference resulting from the immobilization is the fact that it contributed to a broader temperature profile that allows the work in a wider range of conditions. As shown in Figure 19, the immobilized reaction occurs almost at its maximum in a range of temperatures from 45°C to 65°C, whereas the free enzyme reaction only has a rather small range (from 55°C to 60°C) in which the reaction has a relative activity >90%. The improved stability of the immobilized inulinase might be due to its cross-linking with glutaraldehyde, as this reagent can have a protective role upon the active site, protecting it from distortion or heat damage [145], but only up to a limit of 70°C, where the enzyme activity decreases abruptly, probably due to denaturation.

As for the chicory root inulin (Figure 26), the differences in the pH for the PVA immobilized and the free enzyme are basically non-existent in the pH ranges of 3.5–5, but at pH 5.5 it can be said that the immobilization improved the reaction performance as the relative activity increased by 20%. Nonetheless the optimal pH falls within the pH range of 3.5–4. In order to proceed with the forthcoming assays, it was

decided to use the pH 4.5 (conversion of 87%), as at this pH the contribution of the non-enzymatic hydrolysis to the reaction is lower and also because this is the working pH recommended by the enzyme supplier.

Similar results were observed for *A. niger* inulinase immobilized in PVA particles in sucrose hydrolysis, where the immobilized enzyme showed higher activities at more acidic pH (pH 3.5–4.5) than that of the free form (pH 4.5) [137]. Rebroš *et al.* also reported an optimal pH in the range of 3.2–4.5 for PVA-immobilized invertase in sucrose hydrolysis, whereas for the free enzyme occurred only at pH 4–4.5 [35]. These events were assumed to result from secondary interactions that occurred between the enzyme and the PVA matrix during the immobilization. Despite the substrate differences making it impossible for a direct correlation, it can be assumed that the immobilized enzyme generally tends to have higher activities at more acidic environments than when in the free form.

Regarding the temperature, the optimal values were obtained at 65°C for both the free and immobilized enzyme. Similarly to the observed in Chapter 4.1.1, the immobilized enzyme shows improved activities at lower temperatures relatively to the free enzyme, also supporting the theory that immobilization increased the overall enzyme's tolerance to heat. However, the remaining experiments were carried at 50°C due to previously reported significant restrictions regarding the mechanical strength of the PVA beads and lens-shaped capsules (also known as Lentikats®) at temperatures equal or higher than 55°C [35], [146], [147].

Besides inulinase, other enzymes (e.g. β -glucosidase [148]) have shown similar observations regarding the optimum pH profile not becoming significantly altered with immobilization. Inulinase entrapped in a sol-gel (silica xerogel) matrix also reported unchangeable optimal temperatures of 65°C even upon immobilization [149]. Likewise, inulinase immobilized in cross-linked chitosan beads showed the same optimal temperature at 60°C as the free enzyme [142].

Considering the applications of immobilized enzymes, this approach proves to be advantageous from the economic point of view not only coming from biocatalyst reuse and downstream processing but also in terms of better reaction performance under acidic pH and in a wider range of lower temperatures.

5.2. Biotransformation with the free and immobilized enzyme

Preliminary studies on the overall reaction performance were done and it was concluded that inulin hydrolysis showed better yields in agitated reaction vessels than in similar non-agitated reaction vessels and that agitation did not seem to play a crucial role in small reactional volumes (data not shown). Nonetheless, further studies involving agitated and non-agitated 1, 3 and 10 mL systems were performed to get deeper insights into this subject. The role that agitation plays in the reaction performance was assessed by accompanying the first hour of the reaction and quantifying the amount of reduced sugars formed. The results regarding the reaction rates of all reactional systems are in Table 9.

Table 9 – Inulin hydrolysis rates (g.L⁻¹.min⁻¹) at 1, 3 and 10 mL, with and without agitation (440 rpm) for the different immobilization methods tested and the free enzyme. In all cases the R² was higher than 0.94, except for Amberlite IRC-86 without agitation at 3 and 10 mL where no linear correlation was observed.

	1 mL		3 mL		10 mL	
	With agitation	Without agitation	With agitation	Without agitation	With agitation	Without agitation
Free	0.786	0.787	0.926	0.999	0.934	0.954
Amberlite IRC-86	0.149	0.149	0.158	–	0.242	–
PVA	0.229	0.206	0.230	0.236	0.197	0.221

Free enzyme with Dahlia tubers substrate

Contrary to the observed for the majority of the reactions followed with both immobilized enzymes, when concerning with the free enzyme, the linear evolution of the reaction can only be assured in the very beginning (appx 30 min) as afterwards the system starts to show signs of almost total substrate conversion, and therefore losing the linear behavior.

At 1 mL, the non-agitated enzyme tends to have higher concentrations of reducing sugars over the time in which it was followed than the agitated reaction. Nonetheless, in terms of reaction rates both agitated and non-agitated reactions show the same performance and no clear advantages in using, or not, agitation are noticed. Such observation might suggest that the diffusion phenomena is enough for the reaction to occur.

Even though the reducing sugars concentration is higher for the free agitated enzyme at 3 mL, the reaction rate shows otherwise, as it is the non-agitated reaction that has the highest value. At the 10 mL scale both reactions, with and without agitation, evolve linearly in the first 30 minutes, where the amount of reducing sugars released in the non-agitated reaction starts to be lower than in the agitated reaction. Even though, it is in the non-agitated reaction that the hydrolysis rate is higher. The lower reaction rates in these two agitated reactional volumes could be due to inadequate mixing, however as the reaction with the free enzyme is relatively fast, leading to almost completion after one hour it is difficult to clearly see such effects. Nonetheless, when comparing the reaction performance at 3 mL and 10 mL it is possible to see that at 3 mL the reaction does not achieve conversions as high as the ones at 1 mL and 10 mL.

Amberlite IRC-86 immobilized enzyme with Dahlia tubers substrate

Regarding the enzyme immobilized in Amberlite IRC-86, the importance that agitation plays as the reactional volume increases is well evident as the linear evolution of product formation over the course of the reaction (Figure 20) is gradually lost (Figure 21 and Figure 22). This trend is well reflected in the hydrolysis rates present in Table 9, as the more random and disperse measurements at 3 mL and 10 mL without agitation, suggestive of increasing heterogeneity and poor mixing, do not show any linear

correlation. Interestingly enough, just like the registered for the free enzyme, no differences in the hydrolysis rate of the lowest reaction volume with and without agitation were seen.

Therefore, these results seem to indicate that as the reactional volume increases, so does the importance of having optimized agitation to overcome the mass transfer limitations of the substrate and the enzyme, suggesting the need for convective flow in solid-liquid systems even for relatively low reaction volumes, unlike what is observed for homogeneous systems.

As for the agitated reaction, it is possible to see a trend towards higher hydrolysis rates at higher reactional volumes, as observed with the free enzyme (Table 9). Yet, at 10 mL (Figure 22) it was possible to observe that the linear correlation was the weakest ($R^2 = 0.94$), which might suggest that the agitation input was reaching a value where it was not enough to maintain the homogeneity of the reaction.

In a last look at Figure 20, Figure 21 and Figure 22 it is yet possible to observe that after 1 hour the amount of sugars that were hydrolyzed in the immobilized agitated enzyme system is the lowest for the 3 mL volume (18%) and the highest for the 10 mL volume (35%). Similar observations were also made regarding the free enzyme. Overall it was expected for the systems to show similar performances since the scale up (from the 1 mL to the 10 mL reaction) was proportional, however the results suggest that a further insight into the system hydrodynamics' could be of relevance. The fact that the 3 mL reaction was performed in the same vessels as the 1 mL reaction, and that the 10 mL was proportional to the 1 mL vessel, strengthens this hydrodynamic-based premise.

PVA immobilized enzyme with Dahlia tubers substrate

Contrary to the observed with the Amberlite-based immobilization system, in the case in which the enzyme was immobilized in PVA, the overall diffusional effects related with the presence or absence of agitation were not as evident. In the case of the 1 and 10 mL reactional systems, the evolution of the reaction with agitation showed to perform equally good or even better over time than without agitation.

Considering the 1 mL reactional volume (Figure 23), it is possible to observe that the presence of agitation only seems to start being relevant after 30 minutes as, until then, both agitated and non-agitated reactions show a very similar linear behavior. After the first 30 minutes, higher reducing sugars concentrations in the agitated reaction might be the consequence of the higher homogeneity level given to the medium through agitation. The higher hydrolysis rate for the agitated reaction (Table 9) might support such statement. These results show to be in contrast with the observed with the free and Amberlite IRC-86 immobilized enzyme, where the systems showed that the intrinsic diffusional mechanisms in the non-agitated reactions were enough to keep up with the agitated reaction.

Just like the observed for the free enzyme, at the 10 mL scale the differences regarding the reducing sugars concentrations throughout the time (Figure 25) are practically null. However, the hydrolysis rates (Table 9)

show slightly higher values for the non-agitated reaction. With PVA the diffusional restrictions that affect the overall reaction are not as intense as with the covalently linked enzyme (evidenced through linearity losses) but, theoretically, they should be higher than with the free enzyme. Therefore, the fact that the agitated reaction evolves in the same way as the non-agitated, and at lower rates than with the remaining volumes, might be a signal of poor mixing, or in other words the stirring speed might need to be readjusted.

As for the 3 mL reactional volume (Figure 24), the non-agitated reaction tends to show higher reducing sugars concentrations throughout the time whereas the agitated reaction concomitantly tends to show a more linear evolution. Still, the difference in the reaction rates with and without agitation is virtually negligible (Table 9). It is worthy to note that, as previously said, the vessel used for this reactional volume is not properly designed, meaning that there might be some space limitations upon the PVA beads that could compromise their availability or interactions towards the substrate.

Overview on the biotransformation reaction

While the overall results suggest that agitation does not have a crucial role in the smaller reaction volumes, where the diffusional effects seem to be enough to power the reaction, the tests with the enzyme immobilized in Amberlite IRC-86 were pretty clear in showing how important agitation becomes with increasing reactional volumes. Such was corroborated by the fact that no differences between the agitated and non-agitated reaction were seen at 1 mL (as with the free enzyme) whilst at 3 mL the system already started to show signs of heterogeneity, which continued at 10 mL. With the enzyme immobilized in PVA such evidences started readily at the 1 mL scale. Interestingly, both reactions seem to have different ways to evidence the diffusional limitations and need for agitation. While for the enzyme immobilized in Amberlite IRC-86 that was noticed through the loss of the linear behavior of the reaction over the time, with the enzyme immobilized in PVA that seemed to happen through a decrease in the velocity of the reaction, still under a linear evolution of the reaction.

As previously mentioned, the differences in the size of the immobilization supports may be responsible for such observation. While the PVA beads are relatively large (appx diameter of 3-4 mm), the same does not happen for Amberlite IRC-86, as when these particles are in non-agitated vessels the packing is, in great part, responsible for hindering enzyme that otherwise would be available for reaction. With PVA this packing effect is less significant due to the higher volume of the beads, which leaves more inter particle space to allow the occurrence of the normal diffusion mechanisms.

Considering only the increasing reactional volumes in the agitated reactions, there is enough evidence to believe that both immobilized systems could use an optimization in the stirring rates. Therefore, further increases in the reaction volume and/or stirring speeds would be interesting to corroborate this hypothesis. Yet, the overall results corroborated the hypothesis formulated during the preliminary studies.

In a quick look to the hydrodynamics, namely the liquid column height to vessel diameter ratio (H/D) (Table 10), one can see that the H/D of the 1 and 10 mL volumes are very similar, as opposed to the 3 mL reactional volume. Once again, this evidence supports that the vessel geometry could be compromising the proper reaction scale up.

Table 10 – Liquid height to vessel diameter ratio for the different reactional volumes under study.

Reaction Volume / mL	1	3	10
D_{vessel} / cm	1.2	1.2	2.5
H_{liquid} / cm	0.9	2.7	2.0
H/D	0.7	2.2	0.8

It is possible to notice that the PVA immobilization tends to show higher hydrolysis rates than the immobilization with Amberlite IRC-86, which could not only be related to the immobilization efficiency but also to the immobilization method itself. In the case of PVA the enzyme is entrapped within a network which protects the enzyme from the direct contact with the environment and minimizes the shear effects that might affect its activity [6]. While the enzyme is not bound to the membrane, some enzyme leaking might occur, which might also be responsible for the higher hydrolysis rates. There are reported studies on the stabilizing effects of PVA and PEG on the hydrolysis activity of some enzymes that show that in their presence the enzyme turns to be more active [37].

Table 11 – Qualitative comparison between Amberlite IRC-86 and PVA-based immobilization systems.

Parameter	Amberlite IRC-86	PVA
Immobilization Procedure (Laboriousness)	+++	+
Immobilization Efficiency	+	+++
Diffusional Limitations	+++	+
Hydrolysis Rate	+	+++

From Table 11 it is possible to make some general assumptions for practical purposes e.g., we can infer that the Amberlite IRC-86 immobilized enzyme system is the one that shows more limitations in being implemented for similar processes in the sense that it is the one that shows higher diffusional limitations, lower immobilization efficiencies and lower rates of hydrolysis. When considering an industrial purpose, the PVA immobilization approach seems to be the most benefic, relatively to Amberlite IRC-86, due to its relative inexpensiveness, easiness of application and downstream procedures [35].

5.3. Hydrodynamic environment within scale up

Regarding the hydrodynamic aspects of the reactional system, it was observed that the n values assumed did not correctly describe the system under study, as the reaction rates in a 10 mL scale were rather lower than the ones in the 1 mL scale (Figure 27). Such observation can suggest that this particular system for inulin hydrolysis is not well described by such scale up criteria and that further studies should be focused on it. Another important factor to consider is that the ratio on the scale up of the vessels and magnetic agitators is not exactly the same ($T_2/T_1 = 2.08$ vs. $Z_2/Z_1 = 2.22$; $D_2/D_1 = 1.67$ vs. Length of the magnet_{10mL}/Length of the magnet_{1mL} = 1.88), neither the H/D ratio of the 1 and 10 mL reactional system (Table 10). Therefore, it can be inferred that both the n value as well as the dimensions should be further optimized in order to obtain similar reaction rates in both scales.

In another test, to study the overall behavior of the reaction by only changing the stirring speed of the magnetic agitator, it was observed that the initial velocity of the reactions tend to increase as the stirring speed increases, but up to a limit of 900 rpm, where then the velocity starts to fall (Figure 28). Such observation can suggest the existence of some enzyme deactivation or the existence of shear stress effects, due to the intense agitation, on the enzyme, especially at 1200 rpm, where the reaction basically does not occur. In fact, as the magnetic stirrer stands in the bottom of the vessel, there could have been some severe enzyme abrasion occurring between the bottom of the vessel and the agitator [150]. Studies to assess the size and shape of the particles at the end of the tests are suggested.

5.4. Microtiter plates assays

The hydrodynamic studies regarding the reaction performance in MTP were conducted with both immobilization supports.

Dimensionless numbers (Fr_a , Re and Ph) were used to characterize the mixing process, which are intrinsically correlated with the shaking diameter and the shaking speed (Table 3). Regarding the agitation with the Agitator 1, all of the conditions, except for Plate A when agitated at 700 rpm, showed to be out-of-phase, meaning that the operating conditions were not the most favorable and that the liquid did not follow the movements of the shaker. For Agitator 2, the influence of the agitation rate on the fluid flow is quite evident, as at 110 rpm the system is always out-of-phase whereas when this value is increased to 170 rpm, the system enters in-phase – the most favorable conditions. The presence of in-phase conditions is important to guarantee that the fluid in the wells moves consistently with the shaking input, optimizing mixing and, therefore, making the substrate more available to the enzyme [113], [117].

As previously mentioned, the fact that plates B and C in Agitator 1 are out-of-phase at 700 rpm is related with the limitations associated with the unrealistic demands of the shaking speed. Considering the variables used for the calculations (Equation 6 and 7) and the filling volume in Plate A, such difference is probably

due to the large diameter of the wells in these plates. On the other hand, lower volumes and slight increases in the shaking speed could have changed the system to in-phase conditions. However, that was not done as the intentions of keeping the same conditions across the assays would be compromised if so.

In a quick look at Figure 29 it is possible to see better rates for the enzyme immobilized in Amberlite IRC-86 than in PVA. On the other side it is also with Amberlite IRC-86 that the differences between the plates tested is higher. Such results might be explained by the diffusional limitations inherent to each method, however that is not the only factor influencing the system.

Impact of the agitation rate and shaking diameter

Regarding the PVA immobilized enzyme system, in general, increases in the shaking frequency of Agitator 1 ($D_o = 1.5$ mm) lead to faster reactions, however all of these results occurred under out-of-phase conditions, except for Plate A. In Plate A at 700 rpm, the conditions are in-phase and showed to be slightly lower than those at 450 rpm, which is out-of-phase. The fact that the plates under out-of-phase conditions always show considerably better outputs to higher shaking speeds than the plate with the supposed optimal conditions might suggest that the poor mixing and reproducibility of these might have contributed to some in-well inhomogeneity. However, as no other valid results are available for comparison, no further conclusions regarding the effect of the agitation rate in Agitator 1 were made. In Agitator 2 ($D_o = 25$ mm), the increases in the shaking frequency that changed the out-of-phase to in-phase conditions slowed the reaction in the three plates. Once again, the lower reaction rate at 170 rpm and in-phase conditions might be a result of the better mixing conditions, as in these the liquid does not tend to stay motionless at the bottom of the well.

Regarding the system with the enzyme immobilized in Amberlite IRC-86, the complete opposite was observed with Agitator 1: increases in the shaking frequency lead to slower reactions, however all of these results occurred under out-of-phase conditions, except for Plate A, in which the reaction rate showed higher values under in-phase conditions. For Agitator 2 the results are very different from plate to plate, suggesting a more complex system where the agitation rate cannot be considered independently and additional factors might be influencing the result.

Considering that the experiments occurred in parallel under the same conditions, the reason for such differences might be related to the filling content of the wells, and most probably to the volume differences of the very small Amberlite IRC-86 particles relatively to the bigger PVA beads.

Impact of the well shape

To assess the effects of the well shape in the hydrolysis reaction, a 24-square well, pyramidal bottom MTP (Plate B) is compared to a 24-round well, flat bottom MTP (Plate C) (Figure 29). Given that the only time in which these two MTP are under favorable fluid flow conditions is in Agitator 2 ($D_o = 25$ mm) at 170 rpm, the

comparison is made solely by relying in these points. Once again the conclusions are influenced by the immobilization method used. With Amberlite IRC-86 the change from square to round wells shows an increase of 8% in the hydrolysis reaction whereas with PVA a decrease of 9% is observed.

The effects of this change of shape under out-of-phase conditions also always shows an increase in the reaction rate with Amberlite IRC-86. For PVA, in general very slight decreases are seen with the exception of PVA in Agitator 2 at 110 rpm. Still, these last observations will not be further considered as the conditions were not the most appropriate.

Impact of the well dimensions

The effect of the well dimensions upon the reaction can be studied by comparing Plate A with Plate B, when both are operated with a filling volume of 1 mL. The results must be carefully analyzed though as the considerations must be made when the system is under the most favorable conditions for fluid flow. Therefore the observations for Plate A vs. B in Agitator 1 should be discarded.

Considering only the data for Agitator 2 at 170 rpm, the reaction rates shown in Figure 29 show that, for both immobilized enzymes, the reaction rate tends to decrease when the operation changes from a 0.8 x 0.8 mm well to a 17 x 17 mm well. However while such decrease is almost negligible with the enzyme immobilized in PVA, the same does not happen for Amberlite IRC-86, where the change is to almost half.

Impact of the filling volume

To study the impact of the filling volume, Plate B will be used, as the assays included a filling volume of 1 and 3 mL (Figure 29). Even though the results follow the same trend regardless of the agitation rate, the comparisons will only be made for the plates subjected to orbital agitation at 170 rpm, which were the most favorable in terms of fluid flow.

For the Amberlite IRC-86 immobilized enzyme is possible to notice an increase of almost 95% in the reaction rate whereas for PVA the reaction rate does not suffer alterations.

Considering that the proportions of the enzyme and substrate solution were kept the same, the differences observed must arise from the fact that the changes in the filling volume are not accompanied by proportional changes in the well dimensions, which results in a difference in the height of the liquid column.

Overall discussion of MTP

The characterization of the mixing mechanisms in MTP is not yet fully established. Although there is some information relative to their influence in fermentations, mainly based in OTRs, the information regarding the influence of hydrodynamic aspects and flow dynamics in MTP is not very abundant.

Overall the results obtained were a bit conditioned due to the fact that not all of the conditions studied for the higher shaking speeds in Agitator 1 were in-phase. Still, comparisons were made relying on the data obtained for Agitator 2. It was possible to observe that the systems showed very different behaviors accordingly to the immobilization support used.

Regarding the agitation rates and the orbital diameters tested, the results showed that in general when the conditions changed from out-of-phase to in-phase the reaction rate tended to become a little slower for PVA-immobilized enzyme (Plate A in Agitator 1 and all plates in Agitator 2) whereas with Amberlite IRC-86 immobilized enzyme the results were not that straightforward, as increases were registered for Agitator 1 and oscillating behaviors are seen throughout the plates in Agitator 2.

Studies in 8 x 8 mm wells in 96-well MTP focused in the increase of the shaking frequency from 200 to 400 rpm at a shaking diameter of 25 mm have shown to promote a 6-fold increase in the OTR of the system. However such increase decreased only to the double when the shaking diameter was 50 mm [151]. Similar results were also observed for 48-well MTP [113], [118]. The higher OTRs were ascribed to the thin fluid layer and higher gas/liquid mass transfer area present in the smaller shaking diameters resulting from the complete fluid distribution over the walls of the wells instead of just a portion, as observed at higher shaking diameters [118]. Even though the studies performed do not involve gas/liquid mass transfer phenomena, these reports might help to establish a set equilibrated conditions between the shaking frequency and diameter in order to obtain better results.

Additional studies with the theoretical angle formed between the liquid inside the wells and the walls could complement such observations. The angles predicted were of 9.65° and 22.35° , but their influence was not further studied. Nonetheless it seems pertinent to consider such factor as reports regarding OTRs in MTP equivalent to Plates A and B have shown to require angles as high as 70° and 45° , respectively, in order to provide good culture conditions [123].

As for the remaining parameters under study, it seems that the enzyme immobilized in Amberlite IRC-86 benefited from the change from square to round wells whereas with PVA did not.

Contrary to the observed herein with inulinase immobilized in PVA, in a similar study using naringinase entrapped in PVA, operation in 24-round well, flat bottom MTP (Plate C) favored the reaction rate when compared to 24-square well, pyramidal bottom MTP (Plate B) [123]. Other authors although have reported improved biocatalyst performances in 96-square-well MTP than in 96-round-well MTP however, the studies were performed with cells and lower filling volumes [138].

Measurements of the liquid height were made in 48-round well MTP to reveal that as the shaking frequency increased, the liquid height decreased whereas for 48-square well MTP the liquid height tended to be higher comparatively to the round wells, which is in agreement with the fact that higher centrifugal forces drain off the well bottoms by sending the liquid against the walls of the wells [152]. However in squared shaped wells the higher baffling degree, responsible for reducing the liquid motion, combined with the higher breakup of the bulk, responsible for the increase in the superficial area, resulted in higher OTR_{max} [152].

Accordingly, better outputs in square wells have been widely credited to the higher turbulences achieved in such geometry [153] that has been reported as having a similar effect to those of baffles in shake flasks [121]. Still, reports highlight a limit to the baffling degree not to compromise the systems, as for example star-shaped and baffled-cylinder geometries could in fact prejudice the system by stopping liquid motion [152].

Usually in shaken bioreactors a strategy to obtain higher OTRs is by increasing of the vessel diameter [152]. This approach is supported partly in the increase of the surface-to-volume ratio and in the attenuation of the capillarity forces, as these forces can compromise the shaking effectiveness and, in turn, the mass transfer mechanisms [113], [118]. Therefore, changes in the operation from 96-well to 48-well (or even further, 24-well) MTP can minimize such negative effects [153].

The influence of the well dimensions was more significant for the covalently-bonded than for the entrapped enzyme. The fact that the same filling volume went from a smaller to a larger well, decreasing the height of the liquid column was expected to benefit the reaction, which did not occur. Although, such expectation was based on reports that depend on high superficial areas to allow gas/liquid mass transfer, and keep the microorganisms in cultivation alive, which is not the case. In here, as the size of the wells increased, so did the dispersion of the solution and the fact that both plates have different bottom configurations might help to understand the results obtained.

The fact that, Plate A has a U-shaped form and Plate B has a pyramidal one, might have contributed to the poorer reaction with Amberlite IRC-86 and to evidence some particle hindering that could have affected negatively the reaction. Once again the spatial distribution of the enzyme particles might be of relevance specially when considering that the differences in the bottom geometries might require different agitations to keep the particles in suspension. In the case of Amberlite IRC-86, there might be some hindering by the particles closer to the bottom (at the top of the inverted pyramid) due to spatial restrictions that delayed the reaction. With PVA the differences regarding the changes in well dimensions and bottom configurations are practically null, and the fact that there were only present 3 beads per well without significant hindering (visual observation) might support such hypothesis.

Regarding the filling volume, literature reports show that higher OTRs are obtained with lower filling volumes [113], [152]. This observation was also not observed in the results obtained and it might also be due to the differences in the liquid height and particle dispersion inside the wells, as already discussed. Still, the high

increase in the initial velocity seen for Amberlite IRC-86 might be due to the higher amount of biocatalyst that might not be hindered at the bottom of the vessel (now there is 3 times more enzyme present), as what was assumed to occur at the reactional volume of 1 mL. For PVA the changes were unnoticeable, which might support the previously comment regarding the changes in the well dimensions. However further insights should be focused on this specific observations.

Overall the Amberlite IRC-86 showed to be the most susceptible system to the alterations imposed while with PVA the alterations observed were always more discrete and at lower values, which might suggest that the reaction is slower due to intrinsic restrictions of the immobilization method itself. There is a great amount of literature regarding the influence of the tested parameters in microbial cultures that also highlight the importance of not considering each parameter as one but rather focusing on the importance in combining experiments and take full advantage of the high throughput capacity of microtiter plates.

5.5. Enzyme activity

Immobilization can sometimes change significantly the kinetics of an enzyme due to the inherent conformational changes of the immobilization process itself or the support in which the immobilization occurs. Thus, to assess if immobilization improved or not the kinetics of the enzyme, the kinetics of the free enzyme in solution were compared to the kinetics of the immobilized fructanase (Table 5 and Table 6). In order to do so, it was assumed that the reaction followed a Michaelis-Menten kinetics [141].

The Michaelis constant, K_M , is a kinetic parameter that represents the substrate concentration at which the reaction rate is half its maximum value. Since enzymes with small K_M values achieve their maximum catalytic efficiency at lower substrate concentrations, the smaller the value of K_M , the more efficient is the catalyst.

The data obtained (Table 5 and Table 6) shows higher K_M^{app} values for both immobilized enzyme systems than the K_M values for the free enzyme, which means that the reactions became less efficient upon immobilization. In fact such result is not, at all, unexpected as the immobilization process can affect the enzyme's catalytic activity, or even its affinity towards the substrate. The effects of mass transfer resistance are common of immobilized systems and have been reported in PVA-alginate matrices, where enzyme (nariginase) entrapment made the substrate access to its active site rather more difficult, which was reflected in the overall reaction performance (K_M increased by 1.5-fold upon immobilization) [140].

In the case of the PVA immobilized and free enzyme with chicory root inulin (Table 6), there is an increase of the K_M and K_M^{app} with the volume, and within a determined volume, it also tends to increase if the agitation is lost, except for the case of the 1 mL non-agitated immobilized enzyme, however such difference might not be that relevant when considering the associated error. These results suggest that the efficiency of the reaction tends to decrease with bigger non-agitated reactional volumes.

As for the Amberlite IRC-86 immobilized and free enzyme with *Dahlia tubers* inulin (Table 5), the results are not that straightforward as, when considering only the 1 mL and 10 mL systems, the Michaelis constant tends to decrease when the volume is increased. However, the parameters calculated are fairly higher than the ones observed with PVA and chicory inulin, meaning that even though a small improvement might be observed when the volume is increased, the overall reaction with *Dahlia tubers* inulin is still much less efficient. As for the agitation, there is not any trending behavior that can be used to formulate conclusions.

Another parameter is the V_{max} , which corresponds to the maximum velocity of the enzymatic reaction, and is reached when all enzyme sites are saturated with substrate.

In the results from Table 2 it is possible to observe that this parameter decreases upon immobilization. Such result is also not surprising as after the immobilization procedures it is usual for the enzyme to lose some activity and thus to decrease the hydrolysis rate [10]. On a different perspective, it is possible to infer that the V_{max} also tends to decrease as the reactional volume increases. However, when considering the same reactional volumes, when the agitation is lost the V_{max} tends to increase, which might suggest that the presence of agitation might not be that beneficial.

However, in the case in which the substrate was inulin from chicory root, the results show that V_{max} actually increases (up from 2-fold to 5-fold for the 1 mL agitated system) upon enzyme immobilization in PVA. Shifting the analysis angle to the effects of increasing the volume from 1 mL to 10 mL, it can be seen that this alteration has little effect on the free enzyme system, just like the loss of agitation, as the V_{max} parameter is barely affected.

For the PVA immobilized system, increasing the reactional volume translates in a decrease of the V_{max} parameter, however the overall results show that the only reaction that seems to be truly affected and slowed down by the loss of agitation is with the immobilized enzyme at 1 mL.

A similar study performed with Fructozyme L from *A. niger* and inulin from chicory (Fibrulin Instant – Cosucra) with a degree of polymerization of 10. While the free enzyme showed a K_M of $26 \pm 3 \text{ g.L}^{-1}$ and a V_{max} of $2.7 \pm 0.1 \text{ g.g}_{enzyme}^{-1} \cdot \text{s}^{-1}$ its immobilization in Lentikats[®] increased the K_M^{app} to $43 \pm 8 \text{ g.L}^{-1}$ and decreased the V_{max}^{app} to $1.1 \pm 0.2 \text{ g.g}_{enzyme}^{-1} \cdot \text{s}^{-1}$ [146]. In the case of the Michaelis constant, the change in the value due to immobilization is of 1.7 fold in the reference values while in the observed ones is, at maximum, 1.5 fold. Using the same methodology with Fibruline S-20 (degree of polymerization of about 10-12 units) resulted in a K_M of $17 \pm 7 \text{ g.L}^{-1}$ and a V_{max} of $3 \pm 0.3 \text{ g.g}_{enzyme}^{-1} \cdot \text{s}^{-1}$ for the free enzyme and a K_M^{app} of $22 \pm 8 \text{ g.L}^{-1}$ and a V_{max}^{app} to $0.6 \pm 0.1 \text{ g.g}_{enzyme}^{-1} \cdot \text{s}^{-1}$ for the enzyme immobilized in Lentikat[®] PVA hemispheric beads [88].

Nonetheless it can be said that by using a very similar immobilization method (Lentikats® vs. beads), and despite the fact that the enzyme and the substrate used being different from the reference ones, the results obtained are fairly similar.

It should be noted that the kinetics of this reaction can vary greatly with the degree of polymerization of inulin, as the size of the molecule can affect the hydrolysis rate and the affinity between the enzyme and the substrate, and, consequently, the kinetic parameter under study (see Chapter 1.3.3.2) [85]. Therefore it is suggested the realization of tests to relate the K_M with the polymerization degree, specially focused on the commercial available inulin sources under study, which have been reported to have an average DP of 28 [154]. In fact it has already been reported that the degree of polymerization of chicory root inulin affected the kinetics of inulinase (Fructozyme L™) covalently immobilized into Sepabeads®. It was observed that real inulin, from crude extracts, with a DP of 6.4 showed a K_M of 7.0 g.L⁻¹ and a V_{max} of 0.2 g.L⁻¹.min⁻¹ while pure inulin, of reagent grade, with a DP of 28 showed a K_M of 49 g.L⁻¹ and a V_{max} of 0.2 g.L⁻¹.min⁻¹, i.e. it was observed that the higher the degree of polymerization the higher the K_M and, consequently, the less efficient the biocatalyst, as the affinity between the enzyme and the substrate is lower [155]. This is of particular importance since this property can significantly influence the overall design and/or performance of a process, with clear economic repercussions.

In that sense, a kinetic model to describe the enzymatic hydrolysis of chicory root inulin by immobilized inulinase considering the changes of inulin MW over the course of the reaction was developed to account for the significant effects this variation could have in the reaction, namely in the enzyme kinetics and in mass transfer phenomena [154]. The model was reported to show satisfactory results in considering the phenomena that can affect the reaction rate and in predicting the kinetic parameters [154].

Besides the factors related with the immobilization method and the properties of the support and or substrate, the overall rate of the reaction is also affected by external and internal mass transfer resistance phenomena between the solid and liquid phase (support and substrate in the bulk phase) [156] and pore diffusion, respectively [157], which is why ideally the intrinsic kinetics of the reaction should be determined in the absence of such.

6. CONCLUSIONS AND FUTURE WORK

For the work developed, two immobilization protocols were used: Amberlite IRC-86 was used as support for the covalent binding of inulinase and PVA was used for entrapment. Both methods showed satisfactory results to be used in the upcoming experiments, however it became clear that Amberlite IRC-86 showed rather poor immobilization efficiencies (appx 60%) when compared to the good performance of PVA (94%). For future reference it is highly advised to carry studies regarding the optimization of the Amberlite IRC-86 immobilization protocol, more precisely regarding the glutaraldehyde incubation conditions (e.g. incubation time, temperature, pH and concentration), and also to carry experiments to analyze the enzyme distribution throughout the support.

Enzyme characterization in terms of optimal pH and temperature was done for both immobilized forms. For the immobilization in Amberlite IRC-86 and PVA no major differences regarding the optimal temperature, 55°C and 65°C, respectively, were seen upon immobilization. However, both forms showed increased activities for the lower temperatures tested (from 45°C to 65°C), being the outcome more obvious for the covalently immobilized enzyme. Yet, the forthcoming procedures with PVA would have had to be done at 50°C due to the mechanical strength restrictions of this hydrogel to high temperatures (>55°C). Regarding the pH, enzyme entrapment led to practically no changes in the optimal pH range of 3.5–5, observed for both free and immobilized forms, but improvements on the immobilized form activity were registered for pH 5.5. As for Amberlite IRC-86, a shift from pH 5 to 4 was observed upon immobilization. Overall, enzyme immobilization proved to be a solid method of increasing enzyme's tolerance to heat and lower pH, a combination of special relevance in the industrial sectors to which this reaction can be applied.

The tests to investigate the influence of agitation in the reaction with the free and both immobilized enzymes revealed that the reaction with Amberlite IRC-86 was the one who struggled the most with the increasing volumes under non-agitated conditions. Still, whereas for Amberlite IRC-86 the need for agitation was only noticed for volumes higher than 3 mL, for the enzyme immobilized in PVA such occurred at 1 mL. Interestingly, the mechanisms through which those evidences were noticed were different, as for Amberlite IRC-86 non-correlated measurements occurred whereas for PVA the reaction rate decreased. Overall, agitation does not seem have a crucial role in the smaller reaction volumes, where the diffusional effects seem to be enough to control the reaction. There were also reasons to believe that the non-optimized conditions in the 3 mL vessel could have negatively influenced the reaction and that both immobilized enzymes could use an optimization in the stirring rates at volumes higher than 10 mL. Therefore, it would be interesting to further design an appropriate 3 mL vessel and to increase the reaction volume and/or stirring speeds to corroborate these hypothesis.

A scale up attempt from 1 to 10 mL based on common scale up criteria was not well succeeded as the reaction performance changed significantly. The correct prediction of the scale up factor that correctly

describes the system under study and the use of properly and case-specific dimensioned vessels and magnets, with proportional ratios between every length, is strongly suggested.

The kinetic parameters determined showed an overall decrease in the enzyme efficiency ($K_M < K_M^{app}$) upon immobilization for both supports. With PVA a further decrease in the reaction efficiency was registered for increasing non-agitated reactional volumes. Struggles to formulate conclusions on the behavior of Amberlite IRC-86 immobilized enzyme to volume increases and agitation loss arose but it was evident that its performance was much less efficient than with PVA. As for the V_{max} , Amberlite IRC-86 data showed that the reaction slowed down upon immobilization but it could become faster at higher volumes, although the presence of agitation did not seem to be that beneficial. For PVA, an increase in the V_{max} was observed upon immobilization and the behavior to higher reactional volumes was similar to the observed for Amberlite IRC-86. The only situation that seemed to be truly affected and slowed down by the loss of agitation was at 1 mL.

Lastly, MTP were used to find the best conditions for inulin hydrolysis. The results varied greatly with the type of immobilized enzyme used and showed a great dependence on the conditions of the fluid flow. No straightforward correlation regarding the agitation rate or the shaking diameter across the different plates could be made, however it was evident that under in-phase conditions increases in the shaking frequency at high shaking diameters slowed the reaction with PVA and had different effects with Amberlite IRC-86, depending on the plate's geometry. In terms of well shape, round-wells showed to be the most benefic for Amberlite IRC-86 and squared-shaped for PVA. The increase in the well's dimensions decreased the reaction rate with Amberlite IRC-86 to almost half of the value registered in the smaller wells, whereas when the filling volume was triplicated, the reaction rate almost doubled. In both situations, with PVA the alterations were so discrete that it could be said that no alterations were seen upon increasing well dimensions or filling volume.

One of the factors that seemed to affect the reaction in the MTP experiments was the size of the particles, although no further studies on this topic were followed. Therefore, it would be interesting to further assess the influence of this parameter. It was also assumed that the temperature variation across the wells and the evaporation rate were negligible, but that is not always the case. In that sense further investigation towards the impact of these factors, as well as the assessment of the existence of pH microenvironments around the immobilized enzyme, would be of interest.

The establishment of a set of optimal conditions for inulin hydrolysis in MTP with higher outputs than those of small vessels would be an interesting way to establish these miniaturized devices as crucial for bioprocess development and intensification.

7. REFERENCES

- [1] S. Li, X. Yang, S. Yang, M. Zhu, and X. Wang, "Technology Prospecting on Enzymes: Application, Marketing and Engineering," *Comput. Struct. Biotechnol. J.*, vol. 2, no. 3, pp. 1–11, Sep. 2012.
- [2] O. Kirk, T. V. Borchert, and C. C. Fuglsang, "Industrial enzyme applications," *Curr. Opin. Biotechnol.*, vol. 13, no. 4, pp. 345–351, Aug. 2002.
- [3] M. Ghaffari-Moghaddam, H. Eslahi, D. Omay, and E. Zakipour-Rahimabadi, "Industrial applications of enzymes," *Rev. J. Chem.*, vol. 4, no. 4, pp. 341–361, Oct. 2014.
- [4] "Industrial Enzymes Market worth 6.2 Billion USD by 2020." [Online]. Available: <http://www.marketsandmarkets.com/PressReleases/industrial-enzymes.asp>. [Accessed: 13-Dec-2015].
- [5] A. Liese, K. Seelbach, and C. Wandrey, Eds., *Industrial biotransformations*, 2nd ed. Weinheim: Wiley-VCH, 2006.
- [6] R. A. Sheldon, "Enzyme Immobilization: The Quest for Optimum Performance," *Adv. Synth. Catal.*, vol. 349, no. 8–9, pp. 1289–1307, Jun. 2007.
- [7] J. C. Y. Wu, C. H. Hutchings, M. J. Lindsay, C. J. Werner, and B. C. Bundy, "Enhanced Enzyme Stability Through Site-Directed Covalent Immobilization," *J. Biotechnol.*, vol. 193, pp. 83–90, Jan. 2015.
- [8] B. M. Brena and F. Batista-Viera, "Immobilization of enzymes," in *Immobilization of enzymes and cells*, Springer, 2006, pp. 15–30.
- [9] S. Datta, L. R. Christena, and Y. R. S. Rajaram, "Enzyme immobilization: an overview on techniques and support materials," *3 Biotech*, vol. 3, no. 1, pp. 1–9, Feb. 2013.
- [10] J. M. Bolivar, I. Eisl, and B. Nidetzky, "Advanced characterization of immobilized enzymes as heterogeneous biocatalysts," *Catal. Today*, vol. 259, pp. 66–80, Jan. 2016.
- [11] D. Brady and J. Jordaan, "Advances in enzyme immobilisation," *Biotechnol. Lett.*, vol. 31, no. 11, pp. 1639–1650, Nov. 2009.
- [12] R. DiCosimo, J. McAuliffe, A. J. Poulouse, and G. Bohlmann, "Industrial use of immobilized enzymes," *Chem. Soc. Rev.*, vol. 42, no. 15, p. 6437, 2013.
- [13] S. S. Betigeri and S. H. Neau, "Immobilization of lipase using hydrophilic polymers in the form of hydrogel beads," *Biomaterials*, vol. 23, no. 17, pp. 3627–3636, 2002.
- [14] A. Kumari and A. M. Kayastha, "Immobilization of soybean (*Glycine max*) α -amylase onto Chitosan and Amberlite MB-150 beads: Optimization and characterization," *J. Mol. Catal. B Enzym.*, vol. 69, no. 1–2, pp. 8–14, Apr. 2011.
- [15] A. Dwevedi and A. M. Kayastha, "Stabilization of β -Galactosidase (from Peas) by immobilization onto Amberlite MB-150 beads and its application in lactose hydrolysis," *J. Agric. Food Chem.*, vol. 57, no. 2, pp. 682–8, Jan. 2009.
- [16] A. Anita, C. A. Sastry, and M. A. Hashim, "Immobilization of urease using Amberlite MB-1," *Bioprocess Eng.*, vol. 17, no. 6, pp. 355–359, 1997.
- [17] R. Catana, M. Eloy, J. R. Rocha, B. S. Ferreira, J. M. S. Cabral, and P. Fernandes, "Stability evaluation of an immobilized enzyme system for inulin hydrolysis," *Food Chem.*, vol. 101, no. 1, pp. 260–266, Jan. 2007.
- [18] V. Minovska, E. Winkelhausen, and S. Kuzmanova, "Lipase immobilized by different techniques on various support materials applied in oil hydrolysis," *J. Serbian Chem. Soc.*, vol. 70, no. 4, p. 609, 2005.
- [19] M. C. Koetting, J. T. Peters, S. D. Steichen, and N. A. Peppas, "Stimulus-responsive hydrogels: Theory, modern advances, and applications," *Mater. Sci. Eng. R Rep.*, vol. 93, pp. 1–49, Jul. 2015.
- [20] J. M. Bolivar, S. Schelch, T. Mayr, and B. Nidetzky, "Mesoporous silica materials labeled for optical oxygen sensing and their application to development of a silica-supported oxidoreductase biocatalyst," *ACS Catal.*, vol. 5, no. 10, pp. 5984–5993, Oct. 2015.

- [21] C. Boniello, T. Mayr, J. M. Bolivar, and B. Nidetzky, "Dual-lifetime referencing (DLR): a powerful method for on-line measurement of internal pH in carrier-bound immobilized biocatalysts," *BMC Biotechnol.*, vol. 12, no. 1, p. 11, 2012.
- [22] D. Brugger *et al.*, "Convenient microtiter plate-based, oxygen-independent activity assays for flavin-dependent oxidoreductases based on different redox dyes," *Biotechnol. J.*, vol. 9, no. 4, pp. 474–482, Apr. 2014.
- [23] S. Bidmanova *et al.*, "Microscopic monitoring provides information on structure and properties during biocatalyst immobilization," *Biotechnol. J.*, vol. 9, no. 6, pp. 852–860, Jun. 2014.
- [24] A. K. Gupta, M. Kaur, N. Kaur, and R. P. Singh, "A comparison of properties of inulinases of *Fusarium oxysporum* immobilized on various supports," *J. Chem. Technol. Biotechnol.*, no. 53, pp. 293–296, 1992.
- [25] J. Lalonde and A. Margolin, "Immobilization of enzymes," in *Enzyme Catalysis in Organic Chemistry*, 2nd ed., Weinheim: Wiley-VCH, 2002, pp. 163–184.
- [26] S. Ohlson, P.-O. Larsson, and K. Mosbach, "Steroid transformation by living cells immobilized in calcium alginate," *Eur. J. Appl. Microbiol. Biotechnol.*, vol. 7, no. 2, pp. 103–110, 1979.
- [27] J. Fan *et al.*, "Cubic Mesoporous Silica with Large Controllable Entrance Sizes and Advanced Adsorption Properties," *Angew. Chem.*, vol. 115, no. 27, pp. 3254–3258, Jul. 2003.
- [28] C. Ispas, I. Sokolov, and S. Andreescu, "Enzyme-functionalized mesoporous silica for bioanalytical applications," *Anal. Bioanal. Chem.*, vol. 393, no. 2, pp. 543–554, Jan. 2009.
- [29] Y. Han, S. S. Lee, and J. Y. Ying, "Pressure-Driven Enzyme Entrapment in Siliceous Mesocellular Foam," *Chem. Mater.*, vol. 18, no. 3, pp. 643–649, Feb. 2006.
- [30] V. Zlateski, T. C. Keller, J. Pérez-Ramírez, and R. N. Grass, "Immobilizing and de-immobilizing enzymes on mesoporous silica," *RSC Adv.*, vol. 5, no. 106, pp. 87706–87712, Oct. 2015.
- [31] N. Angelova and D. Hunkeler, "Rationalizing the design of polymeric biomaterials," *Trends Biotechnol.*, vol. 17, pp. 409–421, 1999.
- [32] O. Ariga, H. Takagi, H. Nishizawa, and Y. Sano, "Immobilization of microorganisms with PVA hardened by iterative freezing and thawing," *J. Ferment. Technol.*, vol. 65, no. 6, pp. 651–658, Dec. 1987.
- [33] K. Imai, T. Shiomi, K. Uchida, and M. Miya, "Immobilization of Enzyme into Poly(vinyl alcohol) Membrane," *Biotechnol. Bioeng.*, vol. 28, no. 11, pp. 1721–1726, Nov. 1986.
- [34] P. Fernandes, L. P. Fonseca, S. Cattorini, F. Carvalho, M. P. C. Marques, and J. M. S. Cabral, "Inulin hydrolysis by inulinase immobilized in polyvinyl alcohol based hydrogel," presented at the XVIth International Conference on Bioencapsulation, Dublin, Ireland, 2008.
- [35] M. Rebros, M. Rosenberg, Z. Mlichova, and L. Kristofikova, "Hydrolysis of sucrose by invertase entrapped in polyvinyl alcohol hydrogel capsules," *Food Chem.*, vol. 102, no. 3, pp. 784–787, 2007.
- [36] J. C. Santos, A. V. Paula, C. G. F. Rocha, G. F. M. Nunes, and H. F. de Castro, "Morphological and mechanical properties of hybrid matrices of polysiloxane–polyvinyl alcohol prepared by sol–gel technique and their potential for immobilizing enzyme," *J. Non-Cryst. Solids*, vol. 354, no. 42–44, pp. 4823–4826, Nov. 2008.
- [37] C. M. Soares, O. A. dos Santos, H. F. de Castro, F. F. de Moraes, and G. M. Zanin, "Studies on immobilized lipase in hydrophobic sol-gel," in *Proceedings of the Twenty-Fifth Symposium on Biotechnology for Fuels and Chemicals Held May 4–7, 2003, in Breckenridge, CO, 2004*, pp. 307–319.
- [38] K. M. Khoo and Y. P. Ting, "Polyvinyl alcohol as an immobilization matrix—a case of gold biosorption," *Water Sci. Technol.*, vol. 43, no. 11, pp. 17–23, 2001.
- [39] H. Gröger, E. Capan, A. Barthuber, and K.-D. Vorlop, "Asymmetric Synthesis of an (R)-Cyanohydrin Using Enzymes Entrapped in Lens-Shaped Gels," *Org. Lett.*, vol. 3, no. 13, pp. 1969–1972, 2001.
- [40] Q. Shen, R. Yang, X. Hua, F. Ye, W. Zhang, and W. Zhao, "Gelatin-templated biomimetic calcification for β -galactosidase immobilization," *Process Biochem.*, vol. 46, no. 8, pp. 1565–1571, Aug. 2011.

- [41] T. Jesionowski, J. Zdarta, and B. Krajewska, "Enzyme immobilization by adsorption: a review," *Adsorption*, vol. 20, no. 5–6, pp. 801–821, Aug. 2014.
- [42] O. Barbosa, C. Ortiz, Á. Berenguer-Murcia, R. Torres, R. C. Rodrigues, and R. Fernandez-Lafuente, "Strategies for the one-step immobilization–purification of enzymes as industrial biocatalysts," *Biotechnol. Adv.*, vol. 33, no. 5, pp. 435–456, Sep. 2015.
- [43] A. G. Cunha *et al.*, "Immobilization of *Yarrowia lipolytica* Lipase—a Comparison of Stability of Physical Adsorption and Covalent Attachment Techniques," *Appl. Biochem. Biotechnol.*, vol. 146, no. 1–3, pp. 49–56, Mar. 2008.
- [44] N. Rueda *et al.*, "Reversible immobilization of lipases on octyl-glutamic agarose beads: A mixed adsorption that reinforces enzyme immobilization," *J. Mol. Catal. B Enzym.*, no. 128, pp. 10–18, 2016.
- [45] N. Rueda *et al.*, "Reversible immobilization of lipases on heterofunctional octyl-amino agarose beads prevents enzyme desorption," *Molecules*, vol. 51, no. 646, pp. 1–18, 2016.
- [46] N. Rueda, J. C. S. dos Santos, R. Torres, C. Ortiz, O. Barbosa, and R. Fernandez-Lafuente, "Improved performance of lipases immobilized on heterofunctional octyl-glyoxyl agarose beads," *RSC Adv*, no. 5, pp. 11212–11222, 2015.
- [47] J. Krenková and F. Foret, "Immobilized microfluidic enzymatic reactors," *Electrophoresis*, no. 25, pp. 3550–3563, 2004.
- [48] P. Bonomi, T. Bavaro, I. Serra, A. Tagliani, M. Terreni, and D. Ubiali, "Modulation of the Microenvironment Surrounding the Active Site of Penicillin G Acylase Immobilized on Acrylic Carriers Improves the Enzymatic Synthesis of Cephalosporins," *Molecules*, vol. 18, no. 11, pp. 14349–14365, Nov. 2013.
- [49] A. Basso *et al.*, "Endo- and Exo-Inulinases: Enzyme-Substrate Interaction and Rational Immobilization," *Biotechnol. Prog.*, vol. 26, no. 2, pp. 397–405, Nov. 2009.
- [50] L. Shen *et al.*, "Immobilization of enzyme on a polymer surface," *Surf. Sci.*, vol. 648, pp. 53–59, Jun. 2016.
- [51] J. M. Bolivar and B. Nidetzky, "Oriented and selective enzyme immobilization on functionalized silica carrier using the cationic binding module Zbasic2: Design of a heterogeneous D-amino acid oxidase catalyst on porous glass," *Biotechnol. Bioeng.*, vol. 109, no. 6, pp. 1490–1498, Jun. 2012.
- [52] F. López-Gallego *et al.*, "Enzyme stabilization by glutaraldehyde crosslinking of adsorbed proteins on aminated supports," *J. Biotechnol.*, vol. 119, no. 1, pp. 70–75, Sep. 2005.
- [53] S. Velasco-Lozano, F. López-Gallego, J. C. Mateos-Díaz, and E. Favela-Torres, "Cross-linked enzyme aggregates (CLEA) in enzyme improvement – a review," *Biocatalysis*, vol. 1, no. 1, Jan. 2016.
- [54] L. Cao, L. van Langen, and R. Sheldon, "Immobilised enzymes: Carrier-bound or carrier-free?," *Curr. Opin. Biotechnol.*, no. 14, pp. 1–8, 2003.
- [55] H. Noritomi, K. Koyama, S. Kato, and K. Nagahama, "Increased thermostability of cross-linked enzyme crystals of subtilisin in organic solvents," *Biotechnol. Tech.*, no. 12, pp. 467–469, 1998.
- [56] R. A. Sheldon, "Characteristic features and biotechnological applications of cross-linked enzyme aggregates (CLEAs)," *Appl. Microbiol. Biotechnol.*, vol. 92, no. 3, pp. 467–477, Nov. 2011.
- [57] L. Wilson, A. Illanes, B. C. C. Pessela, O. Abian, R. Fernández-Lafuente, and J. M. Guisán, "Encapsulation of crosslinked Penicillin G Acylase aggregates in Lentikats: Evaluation of a novel biocatalyst in organic media," *Biotechnol. Bioeng.*, vol. 86, no. 5, pp. 558–562, Jun. 2004.
- [58] R. A. Sheldon, "Cross-Linked Enzyme Aggregates as Industrial Biocatalysts," *Org. Process Res. Dev.*, vol. 15, no. 1, pp. 213–223, Jan. 2011.
- [59] E. Ricca, V. Calabrò, S. Curcio, and G. Iorio, "Optimization of inulin hydrolysis by inulinase accounting for enzyme time- and temperature-dependent deactivation," *Biochem. Eng. J.*, vol. 48, no. 1, pp. 81–86, Dec. 2009.
- [60] E. Ricca, V. Calabrò, S. Curcio, and G. Iorio, "The State of the Art in the Production of Fructose from Inulin Enzymatic Hydrolysis," *Crit. Rev. Biotechnol.*, vol. 27, no. 3, pp. 129–145, Jan. 2007.

- [61] A. E. Abasaeed and Y. Y. Lee, "Inulin Hydrolysis to Fructose by a Novel Catalyst," *Chem. Eng. Technol.*, no. 18, pp. 440–444, 1995.
- [62] S. E. Fleming and J. W. GrootWassink, "Preparation of high-fructose syrup from the tubers of the Jerusalem artichoke (*Helianthus tuberosus* L.)," *CRC Crit. Rev. Food Sci. Nutr.*, vol. 12, no. 1, pp. 1–28, 1979.
- [63] E. J. Vandamme and D. G. Derycke, "Microbial Inulinases: Fermentation Process, Properties, and Applications," *Adv. Appl. Microbiol.*, vol. 29, pp. 139–176, 1983.
- [64] P. K. Gill, R. K. Manhas, and P. Singh, "Hydrolysis of inulin by immobilized thermostable extracellular exoinulinase from *Aspergillus fumigatus*," *J. Food Eng.*, vol. 76, no. 3, pp. 369–375, Oct. 2006.
- [65] L. Zittan, "Enzymatic Hydrolysis of Inulin - An alternative way to fructose production," *Starch*, vol. 33, no. 11, pp. 373–377, 1981.
- [66] A. Kochhar, A. K. Gupta, and N. Kaur, "Purification and immobilisation of inulinase from *Aspergillus candidus* for producing fructose," *J. Sci. Food Agric.*, pp. 554–594, 1999.
- [67] S. K. Rhee and C. H. Kim, "Fructose production from Jerusalem artichoke by inulinase immobilized on chitin," *Biotechnol. Lett.*, no. 11, pp. 201–206, 1989.
- [68] P. Glibowski and A. Bukowska, "The effect of pH, temperature and heating time on inulin chemical stability," *Acta Sci. Pol. Technol. Aliment.*, vol. 10, no. 2, pp. 189–196, 2011.
- [69] N. Kaur and A. K. Gupta, "Applications of inulin and oligofructose in health and nutrition," *J. Biosci.*, vol. 27, no. 7, pp. 703–714, 2002.
- [70] M. A. Mensink, H. W. Frijlink, K. van der Voort Maarschalk, and W. L. J. Hinrichs, "Inulin, a flexible oligosaccharide I: Review of its physicochemical characteristics," *Carbohydr. Polym.*, vol. 130, pp. 405–419, Oct. 2015.
- [71] M. A. Mensink, H. W. Frijlink, K. van der Voort Maarschalk, and W. L. J. Hinrichs, "Inulin, a flexible oligosaccharide. II: Review of its pharmaceutical applications," *Carbohydr. Polym.*, vol. 134, pp. 418–428, Dec. 2015.
- [72] G. Kelly, "Inulin-type prebiotics—a review: part I," *Altern. Med. Rev.*, vol. 13, no. 4, pp. 315–330, 2008.
- [73] E. Zubaidah and W. Akhadiana, "Comparative Study of Inulin Extracts from *Dahlia*, Yam, and Gembili Tubers as Prebiotic," *Food Nutr. Sci.*, vol. 4, no. 11, pp. 8–12, 2013.
- [74] F. Castelli *et al.*, "Differential scanning calorimetry study on drug release from an inulin-based hydrogel and its interaction with a biomembrane model: pH and loading effect," *Eur. J. Pharm. Sci.*, vol. 35, no. 1–2, pp. 76–85, Sep. 2008.
- [75] J. E. Bailey and D. F. Ollis, *Biochemical Engineering Fundamentals*. Singapore: McGraw-Hill Book Co., 1986.
- [76] Z.-M. Chi, T. Zhang, T.-S. Cao, X.-Y. Liu, W. Cui, and C.-H. Zhao, "Biotechnological potential of inulin for bioprocesses," *Bioresour. Technol.*, vol. 102, no. 6, pp. 4295–4303, Mar. 2011.
- [77] M. Ettalibi and J. C. Baratti, "Molecular and kinetic properties of *Aspergillus ficuum* inulinase," *Agric. Biol. Chem.*, no. 54, pp. 61–68, 1990.
- [78] T. Nakamura, Y. Ogata, A. Shitara, A. Nakamura, and K. Ohta, "Continuous production of fructose syrups from inulin by immobilized inulinase from *Aspergillus niger* Mutant 817," *J. Ferment. Bioeng.*, vol. 80, no. 2, pp. 164–169, 1995.
- [79] M. Fernandes and B. Jiang, "Fungal Inulinases as Potential Enzymes for Application in the Food Industry," *Adv. J. Food Sci. Technol.*, vol. 5, no. 8, pp. 1031–1042, 2013.
- [80] A. Pandey, C. R. Soccol, P. Selvakumar, V. T. Soccol, N. Krieger, and J. D. Fontana, "Recent developments in microbial inulinases," *Appl. Biochem. Biotechnol.*, vol. 80, no. 1, pp. 35–52, 1999.
- [81] J. C. Baratti and M. Ettalibi, "Purification, properties and comparison of invertase, exo-inulinases and endo-inulinases of *Aspergillus ficuum*," *Appl. Microbiol. Biotechnol.*, no. 26, pp. 13–20, 1987.
- [82] Z. Chi, Z. Chi, T. Zhang, G. Liu, and L. Yue, "Inulinase-expressing microorganisms and applications of inulinases," *Appl. Microbiol. Biotechnol.*, vol. 82, no. 2, pp. 211–220, Feb. 2009.

- [83] A. C. Apolinário, B. P. G. de Lima Damasceno, N. E. de Macêdo Beltrão, A. Pessoa, A. Converti, and J. A. da Silva, "Inulin-type fructans: A review on different aspects of biochemical and pharmaceutical technology," *Carbohydr. Polym.*, vol. 101, pp. 368–378, Jan. 2014.
- [84] T. B. Uhm, W. Y. Kim, and S. M. Byun, "Hydrolysis of inulin from Jerusalem artichoke by inulinase immobilized on aminoethylcellulose," *Enzyme Microb. Technol.*, vol. 4, no. 4, pp. 239–244, 1982.
- [85] D. G. Derycke and E. J. Vandamme, "Production and properties of *Aspergillus niger* inulinase," *J. Chem. Technol. Biotechnol.*, vol. 34, no. 1, pp. 45–51, 1984.
- [86] C. Blecker, C. Fournies, J.-C. Van Herck, J.-P. Chevalier, and M. Paquot, "Kinetic Study of the Acid Hydrolysis of Various Oligofructose Samples," *J. Agric. Food Chem.*, vol. 50, no. 6, pp. 1602–1607, Mar. 2002.
- [87] B. Focher, A. Marzetti, P. Carniti, P. L. Beltrame, and D. Guardione, "Hydrolysis of inulin: A kinetic study of the reaction catalyzed by an inulinase from *Aspergillus ficuum*," *Biotechnol. Bioeng.*, vol. 37, no. 6, pp. 575–579, 1991.
- [88] J. Anes and P. Fernandes, "Towards the continuous production of fructose syrups from inulin using inulinase entrapped in PVA-based particles," *Biocatal. Agric. Biotechnol.*, vol. 3, no. 4, pp. 296–302, Oct. 2014.
- [89] J. R. Rocha, R. Catana, B. S. Ferreira, J. M. S. Cabral, and P. Fernandes, "Design and characterisation of an enzyme system for inulin hydrolysis," *Food Chem.*, vol. 95, no. 1, pp. 77–82, Mar. 2006.
- [90] M. F. Silva *et al.*, "Evaluation of enzymatic activity of commercial inulinase from *Aspergillus niger* immobilized in polyurethane foam," *Food Bioprod. Process.*, vol. 91, no. 1, pp. 54–59, Jan. 2013.
- [91] J. Nielsen, J. Villadsen, and G. Lidén, *Bioreaction Engineering Principles*, 2nd ed. New York: Kluwer Academic, 2003.
- [92] E. K. Nauha, O. Visuri, R. Vermasvuori, and V. Alopaeus, "A new simple approach for the scale-up of aerated stirred tanks," *Chem. Eng. Res. Des.*, vol. 95, pp. 150–161, Mar. 2015.
- [93] V. B. Shukla, U. P. Veera, P. R. Kulkarni, and A. B. Pandit, "Scale-up of biotransformation process in stirred tank reactor using dual impeller bioreactor," *Biochem. Eng. J.*, vol. 8, no. 1, pp. 19–29, 2001.
- [94] P. Fernandes and J. M. S. Cabral, "Microlitre/millilitre shaken bioreactors in fermentative and biotransformation processes – a review," *Biocatal. Biotransformation*, vol. 24, no. 4, pp. 237–252, Jan. 2006.
- [95] M. Doble, A. K. Kruthiventi, and V. G. Gaikar, *Biotransformations and Bioprocesses*. New York: Marcel Dekker, Inc., 2004.
- [96] U. Krühne *et al.*, "Biocatalytic process development using microfluidic miniaturized systems," *Green Process. Synth.*, vol. 3, no. 1, Jan. 2014.
- [97] P. M. Doran, *Bioprocess Engineering Principles*. London: Academic Press, 1995.
- [98] P. Fernandes, F. Carvalho, and M. P. C. Marques, "Miniaturization in Biotechnology: Speeding up the Development of Bioprocesses," *Recent Pat. Biotechnol.*, no. 5, pp. 160–173, 2011.
- [99] P. Fernandes, "Miniaturization in Biocatalysis," *Int. J. Mol. Sci.*, vol. 11, no. 3, pp. 858–879, Mar. 2010.
- [100] J. M. Bolivar, J. Wiesbauer, and B. Nidetzky, "Biotransformations in microstructured reactors: more than flowing with the stream?," *Trends Biotechnol.*, vol. 29, no. 7, pp. 333–342, Jul. 2011.
- [101] T. Chován and A. Guttman, "Microfabricated devices in biotechnology and biochemical processing," *Trends Biotechnol.*, vol. 20, no. 3, pp. 116–122, 2002.
- [102] D. Schäpper, S. M. Stocks, N. Szita, A. E. Lantz, and K. V. Gernaey, "Development of a single-use microbioreactor for cultivation of microorganisms," *Chem. Eng. J.*, vol. 160, no. 3, pp. 891–898, Jun. 2010.
- [103] J.-H. Grosch, M. Sieben, C. Lattermann, K. Kauffmann, J. Büchs, and A. C. Spieß, "Enzyme activity deviates due to spatial and temporal temperature profiles in commercial microtiter plate readers," *Biotechnol. J.*, vol. 11, no. 4, pp. 519–529, Apr. 2016.

- [104] D. G. Oliver, A. H. Sanders, R. Douglas Hogg, and J. Woods Hellman, "Thermal gradients in microtitration plates. Effects on enzyme-linked immunoassay," *J. Immunol. Methods*, vol. 42, no. 2, pp. 195–201, Apr. 1981.
- [105] B. J. Battersby and M. Trau, "Novel miniaturized systems in high-throughput screening," *Trends Biotechnol.*, vol. 20, no. 4, pp. 167–173, 2002.
- [106] F. Gielen *et al.*, "A Fully Unsupervised Compartment-on-Demand Platform for Precise Nanoliter Assays of Time-Dependent Steady-State Enzyme Kinetics and Inhibition," *Anal. Chem.*, vol. 85, no. 9, pp. 4761–4769, May 2013.
- [107] J. Z. Baboo, J. L. Galman, G. J. Lye, J. M. Ward, H. C. Hailes, and M. Micheletti, "An automated microscale platform for evaluation and optimization of oxidative bioconversion processes," *Biotechnol. Prog.*, vol. 28, no. 2, pp. 392–405, Mar. 2012.
- [108] E. Fischer and U. Sauer, "Large-scale in vivo flux analysis shows rigidity and suboptimal performance of *Bacillus subtilis* metabolism," *Nat. Genet.*, vol. 37, no. 6, pp. 636–640, Jun. 2005.
- [109] T. Schlepütz, J. P. Gerhards, and J. Büchs, "Ensuring constant oxygen supply during inoculation is essential to obtain reproducible results with obligatory aerobic acetic acid bacteria in vinegar production," *Process Biochem.*, vol. 48, no. 3, pp. 398–405, Mar. 2013.
- [110] T. Schlepütz and J. Büchs, "Scale-down of vinegar production into microtiter plates using a custom-made lid," *J. Biosci. Bioeng.*, vol. 117, no. 4, pp. 485–496, Apr. 2014.
- [111] L. C. Gomes, J. M. R. Moreira, J. M. Miranda, M. Simões, L. F. Melo, and F. J. Mergulhão, "Macroscale versus microscale methods for physiological analysis of biofilms formed in 96-well microtiter plates," *J. Microbiol. Methods*, vol. 95, no. 3, pp. 342–349, Dec. 2013.
- [112] A. B. Bos, P. Luan, J. N. Duque, D. Reilly, P. D. Harms, and A. W. Wong, "Optimization and automation of an end-to-end high throughput microscale transient protein production process: Optimization of an automated microscale transient expression system," *Biotechnol. Bioeng.*, vol. 112, no. 9, pp. 1832–1842, Sep. 2015.
- [113] R. Hermann, M. Lehmann, and J. Büchs, "Characterization of gas–liquid mass transfer phenomena in microtiter plates," *Biotechnol. Bioeng.*, vol. 81, no. 2, pp. 178–186, Jan. 2003.
- [114] G. J. Lye, P. Ayazi-Shamlou, F. Baganz, P. A. Dalby, and J. M. Woodley, "Accelerated design of bioconversion processes using automated microscale processing techniques," *Trends Biotechnol.*, vol. 21, no. 1, pp. 29–37, Jan. 2003.
- [115] V. Hessel, S. Hardt, H. Löwe, and F. Schönfeld, "Laminar mixing in different interdigital micromixers: I. Experimental characterization," *AIChE J.*, vol. 49, no. 3, pp. 566–577, Mar. 2003.
- [116] S. Weiss, G. T. John, I. Klimant, and E. Heinzle, "Modeling of Mixing in 96-Well Microplates Observed with Fluorescence Indicators," *Biotechnol. Prog.*, vol. 18, no. 4, pp. 821–830, Jan. 2002.
- [117] W. Klöckner and J. Büchs, "Advances in shaking technologies," *Trends Biotechnol.*, vol. 30, no. 6, pp. 307–314, Jun. 2012.
- [118] F. Kensy *et al.*, "Oxygen transfer phenomena in 48-well microtiter plates: Determination by optical monitoring of sulfite oxidation and verification by real-time measurement during microbial growth: Oxygen Transfer Phenomena in 48-Well MTP," *Biotechnol. Bioeng.*, vol. 89, no. 6, pp. 698–708, Mar. 2005.
- [119] M. Micheletti and G. J. Lye, "Microscale bioprocess optimisation," *Curr. Opin. Biotechnol.*, vol. 17, no. 6, pp. 611–618, Dec. 2006.
- [120] W. A. Duetz, L. Rüedi, R. Hermann, K. O'Connor, J. Büchs, and B. Witholt, "Methods for Intense Aeration, Growth, Storage, and Replication of Bacterial Strains in Microtiter Plates," *Appl. Environ. Microbiol.*, vol. 66, no. 6, pp. 2641–2646, Jun. 2000.
- [121] M. Funke, S. Diederichs, F. Kensy, C. Müller, and J. Büchs, "The baffled microtiter plate: increased oxygen transfer and improved online monitoring in small scale fermentations," *Biotechnol. Bioeng.*, vol. 103, no. 6, pp. 1118–1128, Aug. 2009.

- [122] S. D. Doig, S. C. R. Pickering, G. J. Lye, and F. Baganz, "Modelling surface aeration rates in shaken microtitre plates using dimensionless groups," *Chem. Eng. Sci.*, vol. 60, no. 10, pp. 2741–2750, May 2005.
- [123] M. A. P. Nunes, P. C. B. Fernandes, and M. H. L. Ribeiro, "Microtiter plates versus stirred mini-bioreactors in biocatalysis: A scalable approach," *Bioresour. Technol.*, vol. 136, pp. 30–40, May 2013.
- [124] C. Walther *et al.*, "Prediction of inclusion body solubilization from shaken to stirred reactors," *Biotechnol. Bioeng.*, vol. 111, no. 1, pp. 84–94, 2014.
- [125] G. Perozziello *et al.*, "A Fluidic Motherboard for Multiplexed Simultaneous and Modular Detection in Microfluidic Systems for Biological Application," *Micro Nanosyst.*, vol. 2, no. 4, pp. 227–238, Dec. 2010.
- [126] M. P. C. Marques and P. Fernandes, "Microfluidic Devices: Useful Tools for Bioprocess Intensification," *Molecules*, vol. 16, no. 12, pp. 8368–8401, Sep. 2011.
- [127] R. H. Liu, Q. Yu, and D. J. Beebe, "Fabrication and characterization of hydrogel-based microvalves," *J. Microelectromechanical Syst.*, vol. 11, no. 1, pp. 45–53, Feb. 2002.
- [128] M. Mehling and S. Tay, "Microfluidic cell culture," *Curr. Opin. Biotechnol.*, vol. 25, pp. 95–102, Feb. 2014.
- [129] J. G. Kralj, H. R. Sahoo, and K. F. Jensen, "Integrated continuous microfluidic liquid-liquid extraction," *Lab. Chip*, vol. 7, no. 2, pp. 256–263, Feb. 2007.
- [130] P. Žnidaršič-Plazl and I. Plazl, "Steroid extraction in a microchannel system—mathematical modelling and experiments," *Lab Chip*, vol. 7, no. 7, pp. 883–889, 2007.
- [131] M. Tokeshi, T. Minagawa, and T. Kitamori, "Integration of a microextraction system: Solvent extraction of a Co–2-nitroso-5-dimethylaminophenol complex on a microchip," *J. Chromatogr. A*, vol. 894, no. 1–2, pp. 19–23, Oct. 2000.
- [132] D. M. Roberge, L. Ducry, N. Bieler, P. Cretton, and B. Zimmermann, "Microreactor Technology: A Revolution for the Fine Chemical and Pharmaceutical Industries?," *Chem. Eng. Technol.*, vol. 28, no. 3, pp. 318–323, Mar. 2005.
- [133] T. Honda, M. Miyazaki, H. Nakamura, and H. Maeda, "Immobilization of enzymes on a microchannel surface through cross-linking polymerization," *Chem. Commun. Camb. Engl.*, no. 40, pp. 5062–5064, Oct. 2005.
- [134] C. G. Frost and L. Mutton, "Heterogeneous catalytic synthesis using microreactor technology," *Green Chem.*, vol. 12, no. 10, pp. 1687–1703, Oct. 2010.
- [135] S. Kundu *et al.*, "Continuous Flow Enzyme-Catalyzed Polymerization in a Microreactor," *J. Am. Chem. Soc.*, vol. 133, no. 15, pp. 6006–6011, Apr. 2011.
- [136] J. M. Obón, M. R. Castellar, J. L. Iborra, and A. Manjón, "β-Galactosidase immobilization for milk lactose hydrolysis: a simple experimental and modelling study of batch and continuous reactors," *Biochem. Educ.*, vol. 28, no. 3, pp. 164–168, 2000.
- [137] P. Fernandes, M. P. C. Marques, F. Carvalho, and J. M. S. Cabral, "A simple method for biocatalyst immobilization using PVA-based hydrogel particles," *J. Chem. Technol. Biotechnol.*, vol. 84, no. 4, pp. 561–564, Apr. 2009.
- [138] S. D. Doig, S. C. R. Pickering, G. J. Lye, and J. M. Woodley, "The use of microscale processing technologies for quantification of biocatalytic Baeyer-Villiger oxidation kinetics," *Biotechnol. Bioeng.*, vol. 80, no. 1, pp. 42–49, Oct. 2002.
- [139] G. L. Miller, "Use of dinitrosalicylic acid reagent for determination of reducing sugar," *Anal. Chem.*, vol. 31, no. 3, pp. 426–428, 1959.
- [140] M. A. P. Nunes, H. Vila-Real, P. C. B. Fernandes, and M. H. L. Ribeiro, "Immobilization of Naringinase in PVA–Alginate Matrix Using an Innovative Technique," *Appl. Biochem. Biotechnol.*, vol. 160, no. 7, pp. 2129–2147, Apr. 2010.

- [141] E. Ricca, V. Calabrò, S. Curcio, and G. Iorio, "Fructose production by chicory inulin enzymatic hydrolysis: A kinetic study and reaction mechanism," *Process Biochem.*, vol. 44, no. 4, pp. 466–470, Apr. 2009.
- [142] S. Trivedi, J. Divecha, T. Shah, and A. Shah, "Rapid and efficient bioconversion of chicory inulin to fructose by immobilized thermostable inulinase from *Aspergillus tubingensis* CR16," *Bioresour. Bioprocess.*, vol. 2, no. 1, Dec. 2015.
- [143] A. Martino, M. Durante, P. G. Pifferi, G. Spagna, and G. Bianchi, "Immobilization of β -glucosidase from a commercial preparation. Part 1. A comparative study of natural supports," *Process Biochem.*, vol. 31, no. 3, pp. 281–285, Jan. 1996.
- [144] J. M. Bolivar, T. Consolati, T. Mayr, and B. Nidetzky, "Shine a light on immobilized enzymes: real-time sensing in solid supported biocatalysts," *Trends Biotechnol.*, vol. 31, no. 3, pp. 194–203, Mar. 2013.
- [145] Q. D. Nguyen, J. M. Rezessy-Szabó, B. Czukor, and Á. Hoschke, "Continuous production of oligofructose syrup from Jerusalem artichoke juice by immobilized endo-inulinase," *Process Biochem.*, vol. 46, no. 1, pp. 298–303, Jan. 2011.
- [146] S. Cattorini, M. P. C. Marques, F. Carvalho, V. Chheub, J. M. S. Cabral, and P. Fernandes, "Lentikat®-based biocatalysts: effective tools for inulin hydrolysis," *Chem. Biochem. Eng. Q.*, vol. 23, no. 4, pp. 429–434, 2009.
- [147] J. Figueira, F. Dias, H. Sato, and P. Fernandes, "Screening of Supports for the Immobilization of β -Glucosidase," *Enzyme Res.*, vol. 2011, pp. 1–8, 2011.
- [148] H. Nagatomo, Y. Matsushita, K. Sugamoto, and T. Matsui, "Preparation and properties of gelatin-immobilized beta-glucosidase from *Pyrococcus furiosus*," *Biosci. Biotechnol. Biochem.*, vol. 69, no. 1, pp. 128–136, Jan. 2005.
- [149] G. L. M. Santa *et al.*, "From Inulin to Fructose Syrups Using Sol–Gel Immobilized Inulinase," *Appl. Biochem. Biotechnol.*, vol. 165, no. 1, pp. 1–12, Sep. 2011.
- [150] J. M. Guisan, *Immobilization of Enzymes and Cells*. Springer Science & Business Media, 2006.
- [151] W. A. Duetz and B. Witholt, "Oxygen transfer by orbital shaking of square vessels and deepwell microtiter plates of various dimensions," *Biochem. Eng. J.*, vol. 17, no. 3, pp. 181–185, Mar. 2004.
- [152] C. Lattermann, M. Funke, S. Hansen, S. Diederichs, and J. Büchs, "Cross-section perimeter is a suitable parameter to describe the effects of different baffle geometries in shaken microtiter plates," *J. Biol. Eng.*, vol. 8, no. 18, pp. 1–10, 2014.
- [153] W. A. Duetz, "Microtiter plates as mini-bioreactors: miniaturization of fermentation methods," *Trends Microbiol.*, vol. 15, no. 10, pp. 469–475, Oct. 2007.
- [154] S. Curcio, E. Ricca, A. Saraceno, G. Iorio, and V. Calabrò, "A mass transport/kinetic model for the description of inulin hydrolysis by immobilized inulinase: Modeling of inulin hydrolysis by immobilized inulinase," *J. Chem. Technol. Biotechnol.*, vol. 90, no. 10, pp. 1782–1792, Oct. 2015.
- [155] S. Curcio, E. Ricca, V. Calabrò, and G. Iorio, "Effect of the Degree of Polymerization of Inulin on the Rate of Hydrolysis Using Immobilized Inulinase," *Food Technol. Biotechnol.*, vol. 52, no. 3, p. 317, 2014.
- [156] V. G. Pangarkar, A. A. Yawalkar, M. M. Sharma, and A. A. C. M. Beenackers, "Particle–Liquid Mass Transfer Coefficient in Two-/Three-Phase Stirred Tank Reactors," *Ind. Eng. Chem. Res.*, vol. 41, no. 17, pp. 4141–4167, Aug. 2002.
- [157] F. Khorasheh, A. Kheiriloom, and S. Mireshghi, "Application of an optimization algorithm for estimating intrinsic kinetic parameters of immobilized enzymes," *J. Biosci. Bioeng.*, vol. 94, no. 1, pp. 1–7, 2002.